International Ocean Discovery Program Expedition 400 Scientific Prospectus

NW Greenland Glaciated Margin

Cenozoic evolution of the northern Greenland Ice Sheet exposed by transect drilling in northeast Baffin Bay

Paul Knutz
Co-Chief Scientist
Marine Geology Department
GEUS
Denmark

Anne Jennings
Co-Chief Scientist
INSTAAR
University of Colorado
USA

Laurel B. Childress
Expedition Project Manager/Staff Scientist
International Ocean Discovery Program
Texas A&M University
USA

Publisher's notes

This publication was prepared by the *JOIDES Resolution* Science Operator (JRSO) at Texas A&M University (TAMU) as an account of work performed under the International Ocean Discovery Program (IODP). This material is based upon work supported by the JRSO, which is a major facility funded by the National Science Foundation Cooperative Agreement Number OCE1326927. Funding for IODP is provided by the following international partners:

National Science Foundation (NSF), United States
Ministry of Education, Culture, Sports, Science and Technology (MEXT), Japan
European Consortium for Ocean Research Drilling (ECORD)
Ministry of Science and Technology (MOST), People's Republic of China
Australia-New Zealand IODP Consortium (ANZIC)
Ministry of Earth Sciences (MoES), India

Portions of this work may have been published in whole or in part in other IODP documents or publications.

This IODP *Scientific Prospectus* is based on precruise *JOIDES Resolution* Facility advisory panel discussions and scientific input from the designated Co-Chief Scientists on behalf of the drilling proponents. During the course of the cruise, actual site operations may indicate to the Co-Chief Scientists, the Expedition Project Manager/Staff Scientist, and the Operations Superintendent that it would be scientifically or operationally advantageous to amend the plan detailed in this prospectus. It should be understood that any substantial changes to the science deliverables outlined in the plan presented here are contingent upon the approval of the IODP JRSO Director and/or *JOIDES Resolution* Facility Board.

Disclaimer

Copyright

Citation

Knutz, P., Jennings, A., and Childress, L.B., 2022. Expedition 400 Scientific Prospectus: NW Greenland Glaciated Margin. International Ocean Discovery Program. https://doi.org/10.14379/iodp.sp.400.2022

ISSN

World Wide Web: 2332-1385

September 2022

Abstract

Elucidating the long-term history of the Greenland Ice Sheet (GrIS) is essential for understanding glacial instability thresholds, identified as major climate system tipping points, and how the cryosphere will respond to anthropogenic greenhouse gas emissions. To address current knowledge gaps in the evolution and variability of the GrIS and its role in Earth's climate system, International Ocean Discovery Program (IODP) Expedition 400 will obtain cores from seven sites across the northwest Greenland margin into Baffin Bay where thick Cenozoic sedimentary successions can be directly linked to the evolution of the northern GrIS (NGrIS). The strategy of drilling along this transect is to retrieve a composite stratigraphic succession representing the Late Cenozoic era from the Oligocene/Early Miocene to Holocene. The proposed sites will specifically target high–accumulation rate deposits associated with contourite drifts and potential interglacial deposits within a trough mouth fan system densely covered by seismic data. We seek to test if the NGrIS underwent near-complete deglaciations in the Pleistocene and to assess the ice sheet's response to changes in orbital cyclicities through the mid-Pleistocene transition. Paleoclimate records will be obtained that can provide chronology on the NGrIS expansion and unravel potential linkages between marine heat transport through Baffin Bay and high Arctic warmth during the Pliocene. A deep coring site (980 meters below seafloor) targeting a Miocene and Oligocene strata succession will examine possible linkages between changes in atmospheric CO_2 and climate-ecosystem conditions in Greenland. The overall aim is to investigate the full range of forcings and feedbacks—oceanic, atmospheric, orbital, and tectonic—that influence the GrIS over a range of timescales, as well as conditions prevailing at the time of glacial inception and deglacial to interglacial periods. The data and results gathered from Expedition 400 will effectively constrain predictive models addressing the GrIS response to global warming and its impending effects on global sea levels.

Plain language summary

Sea-level consequences of anthropogenic climate forcing hinge on how the polar ice sheets respond to global warming. If fully melted, the Greenland Ice Sheet has the potential to raise sea level by >7 meters, yet we know very little about its long-term responses to past climate warming or its role in Earth's climate system. Expedition 400 seeks to address current knowledge gaps in the evolution and variability of the northern Greenland Ice Sheet by analyzing sedimentary archives of warm and cold periods of the last ~30 million years, including times when the greenhouse gas content of the atmosphere was higher than it is today.

Sediment archives will be obtained by drilling at seven sites to depths of 300–1000 meters below seafloor along a transect crossing the northwest Greenland margin into Baffin Bay. The seven sites will provide a composite stratigraphic succession that includes preglacial settings, a record of first growth of the northern Greenland Ice Sheet, and glacial and interglacial cycles when the ice sheet grew to its maximum positions at the shelf edge and retreated toward land, possibly melting nearly completely.

1. Schedule for Expedition 400

International Ocean Discovery Program (IODP) Expedition 400 is based on IODP drilling Proposals 909-Full2 and 909-Add (available at **http://iodp.tamu.edu/scienceops/expeditions/nw_greenland_glaciated_margin.html**). Following evaluation by the IODP Scientific Advisory Structure, the expedition was scheduled for the research vessel (R/V) *JOIDES Resolution*, operating under contract with the *JOIDES Resolution* Science Operator (JRSO). At the time of publication of this *Scientific Prospectus*, the expedition is scheduled to start in St. John's, Canada, on 12 August 2023 and to end in St. John's, Canada, on 12 October. A total of 56 days will be available for the transit, drilling, coring, and downhole measurements described in this report (for the current detailed schedule, see **http://iodp.tamu.edu/scienceops**). Further details about the facilities aboard *JOIDES Resolution* can be found at **http://iodp.tamu.edu/labs/index.html**.

2. Introduction

The Greenland Ice Sheet (GrIS) holds a large amount of freshwater, equivalent to ~7.4 m of global sea level (Bamber et al., 2013). Recent studies have highlighted the sensitivity of the GrIS to climate warming and the potential impact its meltwaters would have on sea level rise and the Atlantic Meridional Ocean Circulation (Alley et al., 2010; Khan et al., 2010; Hansen et al., 2016). With the prospect of irreversible ice sheet retreat as one of the major tipping points, documenting the full range of forcing and feedbacks—oceanic, atmospheric, orbital, and tectonic—that influence the GrIS over a range of timescales is crucial for making robust predictions of future climate and sea level change (Intergovernmental Panel on Climate Change [IPCC] Sixth Assessment Report; **https://www.ipcc.ch/assessment-report/ar6**). To this end, high-resolution sedimentary archives proximal to Greenland that capture glacial discharges of meltwater and sediments under different ice sheet configurations as well as biogenic components reflecting marine and terrestrial climate conditions are needed. The objectives of Expedition 400 directly address the critical questions posed in the Climate and Ocean Change theme of the IODP science plan: "How do ice sheets and sea level respond to a warming climate?" and "How does Earth's climate system respond to elevated levels of atmospheric CO_2?"

The response of the GrIS to extreme interglacial warmth is a highly relevant and debated topic although it is poorly constrained by data. During the last interglacial period, Marine Isotope Stage (MIS) 5e, global sea level was likely in the range of 6–9 m higher than present (Dutton and Lambeck, 2012), of which the GrIS may have contributed between 10% and 40% (Neem Community Members, 2013; Dutton et al., 2015). During MIS 11c, described as a super-interglacial (Loutre, 2003; Melles et al., 2012) (Figure **F1**), global sea levels 6–13 m higher than today have been estimated (Dutton et al., 2015). Several studies associate MIS 11c with a significant or near-complete loss of the GrIS (Willerslev et al., 2007; de Vernal and Hillaire-Marcel, 2008; Reyes et al., 2014). The MIS 11c ice sheet loss apparently occurred despite more moderate summer temperatures compared to MIS 5e (Cluett and Thomas, 2021). A compelling result by Schaefer et al. (2016), based on cosmogenic nuclides in subice bedrock, suggests that central Greenland became completely deglaciated during one or more periods over the last 2.5 My (Figure **F1**). This concept raises critical questions: (1) What forcings drove near-complete collapses of the northern GrIS (NGrIS) during the Pleistocene? (2) How did the ice sheet reconfigure to a state of "normal" glacial–interglacial conditions? To answer these questions and test the temporal scenarios for ice sheet instabilities and extended deglaciation through the Pleistocene requires access to semicontinuous records from the continental margins around Greenland (Bierman et al., 2016).

The mid-Pleistocene transition (MPT) signifies a profound shift in glacial–interglacial cycles from 41 to 100 ky periodicities (Hodell and Channell, 2016). Although the 41 ky cycles are strongly linked to orbital forcing, the insolation changes associated with 100 ky cycles are weak and require a persistent amplification mechanism (Yin and Berger, 2010). Explanations for the MPT have focused on various aspects of CO_2 reservoir exchanges between ice, ocean, and atmosphere (Raymo et al., 1996; Paillard, 1998; Ruddiman, 2006; Yin and Berger, 2010; Rial et al., 2013; Lear et al., 2016) and changes in ice sheet dynamics controlled by bedrock/regolith cover of Northern Hemisphere terrains (Clark and Pollard, 1998; Clark et al., 2006; Abe-Ouchi et al., 2013; Willeit et al., 2019). All hypotheses implicate the GrIS, directly or indirectly, but its dynamic behavior across the MPT is scarcely known. A potential linkage between global climate cycles and GrIS dynamics is highlighted by a recent study denoting a major change in northwest GrIS configuration through the MPT (Knutz et al., 2019) (Figure **F1**).

The current understanding of the Cenozoic evolution of the GrIS has been developed largely from North Atlantic deep-sea records (Figures **F2**, **F3A**). In northeast Greenland, marine-based glaciers appear to have been active since the Miocene (~18 Ma) (Thiede et al., 2011), but smaller outlets may have existed as early as the late Eocene (Eldrett et al., 2007; St. John, 2008; Tripati et al., 2008). Deep drilling and seismic evidence indicate that glacially influenced sedimentation on the central-southern East Greenland margin began during the Late Miocene (~7 Ma) (Larsen et al., 1994; Bierman et al., 2016; Pérez et al., 2018). Full-scale glaciation of Greenland is generally considered to be timed with intensification of the Northern Hemisphere glaciations interpreted from elevated

ice rafting in the North Atlantic during the late Pliocene–Pleistocene (Figure F2) (Shackleton et al., 1984; Jansen et al., 2000; St. John and Krissek, 2002). This ice sheet growth phase is possibly linked with a westward expansion of the GrIS into Baffin Bay during the Pliocene (Nielsen and Kuijpers, 2013; Knutz et al., 2019; Aubry et al., 2021), although the chronology is poorly constrained.

A better knowledge of the inception of the GrIS and its sectorized expansion during the late Cenozoic is needed to support sensitivity studies and climate models (DeConto, 2008). In particular, there is a pressing need for understanding the GrIS behavior during the warm, CO_2-driven climates of the Paleocene and Neogene (Figure F2). The Pliocene (5.3–2.6 Ma) is the most recent period when atmospheric CO_2 concentrations were similar to the modern levels of ~400 ppm. This geological time period thus functions as a past analog interval for the ongoing and future response of the ice sheet under warming conditions. Notably, the mid-Pliocene warm period (3.3–3.0 Ma) has been a focal point for paleoclimate reconstruction and modeling (Haywood et al., 2010; Dowsett et al., 2013). To study analogues for future global warming scenarios (e.g., pCO_2 projections >600 ppm beyond 2050), it is necessary to access records going further back in time (Figure F2). Key stratigraphic intervals for gaining knowledge on elevated pCO_2 climate regimes include the Middle Miocene (16–15 Ma) and most of the Oligocene (34–27 Ma) (Zhang et al.,

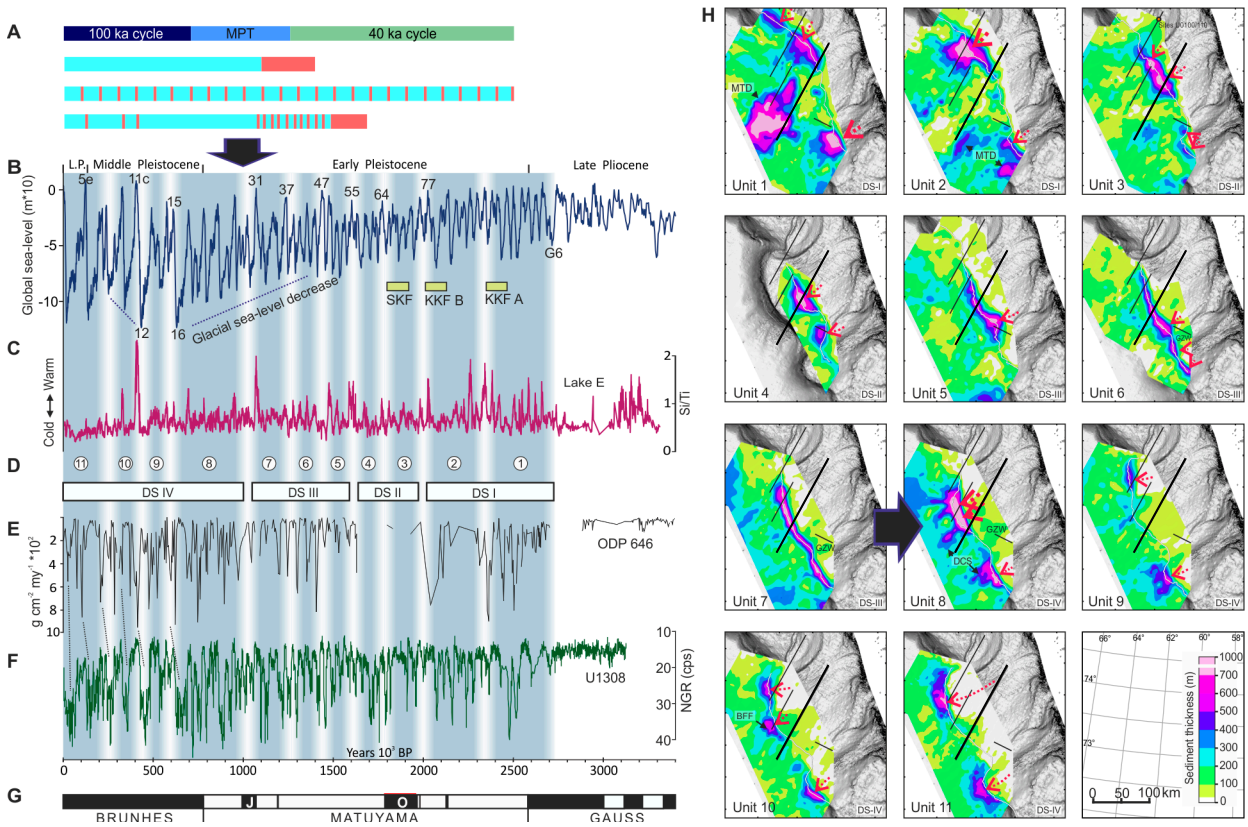

Figure F1. A. Possible scenarios for deglaciation in central Greenland based on cosmogenic bedrock dating (Schaefer et al., 2016). Red = potential near–ice free periods. B. Global sea level curve from Miller et al. (2015) constructed from LR04 benthic $\delta^{18}O$ stack (Lisiecki and Raymo, 2005). MISs for major glacials and interglacials are indicated. LP = Late Pleistocene. Correlation to terrestrial sites are indicated. SKF = Store Koldewey Formation (Bennike et al., 2010), KKF = Kap København Formation (Bennike and Böcher, 1990; Funder et al., 2001). C. Climate record from Lake El'gygytgyn, northeast Russia (Melles et al., 2012). D. Prograding Units 1–11, marked by vertical gray-blue bands, and depositional stages (DS) I–IV of the Melville Bugt/Upernavik TMF complex corresponding to thickness maps in H (Knutz et al., 2019). Age model is based on correlation to nearby boreholes and the assumption that the gross average depositional flux produced by the entire glacial outlet system has been relatively constant over long time periods (approximately several 100 ky cycles). E. Flux of coarse fraction (>63 µm) from ODP Leg 646, eastern Labrador Sea (Knutz et al., 2019; based on Wolf and Thiede, 1991). F. Natural gamma radiation (NGR) variation from Site U1308, reflecting the flux of glacial weathering products to the central North Atlantic ice-rafting belt (Hodell and Channell, 2016). cps = counts per second. G. Paleomagnetic timescale (Ogg, 2020). J = Jaramillo Subchron, O = Olduvai Subchron. H. Sediment thickness maps for prograding Units 1–11 (compare with D and Figure F5) (Knutz et al., 2019). Thick white lines = shelf-break position of top bounding horizon. Black/white background= present bathymetry. White areas = thicknesses below the seismic resolution (<30 m). MTD = mass transport deposit, GZW = grounding zone wedge, DCS = drift-channel system. Red arrows = paleoice stream positions. Large black arrow = major shift in ice stream configuration between Units 7 and 8 corresponding to MPT (D). Bold seismic line = key transect shown in Figure F5. B–H are modified from figs. 5 and 6 of Knutz et al. (2019).

2013; O'Brien et al., 2020; Guillermic et al., 2022). These pre-Quaternary intervals likely exist below the northwest Greenland margin (Knutz et al., 2015) but have yet to be explored by deep drilling.

The vulnerability of the GrIS to global climate change is a major concern, but it also highlights a knowledge gap that limits our ability to confidently project future cryospheric responses, including contributions to sea level rise (Dahl-Jensen et al., 2009; Briner et al., 2017). Cenozoic climate experienced significant changes in atmospheric greenhouse gas concentrations, notably linked to pCO_2 (Pearson and Palmer, 2000; Zachos et al., 2008; Pagani, 2014). Model studies suggest that even the modest atmospheric CO_2 changes (280–400 ppm) observed during the late Cenozoic exert a primary control on GrIS growth across the Pliocene–Pleistocene transition (Lunt et al., 2008; Tan et al., 2018) (Figure **F2**). Other factors controlling ice sheet dynamics include changes in ocean currents (Nielsen et al., 2011; Knutz et al., 2015; Otto-Bliesner et al., 2017), tectonic base-level changes (Solgaard et al., 2013), and variations in geothermal heat flux (Fahnestock et al., 2001; Rogozhina et al., 2016), but these boundary conditions are less constrained by data and are not easily addressed by climate models. For the Oligocene and Miocene time periods, the linkage between global ice volume, surface temperatures and atmospheric pCO_2 is enigmatic. The expansion and dynamic variability of ice sheets in Antarctica during periods of global warming and moderate pCO_2 levels imply a strong nonlinear behavior to climate forcing, with implications for ice sheet tipping points (Foster et al., 2012; Golledge et al., 2017; O'Brien et al., 2020; DeConto et al., 2021) (Figure **F2**). The complex linkages or possible decoupling between pCO_2 and global ice volume (Raymo et al., 1996; Tripati et al., 2009) underscores the importance of evaluating all multiple potential forcings in the earth system. Greenland is surrounded by narrow gateways that over millions of years may have changed configuration, potentially modulating ocean heat fluxes between the Arctic and North Atlantic regions (Thiede and Myhre, 1996) (Figure **F3A**). Unravel-

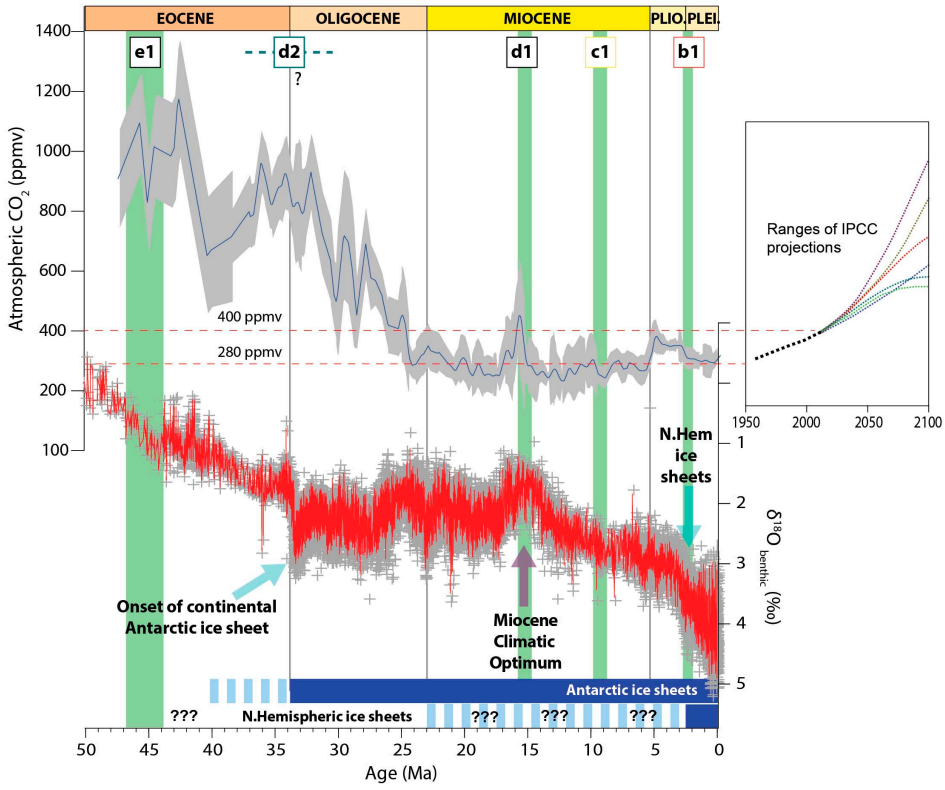

Figure F2. Estimated chronology of seismic stratigraphic horizons abounding mega-units of northwest Greenland margin (see Figure F5) shown in context of Cenozoic climate evolution. Atmospheric CO_2 reconstruction (blue line with gray 2σ errors) is based on all alkenone and boron proxy data (Pagani et al., 2005; Badger et al., 2013; Zhang et al., 2013). Historical and future CO_2 projections from the IPCC AR5 Synthesis Report (**https://www.ipcc.ch/report/ar5/syr**) showing where historical range (red dashed lines) intersects paleo-CO_2 reconstructions. Benthic foraminiferal $\delta^{18}O$ after Zachos et al. (2008). Smoothed line (red) was computed using a Matlab script called Sizer. Figure modified from Śliwińska et al. (unpubl. data).

ing the GrIS response to past global warming events will need to consider regional effects such as those related to ocean gateways, topography, and ecosystems (Otto-Bliesner et al., 2017; Hodson et al., 2010).

With a clear goal of addressing the multiple questions and hypotheses that concern the long-term evolution and stability of the NGrIS, Expedition 400 will obtain a composite sedimentary archive covering the last 25–30 My. The strategy is to drill seven sites along a transect across the northwest Greenland margin from the deep basin of Baffin Bay to the inner continental shelf (Figure **F3**). The transect is positioned between two major trough mouth fan (TMF) systems, the Melville Bugt and the Upernavik TMFs, which avoids drilling through thick glacigenic slope aprons and erosional unconformities within the recent trough features. The proposed sites will primarily core high–accumulation rate deposits that include contourite, hemipelagic, and glacial-marine sediments of Quaternary, Pliocene, and Miocene–Oligocene age. With the data extracted from composite archives obtained in close vicinity of major glacial outlets, we aim to determine maximum and minimum NGrIS configurations throughout the middle to late Cenozoic, from shelf edge glaciation to hypothesized complete ice loss, such as during Pleistocene super-interglacials (Figure **F4**).

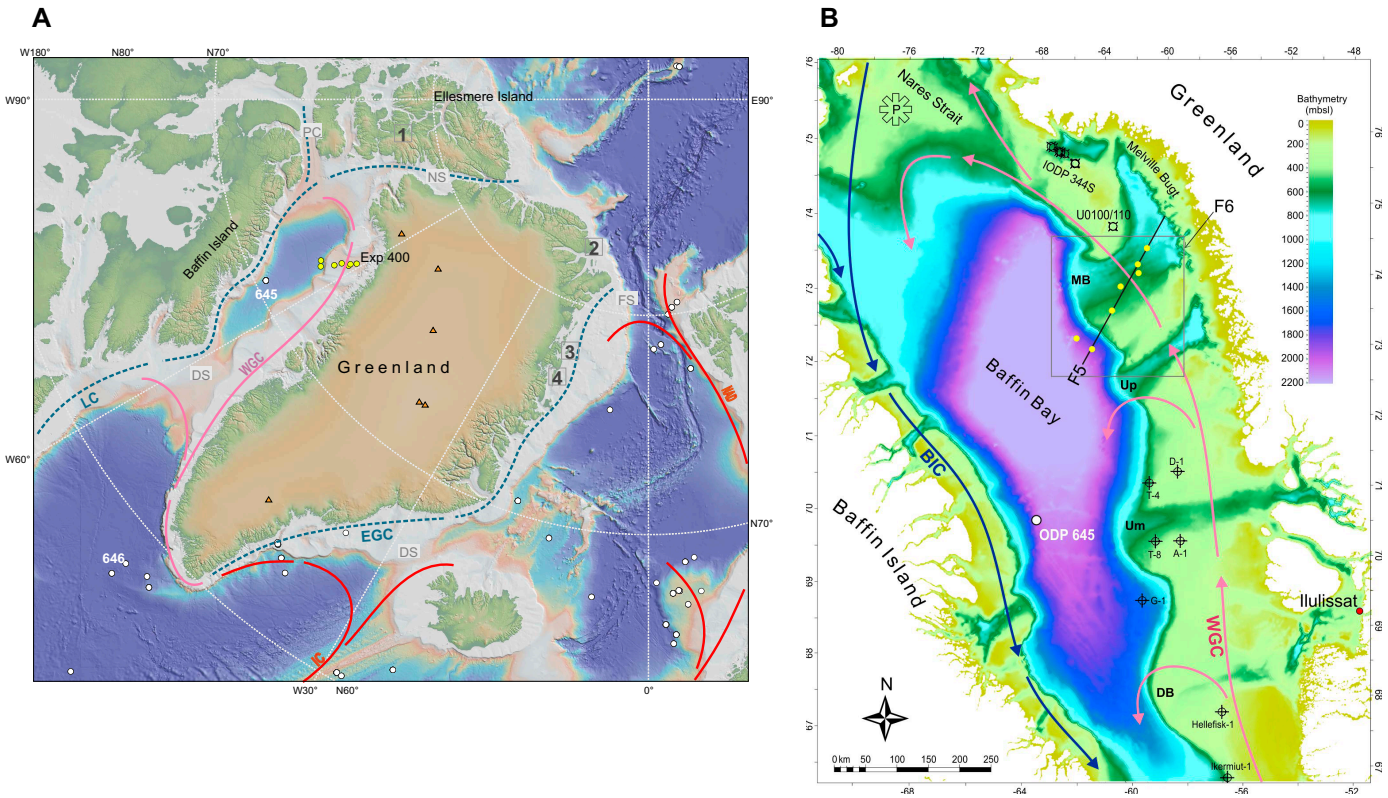

Figure F3. A. Topographic/bathymetric map showing Expedition 400 transect sites in relation to existing ODP/Integrated Ocean Drilling Program/IODP sites (solid circles) and near-surface ocean currents. LC = Labrador Current, WGC = West Greenland Current, IC = Irminger Current, EGC = East Greenland Current, NAD = North Atlantic drift. Ocean gateways surrounding Greenland: DS = Davis Strait, PC = Parry Channel, NS = Nares Strait, FS = Fram Strait, DS = Denmark Strait. Locations of high Arctic Pliocene and Early Pleistocene deposits: 1 = Beaufort Formation, high-level terrace locality on Ellesmere Island (Matthews and Ovenden, 1990; Rybczynski et al., 2013), 2 = Kap København Formation (Bennike and Böcher, 1990; Funder et al., 2001), 3 = Île de France Formation (Bennike et al., 2002), 4 = Store Koldewey Formation (Bennike et al., 2010). Greenland ice core positions (solid triangles) are also shown. The map was produced using the GMRT v4.0 mapping tool. B. Map of Baffin Bay displaying primary Expedition 400 sites along the seismic transect (Figure F5), existing ODP/Integrated Ocean Drilling Program/IODP boreholes, and exploration wells. WGC = West Greenland Current. BIC = Baffin Island Current. Inset box: detailed map in Figure F6. Star = area of the North Water Polynya. TMFs on the West Greenland margin: Melville Bugt (MB), Upernavik (Up), Uummannaq (Um) and Disko Bugt (DB). Bathymetry is based on International Bathymetric Chart of the Arctic Ocean v3 (Jakobsson et al., 2012).

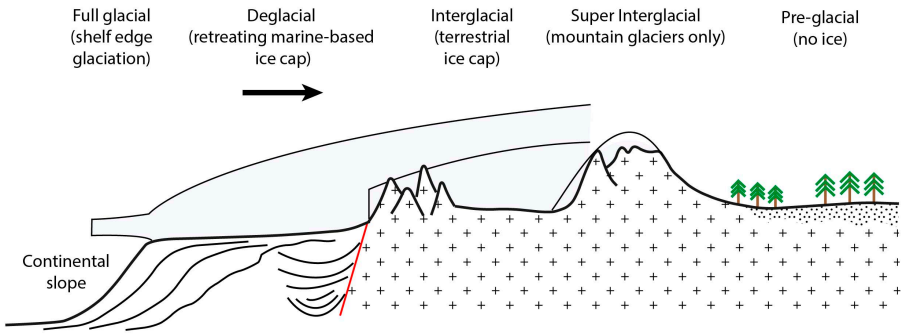

Figure F4. Five conceptual stages of GrIS configurations through the late Cenozoic (approximately the last 30 My).

3. Background

3.1. Baffin Bay hydrology

Baffin Bay is a semienclosed basin with a predominant cyclonic ocean circulation and a pronounced east–west hydrographic gradient (Figure **F3**). The Baffin Island Current transports cold, low-saline Arctic waters along the Canadian margin that exits through the western Davis Strait. In contrast, the West Greenland Current carries warmer (3°–5°C) waters derived from the North Atlantic Irminger Current. The water mass advects over the West Greenland shelf regions at water depths of 100–500 m (Bourke et al., 1989; Hamilton and Wu, 2013). Observations of the deep to intermediate circulation of Baffin Bay are sparse, but hydrographic modeling indicates a southward counter current along the West Greenland slope from 68° to 72°N at depths of 1000–1500 m (Tang et al., 2004). Deepwater formation is possibly taking place in northern Baffin Bay, associated with brine formation during sea ice formation in the North Water Polynya, south of the Nares Strait (Yao and Tang, 2003) (Figure **F3B**). The rates and processes of water-mass conversion in this area are not well understood (Bourke et al., 1989), but there is growing understanding of the role of the North Water Polynya and its influence on the interactions of northern and southern sourced water masses in the deepwater formation in Baffin Bay (Bâcle et al., 2002; Rysgaard et al., 2020).

3.2. Greenland Ice Sheet dynamics

The northwest Greenland shelf region was glaciated on multiple occasions, resulting in prominent TMFs that are the sedimentary expression of former glacial outlets of the NGrIS (Figure **F3B**). Geophysical data and shallow core studies demonstrate the presence of fast-flowing ice streams that reached the outer shelf during the Late Pleistocene (Ó Cofaigh et al., 2013; Dowdeswell et al., 2014; Slabon et al., 2016; Newton et al., 2017). The last glacial retreat from outer shelf grounding positions to fjord outlets in northwest Greenland probably occurred in discrete steps controlled by reverse bed gradients associated with shelf overdeepening (Patton et al., 2016; Newton et al., 2017) and enhanced marine ablation linked to the West Greenland Current (Jennings et al., 2017). Confluent Laurentide, Innuitian, and Greenland ice sheets blocked the Arctic–Atlantic gateways such as Parry Channel and Nares Strait (Figure **F3B**) during the Last Glacial Maximum, eliminating the inflow of Arctic waters into northern Baffin Bay and resulting in a circulation and sea ice regime much different from the modern one (Jennings et al., 2019; Jackson et al., 2021). Arctic–Atlantic gateway closures likely occurred during other glacial periods.

The ice sheets' response to major climate transitions, such as the Pleistocene terminations, is poorly known. A recent study invokes a slow interglacial response to climate forcing, suggesting that the GrIS is in disequilibrium with global warming (Yang et al., 2022). Conversely, during glacial maxima ice shelves may have developed over Baffin Bay, buttressing the ice flow and possibly stabilizing the central ice domes in Greenland (Hulbe et al., 2004; Jennings et al., 2018). Thinning and breakup of stabilizing ice shelves can be triggered by ocean forcing at the grounding line amplified by drainage of surface meltwater to the bed (Holland et al., 2008; Straneo et al., 2012; Scambos et al., 2017; Catania et al., 2020; Jennings et al., 2022). Depending on physiographic fac-

tors such as bathymetry and lateral constraints, ice retreat can be catastrophic or episodic (Alley et al., 2007, 2015; Pollard et al., 2015; Scambos et al., 2017; Hogan et al., 2020). It is important to understand the complex forcings and conditions that initiate retreat and govern the rate of retreat of a previously stable marine-terminating ice sheet to better understand the impacts of ice sheet retreat on sea level, ocean circulation, nutrients, and ecosystems (Catania et al., 2020). Reconstructions of paleo–ice sheet behavior and mass balance change broaden the scope of our understanding of the potential outcomes of continued climate warming on the GrIS.

A better understanding of the boundary conditions and forcings determining long-term ice sheet evolution requires information only attainable by offshore drilling. However, long sedimentary records specifically illuminating NGrIS history are lacking. Previous drilled sites in the North Atlantic recovered sediment shed from elevated terrains in east Greenland (Thiede et al., 2011; Reyes et al., 2014) influenced by semipermanent alpine glaciers since the Late Miocene (Bierman et al., 2016). The only deeply cored site in Baffin Bay (Site 645) was drilled during the early phase of the Ocean Drilling Program (ODP), and its contribution to understanding GrIS history is limited due to its location on the Canadian margin, poor recovery, and age uncertainties (Baldauf et al., 1989). In 2012, shallow coring was carried out in northeast Baffin Bay targeting Mesozoic rift deposits in exhumed sedimentary basins north of the Melville Bugt trough (Expedition 344S; Acton et al., 2012) (Figure **F3B**). However, two sites, U0100 and U0110, penetrated a 124 m thick interval of overcompacted, muddy diamict. Cosmogenic nuclides and other proxy data extracted from these proximal glacigenic sediments suggests that by the Early Pleistocene, a persistent yet dynamic ice sheet existed in northwest Greenland (Christ et al., 2020).

The sensitivity of the GrIS to ocean warming (Holland et al., 2008; Yin et al., 2011) emphasizes the need for high-resolution records near the major glacial outlets of eastern Baffin Bay. Important advances in drilling techniques, dating methodologies, and proxy approaches make new drilling key for advancing understanding of past GrIS dynamics and ice-ocean-climate interactions, which so far have only been addressed by seabed mapping, shallow cores (Jennings et al., 2017, 2018), and seismic stratigraphy correlated to exploration wells (Hofmann et al., 2016).

3.3. Tectonostratigraphic development

The continental margin of northwest Greenland has a complex geological and tectonic history that involves Cretaceous rift phases, extrusive volcanism, and tectonic inversion as seafloor spreading commenced in Baffin Bay. Rifting of the continental margins occurred during the Early and Late Cretaceous forming numerous sedimentary basins and elongate grabens that fringe the Baffin Bay margins (Whittaker et al., 1997; Gregersen et al., 2013; Nøhr-Hansen et al., 2021). Opening of Baffin Bay ensued from the late Paleocene through the Eocene, likely in tandem with the opening of the Labrador Sea (Chalmers et al., 1993). The separation of Greenland relative to the North American continent ceased during the early Oligocene (Chron 13) as seafloor spreading commenced along the Aegir Ridge system of the Icelandic plate boundary (Oakey and Chalmers, 2012; Gregersen et al., 2022). The geological architecture and stratigraphic knowledge of this region is mainly based on seismic and borehole data collected between 2007 and 2012 (Gregersen et al., 2013, 2016, 2022; Knutz et al., 2015, 2019, 2022). Eight seismic mega-units have been described, of which Mega-units A–E are attributed to the Cenozoic interval deposited after continental rifting ceased. The drilling targets of Expedition 400 identified along the key seismic transect cover Mega-units A–D (Figures **F5**, **F6**).

Oblique plate motions between Greenland and North America resulted in a transpressional tectonic regime (strike-slip) on the West Greenland margin, which gave rise to major basin infilling packages and deepwater fan systems guided by structural lineaments along inverted rift basins (Mega-unit E). From the middle late Oligocene through the Middle Miocene, a more passive sedimentation regime ensued with infilling of the remnant rift-basin topography (Mega-units D1 and D2) (Figure **F5**). In the Melville Bay Graben, juxtaposed to the Greenland craton, Mega-unit D2 forms a several kilometer thick succession of continuously stratified deposits that are intensely faulted, primarily as a result of marine clay compaction (Berndt et al., 2003). This package of presumably clay-rich marine sediments overlies stacked fan-type packages that are lodged against the Greenland basement, separated by a major fault. The seismic-stratigraphic division between

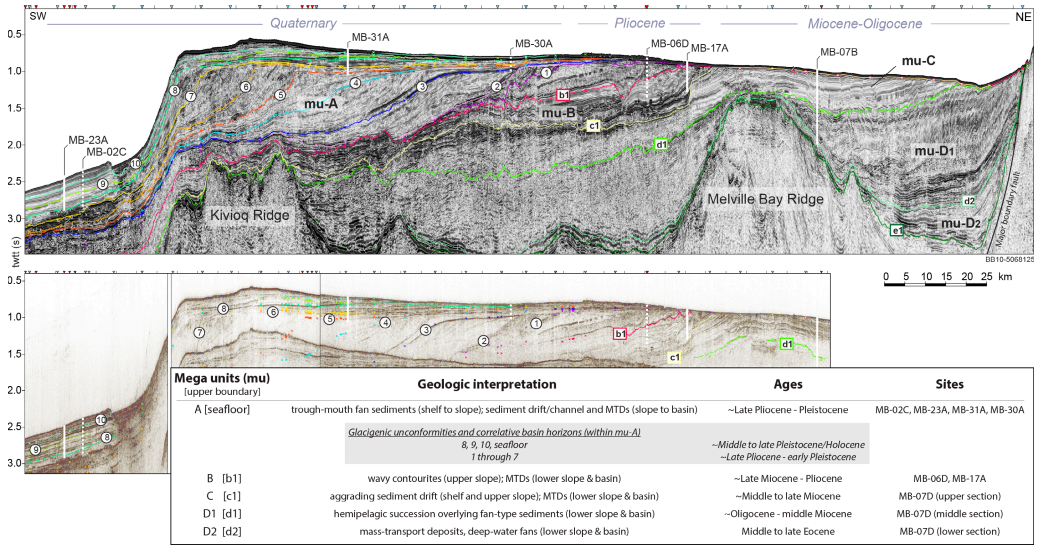

Mega units (mu) [upper boundary]	Geologic interpretation	Ages	Sites
A [seafloor]	trough-mouth fan sediments (shelf to slope); sediment drift/channel and MTDs (slope to basin)	~Late Pliocene - Pleistocene	MB-02C, MB-23A, MB-31A, MB-30A
	Glacigenic unconformities and correlative basin horizons (within mu-A) *8, 9, 10, seafloor* *1 through 7*	*~Middle to late Pleistocene/Holocene* *~Late Pliocene - early Pleistocene*	
B [b1]	wavy contourites (upper slope); MTDs (lower slope & basin)	~Late Miocene - Pliocene	MB-06D, MB-17A
C [c1]	aggrading sediment drift (shelf and upper slope); MTDs (lower slope & basin)	~Middle to late Miocene	MB-07D (upper section)
D1 [d1]	hemipelagic succession overlying fan-type sediments (lower slope & basin)	~Oligocene - middle Miocene	MB-07D (middle section)
D2 [d2]	mass-transport deposits, deep-water fans (lower slope & basin)	Middle to late Eocene	MB-07D (lower section)

Figure F5. Key seismic transect for Expedition 400 coring sites with seismic horizons and units. Top: deep seismic profile (BB10-5068125) courtesy of TGS (Knutz et al., 2019). Bottom: Stitched section of high-resolution seismic data from the LAKO19 site survey. Small triangles over the top axis = positions of crossing seismic profiles, blue = deep seismic lines, red = high-resolution seismic lines. Broken lines = sites projected onto the transect from offset positions (Figure F6). The prograding sequence (Mega-unit [mu] A) forming part of the Melville Bugt/Upernavik TMF system is dissected by 10 horizons, which, including the seabed horizon, correspond to 11 depositional units (Knutz et al., 2019). Horizons are defined by slightly dipping erosional surfaces (high-amplitude reflections in topset strata) with abrupt shelf breaks. The pre-TMF Horizons b1 (approximately Late Pliocene) and c1 (approximately Late Miocene) demarcate a package of wavy contourites formed within a major slide scar that truncates Horizon c1 (Knutz et al., 2015). Horizon d1, likely Middle Miocene in age, defines the base of a late Neogene drift prism forming part of Mega-unit C. Horizon d2 is not constrained by boreholes but is possibly late Oligocene in age. The Melville Bay and Kivioq Ridge systems represent rift-tectonic elements that were modified by compression during late Paleogene (Gregersen et al., 2013, 2016).

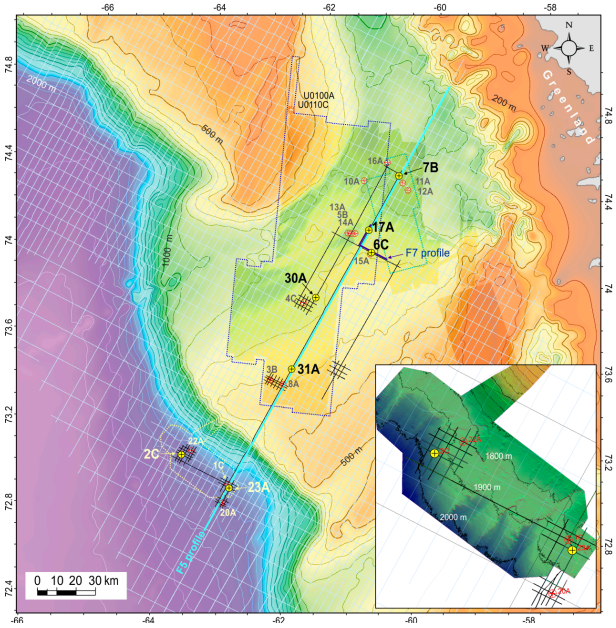

Figure F6. Map of site locations and site survey data for Expedition 400. Yellow dots = primary sites, red crosses = alternate sites. The regular 2D seismic grid (blue-gray lines) constitutes TGS Baffin Bay surveys 2007, 2008, 2009, and 2010 (minimum spacing = ~3.75 km). 3D seismic surveys Shell-ANU-3D-2012 and Cairn-PITU-3D-2011 are marked by broken line polygons (dark and light blue, respectively). High-resolution survey LAKO 2019 is indicated by thin black line grids. The detailed bathymetry on the shelf margin is based on industry multibeam data combined with the first reflection extracted from the 3D seismic data (Newton et al., 2017). Regional bathymetry is based on IBCAO v3 (Jakobsson et al., 2012) shown with 100 m contours. Inset: detail of deepwater sites capturing a sediment drift-channel system developed on the lower slope south of the Melville Bugt trough. Multibeam bathymetry data was collected by Alfred Wegener Institute (Dorschel, 2017). Position of seismic profiles shown in Figures F5 and F7 are indicated.

Mega-units D2 and C is described as the mid-Miocene Unconformity (d1) displaying erosion over structural highs and a conformable development within basin settings (e.g., Melville Bay Graben) (Figure **F5**). Mega-unit C forms an asymmetric sediment prism covering wide parts of the inner shelf in northwest Greenland, with thicknesses up to 1200 m, that is variably modified by glacial erosion. The prism is interpreted as a shelf-bound sediment drift that locally grades into clinoform features associated with prodeltaic environments (Knutz et al., 2015). The boundary between Mega-units C and B is an incised horizon (c1) that is correlated to extensive mass transport deposits on the lower slope and in the Baffin Bay basin, suggesting widespread submarine slope instability. The regional character of this erosion points to a phase of tectonic adjustment affecting the shelf margin, presumably during the Late Miocene (Knutz et al., 2015). Mega-unit B is characterized by distinct lenticular sediment bodies featuring asymmetric sediment waves that have accumulated into expanded sections over the c1 erosion scarp (Figures **F5**, **F7**). The slope component of Mega-unit B is interpreted as a contourite drift with seismic ties to nearby drilled sections suggesting a Pliocene age (Knutz et al., 2015, 2019; Aubry et al., 2021).

3.4. Melville Bugt–Upernavik trough mouth fan system

A prograded shelf package (Mega-unit A) overlying the Neogene sediment drifts reflects deposition under the influence of major ice streams originating from the northwest GrIS sector (Figures **F3**, **F5**). Eleven prograding sedimentary units have been identified, each corresponding to bundles of glacial advance cycles within a major TMF system (Knutz et al., 2019; Newton et al., 2021). The TMF units are numbered according to their top bounding horizons, except for Unit 11, which is capped by the seabed (Figure **F5**). The units are separated by glacial unconformities defining paleotrajectories of shelf break grounding zones that prograded seaward with sediment supplied by successive advances of the NGrIS onto the outer shelf and slope. Between the two, modern cross-shelf troughs (Melville Bugt and Upernavik TMFs) (Figure **F3B**), topset strata of prograding units and associated shelf breaks are extremely well preserved due to high sediment input from paleoice streams and basin subsidence over older rift structures. The Expedition 400 drilling transect was designed with the intention to extract paleoclimate information from this intertrough aggrading sediment wedge (Figure **F6**). Within the topset package, seismic reflections phase reversed from seabed onlap the glacial erosion surfaces or infill intrashelf depressions (Figures **AF3**, **AF4**). These reflections, which have stratal thicknesses of >20–30 m, may represent marine muddy sediments deposited during periods of grounding line retreat and rising sea level, interrupting the glacial advance mega-cycles. An age model for the depositional evolution of the TMF was reconstructed by correlating the seismic horizons to nearby wells/boreholes (Knutz et al., 2019). It is hypothesized that the stratal onlaps, succeeding major shifts in ice stream configuration, may have formed during periods of extreme warmth, such as super-interglacials (Figure **F1**) (Knutz et al., 2019).

Beyond the shelf break, the horizons of Mega-unit A can be traced along clinoformal reflections to the basin strata, resulting in a complete pseudo-3D mapping of the depositional units (Figure

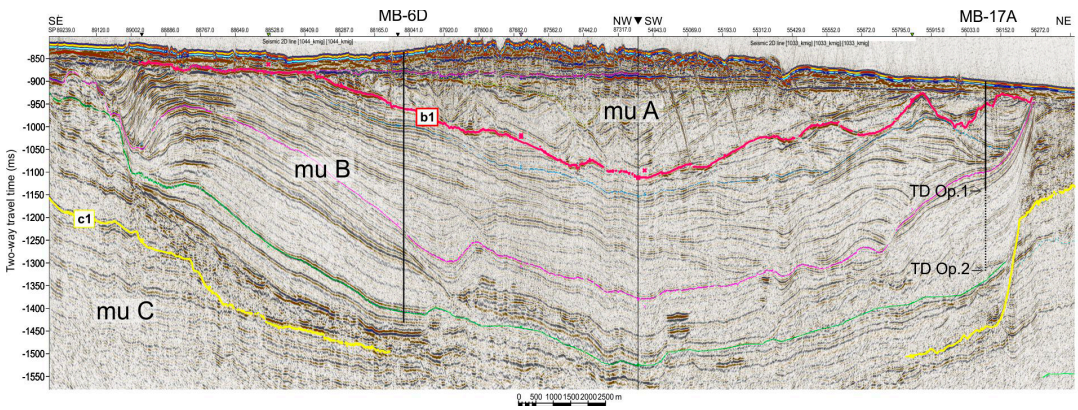

Figure F7. Composite seismic section (LAKO-1033 and 1044) showing the Mega-unit (mu) B contourite drift and Sites MB-06D and MB-17A. Position of profile shown in Figure F6. Dotted lines = internal horizons of Mega-unit B linking the two sites. MB-17A is shown with two target depth (TD) options. See Figure F5 for seismic stratigraphic legend.

F1H). The youngest depositional sequence, comprising Units 8–11, which are likely Middle to Late Pleistocene in age, form a series of contourites intersected by channel deposits on the lower slope (Figures F5, F6). Thus, drilling these contourites will allow high-resolution paleoceanographic reconstructions back to, and potentially through, the MPT.

In summary, there are several reasons for choosing northeast Baffin Bay for documenting the Cenozoic evolution of the NGrIS:

- The area covers a large TMF system primarily constructed by glacial drainage over millions of years;
- It contains a succession of gently dipping strata where a composite sequence of Oligocene–Quaternary deposits may be drilled at relatively shallow depths;
- It has extensive coverage of high-quality 2D and 3D seismic data (Figure F6) with outstanding imaging of glaciogenic sediment progradation, marine deposits formed by along-slope currents, and hemipelagic basin-infilling sediments;
- A detailed seismic stratigraphy tied to well/borehole information illuminates the sediment transport dynamics from the NGrIS (Knutz et al., 2019);
- The western Greenland margin is accessible due to amenable ocean temperatures and reduced sea ice associated with the northbound West Greenland Current (Tang et al., 2004; Holland et al., 2008).
- Expedition 344S demonstrated in 2012 that *JOIDES Resolution* can successfully operate in northeast Baffin Bay, a region that is crossed by icebergs but lacks pack ice (Acton et al., 2012).

3.5. Geophysical data

The supporting site survey data for Expedition 400 are archived at the IODP Site Survey Data Bank (**https://ssdb.iodp.org/SSDBquery/SSDBquery.php**; select P909 for proposal number).

Development of the coring plan for Expedition 400 was facilitated by an extensive seismic database (Figure F6). The core sites initially submitted for IODP drilling Proposal 909-Full1 were located using 2D seismic data, including four regional seismic surveys collected by TGS in 2007–2010. The final placement of sites (IODP drilling Proposals 909-Full2 and 909-Add) was accomplished based on (1) two 3D data volumes, Cairn-PITU-3D-2011 and Shell-ANU-3D-2012, and (2) a dedicated high-resolution seismic survey completed in 2019 as a collaboration between GEUS and Geoscience-Aarhus University using the Danish R/V *Lauge Koch* (LAKO) (Pearce and Knutz, 2019). Both 3D surveys were utilized in a compilation of seabed geomorphology (Newton et al., 2017, 2021) and geohazard assessments for further refining drill site locations (Cox et al., 2020, 2021).

The LAKO 2019 survey data provide high-resolution coverage (vertical resolution = ~4–6 m) of all primary sites and several alternate sites. The multichannel reflection seismic acquisition (15–300 Hz) was optimized to gain enhanced resolution in the uppermost 500 m of the sedimentary section, complementary to the existing industry data. A 90 cubic inch generator-injector (GI) gun was used as a seismic source configured with a 45 inch^3 main chamber and a 45 inch^3 injection chamber. Shot time was 4.0 s for most of the data, and record length varied between 2.0 and 3.5 s. Shots were recorded on a Geometrics GeoEel streamer, which included five 25 m active sections of 8 channels each (40 channels total) with a group spacing of 3.125 m. A total of 861 line kilometers was collected. Initial processing producing a migrated data version was performed on the ship. Onshore final processing included confirmation of static and delay correction, deconvolution to zero-phase data and fk filtering. The overall data quality was excellent, except some of the shelf sections marked by significant short wavelength variations due to a rough seabed (e.g., boulders, glacial scouring, and iceberg plough marks).

Swath bathymetry and high-resolution subbottom profiler (ParaSound) data were collected in 2017 (Alfred Wegener Institute; Expedition MSM66; Dorschel, 2017) over the deepwater sites on the lower slope (Figure F6). Bathymetry covering an area of 900 km^2 was acquired using a Kongsberg EM122 multibeam echosounder on the R/V *Maria S. Merian*. For converting seismic drilling targets into metric depths, the proposed sites were bundled into four groups based on similarities in the depositional setting, geological context, and general target depths. To obtain the most real-

istic time-depth conversion, all available data from the region was reviewed. Velocity information was extracted from existing industry boreholes south of the transect (e.g., Gamma-1), data gained from Expedition 344S sites north of the transect (Figure **F3B**), and an interval velocity cube derived from the Cairn-PITU-3D-2011 seismic volume. The average V_P velocities applied for each setting were 1800 m/s for the deepwater sites (proposed primary Sites MB-23A and MB-02C), 2200 m/s for the glacigenic topset strata on the shelf (proposed primary Sites MB-30A and MB-31A), 1900 m/s for the Pliocene contorite sediments (proposed primary Sites MB-06D and MB-17A), and 2050 m/s for the Miocene succession (proposed primary Site MB-07B).

4. Scientific objectives

The overall objective of Expedition 400 is to provide new insights into the long-term evolution of the NGrIS. To this end, seismic imaging from the deep basin to inner shelf has guided the selection of coring sites and stratigraphic correlation. A multiproxy diagnostic template has been developed, which in concert with a transect-drilling strategy can constrain different phases of ice extent and regional climate regimes (Figure **F8**). This template provides a methodological basis to test hypotheses that are crucial for understanding GrIS history, how the glacial margins will respond to continued warming in the near future, and how this may affect other components of the Earth system.

Subglacial topography exerts a major control on ice sheet drainage, dynamics, and the vulnerability of ice outlets to warm ocean waters (Morlighem et al., 2014, 2017). Instant removal of the ice sheet in a model exercise leaves about 22% of Greenland below sea level, although this configuration would change rapidly due to glacio-isostatic adjustment of the Earth's crust (e.g., water depths would become shallower over the central parts) (Conrad, 2013). Canyon systems that characterize the subglacial topography in Greenland, including the 750 km long, v-shaped trough that termi-

Parameter	Proxy	Full Ice	Termination	Interglacial	Super-interglacial	Pre-GrIS
		Sites MB-23A, MB-02C, MB-31A, MB-30A, MB-06D	Sites MB-23A, MB-02C, MB-31A, MB-30A, MB-06D	Sites MB-23A, MB-02C, MB-31A, MB-30A, MB-06D	Sites MB-23A, MB-02C, MB-31A, MB-30A, MB-06D	Sites MB-06D, MB-17A, MB-07B
Ice sheet configuration indicators						
Iceberg production	*IRD*	0 to ++	++++	0 to +	0	0
Land exposure	*^{10}Be*	0	0	+	++	+++
Ice cover	*^{10}Be/^{26}Al*	<7 (burial)	<7 (burial)	7	7	7
Terrigenous flux	*Volumetric sed. rate, sedimentary magnetism, NGR*	+ to ++	+++++	+	+	+ to ++
Terrestrial productivity	*Pollen, leaf waxes, DNA, fossils*	0	+	++	+++	++++
Sediment sourcing	*Elemental, magnetic, mineral, and isotopic provenance*	Glacial flowline, warm – polythermal bed	Glacial flowline, warm bed	Multiple ice-rafted sources, reworked glacial	Fluvial, reworked glacial, more local	Fluvial, basin only
Weathering intensity	*Mineralogy, grain size and texture*	0	0	+	++	++++
Glacial meltwater	*Salinity reconstructions using $\delta^{18}O$ and trace elements in foraminifera, palmitic acid δD*	0 to +	++++	++	0	0 to +
Environmental indicators						
Depositional processes (Shelf environment)	*Lithofacies description*	Tills	Glacial- marine, diamicton	Hemipelagic	Hemipelagic	Hemipelagic, contourite, deltaic
Depositional processes (Basin environment)	*Lithofacies description*	Glacial- marine, plumites/turbidites	Glacial- marine, plumites/turbidites	Hemipelagic, glacial-marine, contourite	Hemipelagic, contourite	Hemipelagic, contourite
Terrestrial climate	*Pollen, brGDGT, leaf wax δD*	Cold, dry	Transitional	Warm, wet	Warmer, wetter	Warmest, wettest
Ocean water conditions (surface/subsurface)	*Dinoflagellate, diatom and foraminifera; isoGDGTs (e.g. TEX_{86}), shell trace elements*	Cold	Cool, strongly stratified	Warm, highly seasonal	Very warm	Very warm
Sea Ice	*IRD, Dinoflagellates and diatoms; biomarkers (HBIs, e.g. IP_{25})*	+++	++ to +++	+	0-?	0-?

Figure F8. Diagnostic template for proxy interpretation. The combination of different proxy results will provide information on glacial response and paleoenvironmental settings associated with five overall stages of ice sheet configuration. Drill sites linked to each glaciation stage are shown in the second row. Environmental parameters and proxies used to measure those parameters are shown in columns to the left. Hypothesized parameter response to each glaciation stage is shown in columns to the right. IRD = ice-rafted debris, NGR = natural gamma radiation. BrGDGT = branched glycerol dialkyl glycerol tetraethers, IsoGDGTs = iso-glycerol dialkyl glycerol tetraethers, HBIs = highly branched isoprenoids. Descriptors for ice sheet configuration indicators: none (0), minor (+), moderate (++), high (+++), and very high (++++). ^{10}Be/^{26}Al values are based on Biermann et al. (2016).

nates in the Petermann Fjord system, northwest Greenland, have been thought to have a preglacial, fluvial origin (Bamber et al., 2013). Recent modeling work alternatively suggests that the deeply incised topography was generated by catastrophic outburst floods from a fluctuating GrIS (Keisling et al., 2020).

To understand the processes shaping the subglacial landscape, access to sediment archives reflecting GrIS erosion is crucial (Graly et al., 2018; Pedersen et al., 2019; Christ et al., 2020). Most of our current knowledge regarding the long-term GrIS history originates from North Atlantic core sites (Jansen et al., 2000; Thiede et al., 2011; Bierman et al., 2016). However, these records reflect discharges from eastern GrIS outlets predominantly influenced by the orogenic topography of the East Greenland Caledonides (Henriksen et al., 2009). The lack of major mountain belts in the northwest Greenland sector toward Baffin Bay means that proxy records from the adjoining margins are more directly coupled to the dynamics of the central Greenland ice dome. Glacial modeling highlights this region as being particularly sensitive to rapid mass-loss due to the concentration of glacial flow lines with gentle bed topography that reach far into the ice sheet interior (Felikson et al., 2021). Moreover, a fault-bounded lake system in the Camp Century basin reported by Paxman et al. (2021), may have been an important factor for freshwater discharges, and possibly major outbursts, into Melville Bugt. By drilling at all the proposed sites along the Melville Bugt transect we will collect sediment cores necessary to better understand NGrIS evolution, especially as it relates to the major transitions/phases that are key for understanding the late Cenozoic climate.

4.1. How did the NGrIS respond to extreme interglacial warmth?

Cosmogenic nuclides in subice bedrock show that central Greenland was almost completely deglaciated during one or more intervals over the last 2.5 My (Schaefer et al., 2016) (Figure **F1A**). The study cannot determine a unique ice cover history, but three scenarios are proposed varying from ice-free interglacials to a single 280 ky deglacial event during the Early Pleistocene, followed by ~1.1 Ma of uninterrupted ice sheet coverage. The long-term depositional record on the margin of northeast Baffin Bay contains the glaciation history needed to infer when such extreme mass loss occurred. By drilling high-accumulation sites in the basin (primary Sites MB-23A and MB-02C) and on the shelf margin (primary Sites MB-30A and MB-31A) (Figures **F5**, **F6**, **AF1**, **AF2**, **AF3**, **AF4**) targeting potential interglacial deposits, we intend to test the hypothesis that the NGrIS underwent substantial deglaciation on one or more occasions during the Pleistocene. Parameters for identifying warm interglacial periods will be derived from multiple qualitative and quantitative proxies that constrain ice sheet response and environmental conditions in both marine and terrestrial/atmospheric areas (Figure **F8**).

4.2. When did glacial inception occur in northwest Greenland, and how did the NGrIS dynamics evolve through Cenozoic climate transitions?

The relationship between long-term pCO_2 trends, temperature records, and global ice volume is poorly understood (Figure **F2**). A northwest Greenland perspective of this knowledge gap will be gained by retrieving a composite Oligocene, Miocene, and Pliocene interval covered by primary Sites MB-07B, MB-06D, and MB-17A (Figures **F3B**, **AF5**, **AF6**, **AF7**). These archives will provide information on timing, sedimentary processes, and changes in denudation rates of Greenland through periods of large atmospheric CO_2 variations (Figure **F2**). Organic components carried by these sediments in allochthonous or autochthonous fractions will provide insights into terrestrial and marine ecosystems and information on background climate states. We hypothesize that the decrease in pCO_2 from the early middle Oligocene (>600 ppm) to Early Miocene (<300 ppm) coincides with cold and possibly glacial environments in northwest Greenland. (Figure **F2**). This will be tested by recovering a 980 m long climate record from Oligocene–Miocene strata at primary Site MB-07B (Figures **F5**, **AF7**).

A complicating factor, disrupting or modulating a linear response between pCO_2 forcing and ice sheet growth/decay, may involve tectonic base-level adjustments causing snow line lowering (Foster et al., 2010) or changes in heat flux through oceanic gateways (Otto Bliesner et al., 2017).

Extensive submarine landslides into Baffin Bay associated with a late Miocene unconformity (c1) (Figure **F5**) along the northwest Greenland margin may reflect a regional tectonic adjustment apparently predating the first shelf edge advances (Knutz et al., 2015). This erosion event may be linked to hinterland uplift (Japsen et al., 2006), but a more concise understanding of its origin requires recovery of Neogene sediments. Following a full-scale glaciation, physical weathering would redistribute mass from the Greenland craton to the continental slope and consequently accelerate hinterland uplift by isostatic compensation (Berger et al., 2008; Medvedev et al., 2013), prompting the question: did active tectonics play a role in the development of the GrIS (Solgaard et al., 2013), or are the late Neogene basin adjustments along the West Greenland margin a response to mass redistribution caused by glacial erosion (Ruddiman and Kutzbach, 1989; Molnar and England, 1990; Eyles, 1996)?

The timing of the advance of marine-based glaciers onto the northwest Greenland margin is presently ambiguous. Drilling through the initial clinoforms of the first prograding unit and farther into marine contourite sediments of probable Pliocene age (primary Sites MB-06D [Figure **AF5**] and MB-17A [Figure **AF6**]) will test the hypothesis that glacial expansion of the NGrIS is linked with intensification of Northern Hemisphere glaciation (3.3–2.8 Ma).

Understanding the evolution of the NGrIS may hold the key to the origin of Northern Hemisphere glaciation, including the mechanisms of gradual amplification of glacial cycles since the late Pliocene and the shift from 40 to 100 ky cycles across the MPT (Raymo and Huybers, 2008). A major reorganization in the ice flow that drains the NGrIS apparently occurred across the MPT (Figure **F5**) (Knutz et al., 2019). Hence, both local and regional evidence suggests that major changes in the size, erosivity, and responsiveness of the GrIS occurred throughout the Pleistocene (Bierman et al., 2016; Schaefer et al., 2016). By drilling Seismic Units 7–9 at the deepwater sites (primary Sites MB-23A and MB-02C) (Figures **AF1**, **AF2**) and on the shelf (primary Site MB-30A) (Figure **AF4**), we will examine changes in NGrIS dynamics through the MPT pertaining to recent models, in particular the regolith hypothesis (Clark and Pollard, 1998).

4.3. Significance of Pliocene contourite drifts in northeast Baffin Bay

The early mid-Pliocene was characterized by relatively warm and humid forest tundra conditions in the high Arctic of Canada (Matthews and Ovenden, 1990; Fyles et al., 1994; Csank et al., 2011; Rybczynski et al., 2013) and Greenland (Bennike et al., 2002) (Figure **F3A**). A similar environment was inferred from Early Pleistocene interglacial deposits in northern Greenland (Funder et al., 2001), which is when southern Greenland appears to have been forested (de Vernal and Mudie, 1989). These warm Arctic conditions occurred under modest pCO_2 levels (~400 ppm), implying a high sensitivity of the Pliocene Arctic climate to pCO_2 or the influence of other forcing factors (Haywood et al., 2016, 2020; Feng et al., 2022). Pliocene glacial ice was likely limited to high-elevation terrains in eastern and southern Greenland, although climate models are limited by a dearth of proxy archives close to Greenland (Koenig et al., 2015). In the late Neogene, presumably the latest Miocene and Pliocene, the West Greenland/Baffin Bay margin was influenced by contour currents that deposited extensive sedimentary drifts (Knutz et al., 2015). The establishment of persistent oceanic gradients strong enough to maintain a geostrophic boundary current over millions of years is intriguing and may be linked with enhanced Pliocene Atlantic Meridional Ocean Circulation. Past configurations of Arctic gateways (e.g., Davis Strait, Nares Strait, Fram Strait, and Bering Strait) could have played a key role for poleward heat exchange during the Pliocene (Hu et al., 2015; Keisling et al., 2017); however, the tectonic history of these topographic thresholds is poorly known (Eyles, 1996; Knies et al., 2014). The contourite deposits of Mega-unit B, presently exposed at shallow depths below the glacial trough, can illuminate the environmental conditions of this paleocurrent system that appear to have existed prior to the expansion of the NGrIS.

Primary Sites MB-06D (Figure **AF5**) and MB-17A (Figure **AF6**) will provide a composite succession that can constrain Pliocene climate variability and paleotemperatures and test whether or not the high Arctic warmth of the early mid-Pliocene is associated with enhanced heat advection through Baffin Bay.

4.4. Summary of scientific objectives

1. Test the hypothesis that the NGrIS underwent significant deglaciation at intervals within the frequency range of orbital eccentricity (~100–400 ky). Pleistocene sites on the slope (primary Sites MB-23A and MB-02C; Figures **AF1**, **AF2**) and the outer shelf (primary Sites MB-31A and MB-30A; Figures **AF3**, **AF4**) are the key sites for attaining this objective.
2. Test the hypothesis that the general decrease in pCO_2 from the early middle Oligocene to the Early Miocene is linked to cold and possibly glacially dominated environments in northwest Greenland. Primary Site MB-07B (Figure **AF7**) on the middle shelf addresses this objective.
3. Provide information on the timing, sedimentary processes, sediment sources, and Greenland exposure history in the context of late Neogene tectonic adjustments inferred from the seismic record. Pliocene drill sites on the middle shelf (primary Sites MB-06D and MB-17A; Figures **AF5**, **AF6**) and Oligocene to Miocene primary Site MB-07B (Figure **AF7**) on the middle shelf will address this objective.
4. Test the hypothesis that major glacial expansion of the NGrIS is linked with intensification of Northern Hemisphere glaciation (3.3–2.8 Ma). Pliocene drill sites on the middle shelf (primary Sites MB-06D and MB-17A; Figures **AF5**, **AF6**) will address this objective.
5. Assess recent models for the change in orbital cycles through the MPT by analyzing sediment maturity and regolith history. Pleistocene sites on the slope (primary Sites MB-23A and MB-02C; Figures **AF1**, **AF2**) and the outer shelf (primary Sites MB-31A and MB-30A; Figures **AF3**, **AF4**) are the key sites for attaining this objective.
6. Investigate whether high Arctic warmth of the early mid-Pliocene is related to heat advection through the western North Atlantic Ocean and Baffin Bay. Pliocene drill sites on the middle shelf (primary Sites MB-06D and MB-17A; Figures **AF5**, **AF6**) will address this objective.

5. Operations plan/coring strategy

Expedition 400 will include coring and logging along a transect of sites representing the late Cenozoic era from the Oligocene/Early Miocene to Holocene (Figures **F5**, **F6**, **F7**). The primary drill sites, alternate sites, and drilling and coring strategy for each are described below (Tables **T1**, **T2**). Wireline logging will be conducted following coring if hole conditions permit (see **Wireline logging/Downhole measurements strategy**). The general operational plan is to proceed with drilling along the transect in a sequence that prioritizes the primary and alternate sites, generally going from younger to older strata. However, iceberg conditions may require changes to this prioritization that will have to be decided at sea.

5.1. Drill sites

5.1.1. Middle to Late Pleistocene sites on the lower slope

The two lower slope sites in deep water off Melville Bugt are primary Sites MB-23A and MB-02C (Figure **F6**). These sites are expected to recover high-resolution paleoceanographic records of an Early/Middle to Late Pleistocene (up to 1 My) sediment drift system corresponding to the most recent part of the TMF history (Scientific Objectives 1 and 5).

Primary Site MB-23A (Figure **AF1**) is located on the lower slope below the Melville Bugt TMF at a water depth of 1832 m (Figures **F5**, **F6**; Table **T1**). This site is expected to recover mud with scattered dropstones. It is located 0.45 km from the nearest crossing point to avoid disturbances seen at the edge of the channel. This site targets expanded intervals of Seismic Units 9–11. Site MB-23A overlaps stratigraphically with the strata that will be drilled at primary Site MB-02C (Figure **AF2**).

Planned drilling at primary Site MB-23A includes coring from the seafloor to 250 meters below seafloor (mbsf) with the advanced piston corer (APC) system in two holes. A third hole will be cored from the seafloor to 422 mbsf with the APC and extended core barrel (XCB) systems. The third hole will be logged. Two alternate sites for Site MB-23A, proposed Sites MB-01C and MB-20A, have been identified to achieve the key scientific objectives if operations at Site MB-23A are unsuccessful or are not possible (Table **T2**; Figures **AF8**, **AF9**). The drilling and logging strategy for these alternate sites is the same as for the primary site.

Primary Site MB-02C is located on the lower slope below the Melville Bugt TMF at a water depth of 1957 m (Figure **F6**; Table **T1**). It is expected to recover silty-sandy muds, presumably of Early/Middle to Late Pleistocene age. Site MB-02C (Figure **AF2**) targets an expanded interval of Seismic Unit 8, which underlies Unit 9 and is not well represented at Site MB-23A.

Planned drilling at primary Site MB-02C includes coring from the seafloor to 522 mbsf in two holes with the APC and XCB systems; logging is planned for the second hole (Figure **F9**). One

Site	Location (latitude, longitude)	Seafloor depth (mbrf)	Operations description	Transit (days)	Drilling/ Coring (days)	Logging (days)
St John's			Begin expedition 5.0	Port call days		
			Transit ~1553 nmi to MB-23A @ 10.5 kt	6.2		
MB-23A	72°59.0400'N	1832	Hole A - APC/HLAPC to 250 mbsf	0.0	1.8	0.0
EPSP	62°58.8300'W		Hole B - APC/HLAPC to 250 mbsf	0.0	1.3	0.0
to 422 mbsf			Hole C - APC/XCB to 422 mbsf - Log with triple combo, FMS-sonic, and VSI	0.0	2.2	1.3
			Subtotal days on site: 6.6			
			Transit ~16 nmi to MB-02C @ 10.5 kt	0.1		
MB-02C	73°6.9000'N	1968	Hole A - APC/XCB to 522 mbsf	0.0	3.0	0.0
EPSP	63°47.4240'W		Hole B - APC/XCB to 522 mbsf - Log with triple combo, FMS-sonic, and VSI	0.0	2.7	1.4
to 522 mbsf						
			Subtotal days on site: 7.2			
			Transit ~39 nmi to MB-31A @ 10.5 kt	0.2		
MB-31A	73°33.6420'N	542	Hole A - RCB to 282 mbsf - Log with triple combo, FMS-sonic, and VSI	0.0	1.3	1.0
EPSP	62°9.0720'W		Hole B - Drill ahead to 70 mbsf - APC/HLAPC/XCB to 282 mbsf	0.0	1.3	0.0
to 282 mbsf						
			Subtotal days on site: 3.6			
			Transit ~21 nmi to MB-30A @ 10.5 kt	0.1		
MB-30A	73°54.0780'N	629	Hole A - RCB to 303 mbsf - Log with triple combo and FMS-sonic	0.0	1.3	0.9
EPSP	61°51.2400'W		Hole B - Drill ahead to 100 mbsf - APC/HLAPC/XCB to 303 mbsf	0.0	1.3	0.0
to 303 mbsf						
			Subtotal days on site: 2.4			
			Transit ~20 nmi to MB-06D @ 10.5 kt	0.1		
MB-06D	74°7.6980'N	625	Hole A - RCB to 561 mbsf - Log with triple combo, FMS-sonic, and VSI	0.0	2.5	1.4
EPSP	60°58.4640'W		Hole B - RCB to 400 mbsf	0.0	2.0	0.0
to 561 mbsf						
			Subtotal days on site: 5.9			
			Transit ~6 nmi to MB-17A @ 10.5 kt	0.0		
MB-17A	74°13.9380'N	666	Hole A - RCB to 411 mbsf - Log with triple combo and FMS-sonic	0.0	1.9	1.0
EPSP	61°2.2440'W					
to 411 mbsf						
			Subtotal days on site: 3.1			
			Transit ~17 nmi to MB-07B @ 10.5 kt	0.1		
MB-07B	74°29.5500'N	747	Hole A - RCB to 620 mbsf - Log with triple combo, FMS-sonic, and VSI	0.0	2.8	1.4
EPSP	60°34.9920'W		Hole B - HRT reentry system to 600 mbsf	0.0	2.7	0.0
to 978 mbsf			Hole B - RCB to 978 mbsf - Log with triple combo, FMS-sonic, and VSI	0.0	2.8	1.3
			Subtotal days on site: 11.0			
			Transit ~1631 nmi to St John's @ 10.5 kt	6.5		
St John's			End expedition	13.1	30.9	9.7

Port call days:	5.0	Total operating days:	53.7
Subtotal days on site:	40.6	Total expedition days:	58.7

Table T1. Operations and time estimates for primary sites, Expedition 400. EPSP = Environmental Protection and Safety Panel.

Site	Location (latitude, longitude)	Seafloor depth (mbrf)	Operations description	Drilling/ Coring (days)	Logging (days)
MB-01C	73°0.0060'N	1820	Hole A - APC/HLAPC to 250 mbsf	1.4	0.0
EPSP	63°0.3900'W		Hole B - APC/HLAPC to 250 mbsf	1.1	0.0
to 473 mbsf			Hole C - APC/XCB to 473 mbsf - Log with triple combo, FMS-sonic, and VSI	2.2	1.2
			Subtotal days on site: 6.1		
MB-20A	72°54.7080'N	1939	Hole A - APC/HLAPC to 250 mbsf	1.5	0.0
EPSP	63°3.8520'W		Hole B - APC/HLAPC to 250 mbsf	1.1	0.0
to 450 mbsf			Hole C - APC/XCB to 450 mbsf - Log with triple combo, FMS-sonic, and VSI	2.1	1.2
			Subtotal days on site: 5.9		
MB-22A	73°8.3280'N	1861	Hole A - APC/HLAPC to 250 mbsf	1.4	0.0
EPSP	63°38.4120'W		Hole B - APC/XCB to 611 mbsf - Log with triple combo, FMS-sonic, and VSI	3.1	1.1
to 611 mbsf					
			Subtotal days on site: 5.6		
MB-08A	73°29.2200'N	508	Hole A - RCB to 370 mbsf - Log with triple combo, FMS-sonic, and VSI	1.7	1.1
EPSP	62°16.0920'W		Hole B - Drill ahead to 70 mbsf - APC/HLAPC/XCB to 370 mbsf	1.6	0.0
to 370 mbsf					
			Subtotal days on site: 4.4		
MB-03B	73°30.1920'N	509	Hole A - RCB to 375 mbsf - Log with triple combo, FMS-sonic, and VSI	1.7	1.1
EPSP	62°29.1660'W		Hole B - Drill ahead to 70 mbsf - APC/HLAPC/XCB to 375 mbsf	1.6	0.0
to 375 mbsf					
			Subtotal days on site: 4.4		
MB-04C	73°52.4040'N	639	Hole A - RCB to 305 mbsf - Log with triple combo and FMS-sonic	1.4	0.9
EPSP	62°3.1680'W				
to 305 mbsf					
			Subtotal days on site: 2.3		
MB-15A	74°7.3020'N	616	Hole A - RCB to 582 mbsf - Log with triple combo, FMS-sonic, and VSI	2.6	1.4
EPSP	60°59.4540'W		Hole B - RCB to 400 mbsf	2.0	0.0
to 648 mbsf					
			Subtotal days on site: 6.0		
MB-05B	74°12.6960'N	715	Hole A - RCB to 520 mbsf - Log with triple combo and FMS-sonic	2.5	1.1
EPSP	61°20.3830'W				
to 520 mbsf					
			Subtotal days on site: 3.6		
MB-13A	74°12.7080'N	718	Hole A - RCB to 540 mbsf - Log with triple combo and FMS-sonic	2.6	1.1
EPSP	61°23.7480'W				
to 540 mbsf					
			Subtotal days on site: 3.7		
MB-14A	74°12.6540'N	674	Hole A - RCB to 510 mbsf - Log with triple combo and FMS-sonic	2.3	1.1
EPSP	61°16.2240'W				
to 510 mbsf					
			Subtotal days on site: 3.4		
MB-16A	74°33.0420'N	745	Hole A - RCB to 630 mbsf - Log with triple combo, FMS-sonic, and VSI	2.9	1.4
EPSP	60°47.9400'W		Hole B - HRT reentry system to 600 mbsf	2.7	0.0
to 1089 mbsf			Hole B - RCB to 1080 mbsf - Log with triple combo, FMS-sonic, and VSI	3.5	1.4
			Subtotal days on site: 11.8		
MB-11A	74°25.6980'N	758	Hole A - RCB to 630 mbsf - Log with triple combo, FMS-sonic, and VSI	2.9	1.4
EPSP	60°24.5160'W		Hole B - HRT reentry system to 600 mbsf	2.7	0.0
to 1200 mbsf			Hole B - RCB to 1015 mbsf - Log with triple combo, FMS-sonic, and VSI	3.0	1.3
			Subtotal days on site: 11.3		
MB-12A	74°27.5820'N	750	Hole A - RCB to 630 mbsf - Log with triple combo, FMS-sonic, and VSI	2.9	1.4
EPSP	60°30.2940'W		Hole B - HRT reentry system to 600 mbsf	2.7	0.0
to 1186 mbsf			Hole B - RCB to 971 mbsf - Log with triple combo, FMS-sonic, and VSI	2.7	1.3
			Subtotal days on site: 11.0		
MB-10A	74°27.5040'N	709	Hole A - RCB to 630 mbsf - Log with triple combo, FMS-sonic, and VSI	2.9	1.4
EPSP	61°10.7520'W		Hole B - HRT reentry system to 600 mbsf	2.7	0.0
to 1288 mbsf			Hole B - RCB to 1200 mbsf - Log with triple combo, FMS-sonic, and VSI	4.2	1.5
			Subtotal days on site: 12.7		

Table T2. Operations and time estimates for alternate sites, Expedition 400. EPSP = Environmental Protection and Safety Panel.

alternate site for Site MB-02C, proposed Site MB-22A (Figure **AF10**), has been identified to achieve the key scientific objectives in the event that operations at Site MB-02C are unsuccessful or are not possible (Table **T2**). The drilling and logging strategy for the alternate site is the same as that planned for the primary site.

5.1.2. Pleistocene sites on the outer shelf

Two outer shelf sites are primary Sites MB-31A and MB-30A. The overall goal at these sites is to recover the deglacial and interglacial intervals of potentially early mid-Pleistocene age within the top-set strata of the TMF. Both sites are high priorities for Scientific Objectives 1 and 5.

Primary Site MB-31A is located on the outer shelf margin of the Melville Bugt TMF at a water depth of 531 m (Figure **F6**; Table **T1**). This site penetrates a package of flat-lying, semicontinuous reflections that onlap glacial unconformities in Seismic Units 6–8 (Figure **AF3**). The expected lithologies are proximal ice contact and glaciomarine sediments (e.g., diamicton with intercalated pebbly mud and hemipelagic mud).

Planned drilling at primary Site MB-31A includes rotary core barrel (RCB) system coring from the seafloor to 282 mbsf in the first hole. A second hole will include drilling ahead to 70 mbsf, followed by APC/XCB system coring to 282 mbsf. Logging is planned for the second hole. Recovery and lithologies of the first hole will guide adaptations of the drilling strategy in the second hole (Figure **F9**).

Two alternate sites have been selected for primary Site MB-31A (proposed Sites MB-08A and MB-03B; Figures **AF11**, **AF12**) to achieve the key scientific objectives in the event that operations at Site MB-31B are unsuccessful or are not possible (Table **T2**). The drilling and logging strategy for the alternate sites is the same as that planned for the primary site.

Primary Site MB-30A is located northeast of primary Site MB-31A on the outer shelf margin of the Melville Bugt TMF at a water depth of 618 m (Figure **F6**). Site MB-30A (Figure **AF4**) targets a package of flat-lying, continuous reflections that onlap a major glacial unconformity (Seismic Unit

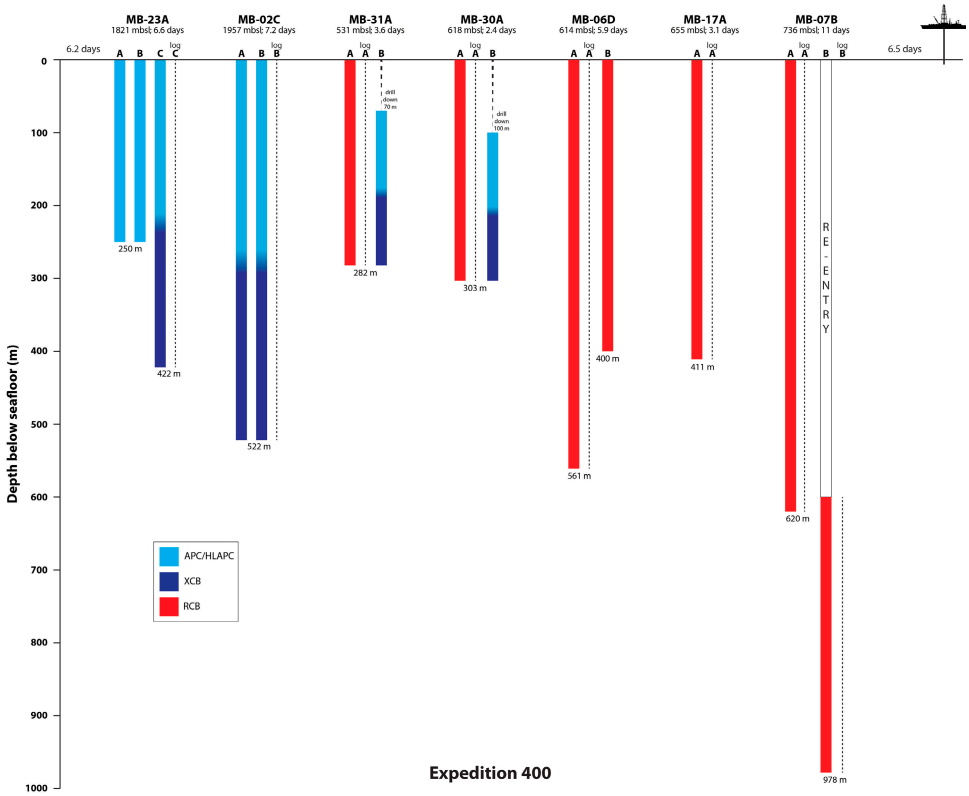

Figure F9. Coring operations plan, including type of coring, target depth, and estimated days on site for Expedition 400.

3). The site is placed to achieve optimal recovery of Seismic Units 3 and 4 of possible Early Pleistocene age. The expected lithologies are proximal ice contact and glaciomarine sediments (e.g., diamicton with intercalated pebbly mud and hemipelagic mud).

Planned drilling at primary Site MB-30A includes RCB coring to 303 mbsf in the first hole (Figure **F9**). Logging is planned for the first hole. The second hole includes drilling ahead to 100 m followed by APC/XCB system coring to 303 mbsf. The recovery and lithologies of the first hole will guide adaptations of the drilling and logging strategy in the second hole.

One alternate site (proposed Site MB-04C) (Figure **AF13**) has been selected for primary Site MB-30A to achieve the key scientific objectives if operations at Site MB-30A are unsuccessful or are not possible (Table **T2**). The drilling strategy for the alternate sites is the same as that planned for the primary site.

5.1.3. Pliocene sites on the middle shelf

Two middle shelf sites, primary Sites MB-06D and MB-17A, will sample a buried Neogene contourite system with the overall goal of studying Greenland climate and ocean circulation during the Pliocene, prior to major basinward expansion of the GrIS. The middle shelf Pliocene sites address Scientific Objectives 3, 4, and 6.

Primary Site MB-06D is located on the middle shelf at a water depth of 614 m (Figure **F6**; Table **T1**). The site overlaps stratigraphically with the lowermost section that will be drilled at primary Site MB-17A. The main target is an expanded section of a mounded contourite drift that may contain a high-resolution Pliocene record of Mega-unit B (Figure **AF5**). The expected lithologies are diamicton and mudstone with silty-sandy intervals such as would be expected in proglacial settings and from nearshore to deep marine environments.

Planned drilling at primary Site MB-06D includes RCB coring to 561 mbsf in the first hole and RCB coring to 400 mbsf in the second hole (Figure **F9**).

One alternate site, proposed Site MB-15A (Figure **AF14**), has been selected to achieve the key scientific objectives in the event that operations at the primary site are unsuccessful or are not possible (Table **T2**). The drilling strategy for the alternate site is a single hole with RCB coring and logging to 582 mbsf.

Primary Site MB-17A (Figure **AF6**) is located on the middle shelf at a water depth of 655 m (Figure **F6**; Table **T1**). There are two goals for this site: (1) capture deposits corresponding to the earliest shelf-based glaciations in northwest Greenland (earliest glacial clinoforms of Mega-unit A) and (2) recover Neogene sediments of likely Early Pliocene age in Mega-unit B that can elucidate paleoceanographic conditions prior to the major expansion of the GrIS (Late Pliocene and Early Pleistocene) (Scientific Objectives 3, 4, and 6). Site MB-17A targets an interval that is stratigraphically younger interval than that targeted at primary Site MB-06D. The expected lithologies are diamicton and mudstone with silty-sandy intervals such as would be expected in proglacial settings and from nearshore to deep marine environments.

Planned drilling at primary Site MB-17A involves RCB coring and logging to 411 mbsf in a single hole (Figure **F9**). Three alternate sites have been selected to achieve the key scientific objectives in the event that operations at the primary site are unsuccessful or are not possible: proposed Sites MB-05B, MB-13A, and MB-14A (Figures **AF15**, **AF16**, **AF17**). The coring and logging strategies at the alternate sites emulate those for primary Site MB-17A, with RCB coring and logging at a single hole.

5.1.4. Late Oligocene and Miocene sites on the middle shelf

Primary Site MB-07B is located at a water depth of 736 m on the middle shelf landward of the Melville Bay Ridge (Figure **F6**). The targeted section includes Mega-units C and D of potentially Late and Middle Miocene age overlying a sedimentary wedge of possible Oligocene age, with a sequence potentially representing 6–30 My (Figures **F5**, **AF7**). The goal is to elucidate past ocean and terrestrial climates in northeast Baffin Bay/Greenland and the onset of ephemeral glaciation in northwest Greenland to satisfy Scientific Objectives 2 and 3. Expected lithology is claystone

with silty to sandy intervals and siliceous ooze, consistent with predicted hemipelagic marine environments.

Planned drilling at Site MB-07B involves RCB coring and logging in the first hole to 620 mbsf (Figure **F9**). The second hole will then begin with the installation of a hydraulic release tool (HRT) reentry system with 600 m of casing. The hole will then be RCB cored from 600 to 978 mbsf and logged (Figure **F9**). Four alternate sites have been selected to achieve the key scientific objectives if operations at the primary site are unsuccessful or are not possible: proposed Sites MB-16A, MB-11A, MB-12A, and MB-10A (Figures **AF18**, **AF19**, **AF20**, **AF21**).

6. Wireline logging/Downhole measurements strategy

As part of APC/half-length APC (HLAPC) coring, formation temperature measurements will be made using the advanced piston corer temperature (APCT-3) tool. If time, sea state, and hole conditions permit, we also anticipate conducting temperature measurements with the Sediment Temperature 2 (SET2) tool during RCB coring of primary Sites MB-02C, MB-06D, and MB-07B.

Planned wireline logging includes the triple combo, Formation MicroScanner (FMS), and FMS-sonic tool strings at all sites (Table **T1**). Additionally, use of the Versatile Seismic Imager (VSI) is planned for primary Sites MB-23A, MB-02C, MB-31A, MB-06D, and MB-07B. The triple combo tool string measures density, natural gamma radiation (NGR), porosity, and resistivity along with borehole diameter (caliper log).

Because variable recovery rates are expected (>80% in hemipelagic and contourite drift sediments and <50% for the sites in the aggradational shelf wedge), the downhole logging data, in conjunction with physical properties measured on the cores, will be important for determining boundaries of lithologic units and to capture the lithologic signature of the entire succession. The FMS image tool should provide a more complete understanding of drilled intervals with poor recovery. VSI calibration and generation of synthetic seismograms will facilitate core-to-seismic integration. For more information on the wireline logging tools see: **http://iodp.tamu.edu/tools** and **http://iodp.tamu.edu/tools/logging**.

7. Risks and contingency

The area of operation (Baffin Bay) involves several risks. Potential hazards may arise from ice conditions, shallow gas, or technical problems. Hence, flexibility will be required and drilling operations will need to move forward as dictated by the drilled material and the potential hazards. Drilling operations could shift between primary and alternate sites; however, due to the generally close proximity of all sites there is no contingency for an alternate region of operations. There are currently ~2 days of contingency time included in the operations plan.

7.1. Ice conditions

Icebergs pose an additional threat to drilling operations, and *JOIDES Resolution* will have to move off site if an iceberg approaches too close to a site location during operations. In these instances, we will have a free-fall funnel (FFF) ready to deploy that would allow for hole reentry after the iceberg passes. Icebergs will be monitored visually by radar and where possible by satellite images.

7.2. Shallow gas

From the wealth of industry seismic data collected in Melville Bay, it is obvious that the margin has been regarded as a potential petroliferous region. The main lithologies expected are (1) hemipelagic and distal glacial-marine muds with thin interbedded sand layers, mainly of turbiditic origin, (2) proximal glacigenic sediments interbedded with intervals of marine/glacial-marine muddy deposits, and (3) thick mudstone-siltstone successions with fine sandy intervals. None of the sites involve drilling into older strata that may have petroleum potential or structural elements (closures or faults), and the density of data means that high-amplitude anomalies and chimney fea-

tures can be avoided. As further mitigation of drilling hazards, a gas anomaly study was carried out based on the 3D seismic volumes (Cox et al., 2020), and the information was used in the final round of site selection (IODP drilling Proposals 909-Full2 and 909-Add).

During Expedition 344S, where Mesozoic shales presented key drilling targets hydrocarbon gases were closely monitored by application of gas chromatography at least once for every core using two sampling techniques: headspace (HS) sampling and gas void (VAC) sampling. Based on the results from Site U0110, methane levels of up to 5000 ppmv may be expected in the Quaternary, although this is probably a high estimate because this site was located directly over the Melville Bay Ridge structure.

For each core, headspace gas will be monitored following established protocols. See **https://wiki.iodp.tamu.edu/display/LMUG/Chemistry#Chemistry-SafetyMonitoring** and **https://www.iodp.org/top-resources/program-documents/policies-and-guidelines/1178-epsp-safety-review-report-guidelines-may-2022/file** for details.

7.3. Coring/logging and operational risks

The proposed penetration depth at primary Site MB-07B (and some alternate sites) presents several challenges. Hole stability is always a risk during coring operations, and the risk increases with time. Casing (especially over intervals of unconsolidated sediment) is an effective method to mitigate this risk and will be employed at Site MB-07B with an HRT reentry system to 600 mbsf.

A stuck drill string is always a risk during coring operations and can consume expedition time while attempting to free the stuck drill string. This can result in the complete loss of the hole, equipment, and time while starting a new hole. *JOIDES Resolution* carries sufficient spare drilling equipment to enable the continuation of coring, but the time lost to the expedition can be significant.

Ice-rafted debris and dropstones may occur in the sedimentary sequences targeted for Expedition 400. This material can be particularly difficult to core with the APC/HLAPC systems, and depending on clast size and frequency it can also present challenges to XCB and RCB coring.

8. Sampling and data sharing strategy

Shipboard and shore-based researchers should refer to the IODP Sample, Data, and Obligations Policy and Implementation Guidelines posted on the Web at **http://www.iodp.org/top-resources/program-documents/policies-and-guidelines**. This document outlines the policy for distributing IODP samples and data to research scientists, curators, and educators. The document also defines the obligations that sample and data recipients incur. The Sample Allocation Committee (SAC; composed of Co-Chief Scientists, Staff Scientist, and IODP Curator on shore and curatorial representative on board the ship) will work with the entire scientific party to formulate a formal expedition-specific sampling plan for shipboard and postcruise sampling.

Shipboard scientists are expected to submit sample requests (at **http://iodp.tamu.edu/curation/samples.html**) ~6 months before the beginning of the expedition. Based on sample requests (shore based and shipboard) submitted by this deadline, the SAC will prepare a tentative sampling plan, which will be revised on the ship as dictated by core recovery and cruise objectives. The sampling plan will be subject to modification depending upon the actual material recovered and collaborations that may evolve between scientists during the expedition. Modification of the strategy during the expedition must be approved by the Co-Chief Scientists, Staff Scientist, and curatorial representative on board the ship.

The minimum permanent archive will be the standard archive half of each core. All sample frequencies and sizes must be justified on a scientific basis and will depend on core recovery, the full spectrum of other requests, and the cruise objectives. Some redundancy of measurement is unavoidable, but minimizing the duplication of measurements among the shipboard party and identified shore-based collaborators will be a factor in evaluating sample requests.

If some critical intervals are recovered, there may be considerable demand for samples from a limited amount of cored material. These intervals may require special handling, a higher sampling density, reduced sample size, or continuous core sampling by a single investigator. A sampling plan coordinated by the SAC may be required before critical intervals are sampled.

Shipboard sampling will be generally restricted to those required for shipboard measurements; any samples that are ephemeral; and possibly limited, low-resolution samples for personal research that are required to define plans for the postexpedition sampling meeting. Whole-round samples may be taken for, but not limited to, interstitial water measurements, microbiology, and petrophysical measurements as dictated by the primary expedition objectives, approved research plans, and the shipboard sampling plan that must be finalized during the first few days of the expedition. Nearly all sampling for postexpedition research will be postponed until a shore-based sampling meeting that will be implemented ~3–5 months after the end of Expedition 400.

9. Expedition scientists and scientific participants

The current list of participants for Expedition 400 can be found at **http://iodp.tamu.edu/scienceops/expeditions/nw_greenland_glaciated_margin.html**.

References

Abe-Ouchi, A., Saito, F., Kawamura, K., Raymo, M.E., Okuno, J.i., Takahashi, K., and Blatter, H., 2013. Insolation-driven 100,000-year glacial cycles and hysteresis of ice-sheet volume. Nature, 500(7461):190–193. **https://doi.org/10.1038/nature12374**

Acton, G., and the Expedition 344S Scientists, 2012. Proceedings of the Baffin Bay Scientific Coring Program: The Hague, Netherlands (Shell).

Aksu, A.E., 1983. Holocene and Pleistocene dissolution cycles in deep-sea cores of Baffin Bay and Davis Strait: Palaeoceano-graphic implications. Marine Geology, 53(4):331–348. **https://doi.org/10.1016/0025-3227(83)90049-X**

Alley, R.B., Anandakrishnan, S., Christianson, K., Horgan, H.J., Muto, A., Parizek, B.R., Pollard, D., and Walker, R.T., 2015. Oceanic forcing of ice-sheet retreat: West Antarctica and more. Annual Review of Earth and Planetary Sciences, 43(1):207–231. **https://doi.org/10.1146/annurev-earth-060614-105344**

Alley, R.B., Anandakrishnan, S., Dupont, T.K., Parizek, B.R., and Pollard, D., 2007. Effect of sedimentation on ice-sheet grounding-line stability. Science, 315(5820):1838–1841. **https://doi.org/10.1016/B978-0-12-817129-5.00009-3**

Alley, R.B., Andrews, J.T., Brigham-Grette, J., Clarke, G.K.C., Cuffey, K.M., Fitzpatrick, J.J., Funder, S., Marshall, S.J., Miller, G.H., Mitrovica, J.X., Muhs, D.R., Otto-Bliesner, B.L., Polyak, L., and White, J.W.C., 2010. History of the Greenland Ice Sheet: paleoclimatic insights. Quaternary Science Reviews, 29(15–16):1728–1756. **https://doi.org/10.1016/j.quascirev.2010.02.007**

Aubry, A.M.R., de Vernal, A., and Knutz, P.C., 2021. Baffin Bay late Neogene palynostratigraphy at Ocean Drilling Program Site 645. Canadian Journal of Earth Sciences, 58(1):67–83. **https://doi.org/10.1139/cjes-2019-0227**

Bâcle, J., Carmack, E.C., and Ingram, R.G., 2002. Water column structure and circulation under the North Water during spring transition: April–July 1998. Deep Sea Research, Part II: Topical Studies in Oceanography, 49(22):4907–4925. **https://doi.org/10.1016/S0967-0645(02)00170-4**

Badger, M.P.S., Lear, C.H., Pancost, R.D., Foster, G.L., Bailey, T.R., Leng, M.J., and Abels, H.A., 2013. CO_2 drawdown following the Middle Miocene expansion of the Antarctic Ice Sheet. Paleoceanography, 28(1):42–53. **https://doi.org/10.1002/palo.20015**

Baldauf, J.G., Clement, B.M., Aksu, A.E., de Vernal, A., Firth, J.V., Hall, F.R., Head, M.J., Jarrard, R.D., Kaminski, M.A., Lazarus, D., Monjanel, A.-L., Berggren, W.A., Gradstein, F.M., Knüttel, S., Mudie, P.J., and Russell, M.D., Jr., 1989. Magnetostratigraphic and biostratigraphic synthesis of Ocean Drilling Program Leg 105: Labrador Sea and Baffin Bay. In Srivastava, S.P., Arthur, M., Clement, B., et al., Proceedings of the Ocean Drilling Program, Scientific Results, 105: College Station, TX (Ocean Drilling Program), 935–956. **https://doi.org/10.2973/odp.proc.sr.105.165.1989**

Bamber, J.L., Griggs, J.A., Hurkmans, R.T.W.L., Dowdeswell, J.A., Gogineni, S.P., Howat, I., Mouginot, J., Paden, J., Palmer, S., Rignot, E., and Steinhage, D., 2013. A new bed elevation dataset for Greenland. The Cryosphere, 7(2):499–510. **https://doi.org/10.5194/tc-7-499-2013**

Bennike, O., Abrahamsen, N., Bak, M., Israelson, C., Konradi, P., Matthiessen, J., and Witkowski, A., 2002. A multiproxy study of Pliocene sediments from Île de France, North-East Greenland. Palaeogeography, Palaeoclimatology, Palaeoecology, 186(1–2):1–23. **https://doi.org/10.1016/S0031-0182(02)00439-X**

Bennike, O., and Böcher, J., 1990. Forest-tundra neighbouring the North Pole: plant and insect remains from the Plio–Pleistocene Kap København Formation, North Greenland. Arctic, 43(4):301–414. **https://doi.org/10.14430/arctic1629**

Bennike, O., Knudsen, K.L., Abrahamsen, N., Böcher, J., Cremer, H., and Wagner, B., 2010. Early Pleistocene sediments on Store Koldewey, northeast Greenland. Boreas, 39(3):603–619. **https://doi.org/10.1111/j.1502-3885.2010.00147.x**

Berger, A.L., Gulick, S.P.S., Spotila, J.A., Upton, P., Jaeger, J.M., Chapman, J.B., Worthington, L.A., Pavlis, T.L., Ridgway, K.D., Willems, B.A., and McAleer, R.J., 2008. Quaternary tectonic response to intensified glacial erosion in an orogenic wedge. Nature Geoscience, 1(11):793–799. **https://doi.org/10.1038/ngeo334**

Berndt, C., Bünz, S., and Mienert, J., 2003. Polygonal fault systems on the mid-Norwegian margin: a long-term source for fluid flow. In Van Rensbergen, P., Hillis, R.R., Maltman, A.J., and Morley, C.K. (Eds.), Subsurface Sediment Mobilization. Geological Society Special Publication, 216: 283–290. **https://doi.org/10.1144/GSL.SP.2003.216.01.18**

Bierman, P.R., Shakun, J.D., Corbett, L.B., Zimmerman, S.R., and Rood, D.H., 2016. A persistent and dynamic East Greenland Ice Sheet over the past 7.5 million years. Nature, 540(7632):256–260. **https://doi.org/10.1038/nature20147**

Bourke, R.H., Addison, V.G., and Paquette, R.G., 1989. Oceanography of Nares Strait and northern Baffin Bay in 1986 with emphasis on deep and bottom water formation. Journal of Geophysical Research: Oceans, 94(C6):8289–8302. **https://doi.org/10.1029/JC094iC06p08289**

Briner, J.P., Alley, R.B., Bender, M.L., Csatho, B., Poinar, K., and Schaefer, J.M., 2017. How stable is the Greenland Ice Sheet? With contributions by Axford, Y., Born, A., Hatfield, R., Jennings, A.J., Keisling, B., Kelly, M., Langebroek, P., Miller, G.H., Morlighem, M., Osterberg, E.C., Otto-Bliesner, B., Robel, A., and Young, N.E. National Science Foundation Report. **http://www.glyfac.buffalo.edu/Faculty/briner/greenlandworkshop/NSF_greenland_stability_whitepaper.pdf**

Catania, G.A., Stearns, L.A., Moon, T.A., Enderlin, E.M., and Jackson, R.H., 2020. Future evolution of Greenland's marine-terminating outlet glaciers. Journal of Geophysical Research: Earth Surface, 125(2):e2018JF004873. **https://doi.org/10.1029/2018JF004873**

Chalmers, J.A., Pulvertaft, T.C.R., Christiansen, F.G., Larsen, H.C., Laursen, K.H., and Ottesen, T.G., 1993. The southern West Greenland continental margin: rifting history, basin development, and petroleum potential. In Parker, J.R., Petroleum Geology of Northwest Europe: Proceedings of the 4th Conference. Geological Society, London, Petroleum Geology Conference Series, 4:915–931. **https://doi.org/10.1144/0040915**

Christ, A.J., Bierman, P.R., Knutz, P.C., Corbett, L.B., Fosdick, J.C., Thomas, E.K., Cowling, O.C., Hidy, A.J., and Caffee, M.W., 2020. The Northwestern Greenland Ice Sheet during the Early Pleistocene was similar to today. Geophysical Research Letters, 47(1):e2019GL085176. **https://doi.org/10.1029/2019GL085176**

Clark, P.U., Archer, D., Pollard, D., Blum, J.D., Rial, J.A., Brovkin, V., Mix, A.C., Pisias, N.G., and Roy, M., 2006. The Middle Pleistocene transition: characteristics, mechanisms, and implications for long-term changes in atmospheric pCO_2. Quaternary Science Reviews, 25(23–24):3150–3184. **https://doi.org/10.1016/j.quascirev.2006.07.008**

Clark, P.U., and Pollard, D., 1998. Origin of the Middle Pleistocene transition by ice sheet erosion of regolith. Paleoceanography, 13(1):1–9. **https://doi.org/10.1029/97PA02660**

Cluett, A.A., and Thomas, E.K., 2021. Summer warmth of the past six interglacials on Greenland. Proceedings of the National Academy of Sciences of the United States of America, 118(20):e2022916118. **https://doi.org/10.1073/pnas.2022916118**

Conrad, C.P., 2013. The solid Earth's influence on sea level. Geological Society of America Bulletin, 125(7–8):1027–1052. **https://doi.org/10.1130/B30764.1**

Cox, D.R., Huuse, M., Newton, A.M.W., Sarkar, A.D., and Knutz, P.C., 2021. Shallow gas and gas hydrate occurrences on the northwest Greenland shelf margin. Marine Geology, 432:106382. **https://doi.org/10.1016/j.margeo.2020.106382**

Cox, D.R., Knutz, P.C., Campbell, D.C., Hopper, J.R., Newton, A.M.W., Huuse, M., and Gohl, K., 2020. Geohazard detection using 3D seismic data to enhance offshore scientific drilling site selection. Scientific Drilling, 28:1–27. **https://doi.org/10.5194/sd-28-1-2020**

Csank, A.Z., Patterson, W.P., Eglington, B.M., Rybczynski, N., and Basinger, J.F., 2011. Climate variability in the Early Pliocene Arctic: annually resolved evidence from stable isotope values of sub-fossil wood, Ellesmere Island, Canada. Palaeogeography, Palaeoclimatology, Palaeoecology, 308(3–4):339–349. **https://doi.org/10.1016/j.palaeo.2011.05.038**

Dahl-Jensen, D., Bamber, J., Bøggild, C.E., Buch, E., Christensen, J.H., Dethloff, K., Fahnestock, M., Marshall, S., Rosing, M., Steffen, K., Thomas, R., Truffer, M., van den Broeke, M., and van der Veen, C.J., 2009. The Greenland Ice Sheet in a changing climate: snow, water, ice and permafrost in the Arctic (SWIPA) 2009. Arctic Monitoring and Assessment Programme Report. **https://pure.au.dk/ws/files/70671287/2009_vdBroeke_AMAP.pdf**

de Vernal, A., and Hillaire-Marcel, C., 2008. Natural variability of Greenland climate, vegetation, and ice volume during the past million years. Science, 320(5883):1622–1625. **https://doi.org/10.1126/science.1153929**

de Vernal, A., and Mudie, P.J., 1989. Pliocene and Pleistocene palynostratigraphy at ODP Sites 646 and 647, eastern and southern Labrador Sea. In Srivastava, S.P., Arthur, M., Clement, B., et al., Proceedings of the Ocean Drilling Program, Scientific Results, 105: College Station, TX (Ocean Drilling Program), 401–422. **https://doi.org/10.2973/odp.proc.sr.105.134.1989**

DeConto, R.M., Pollard, D., Alley, R.B., Velicogna, I., Gasson, E., Gomez, N., Sadai, S., Condron, A., Gilford, D.M., Ashe, E.L., Kopp, R.E., Li, D., and Dutton, A., 2021. The Paris Climate Agreement and future sea-level rise from Antarctica. Nature, 593(7857):83–89. **https://doi.org/10.1038/s41586-021-03427-0**

DeConto, R.M., Pollard, D., Wilson, P.A., Pälike, H., Lear, C.H., and Pagani, M., 2008. Thresholds for Cenozoic bipolar glaciation. Nature, 455(7213):652–656. **https://doi.org/10.1038/nature07337**

Dorschel, B., 2017. Cruise Summary Report Maria S. Merian - MSM66, Nuuk–Reykjavik 22.07.2017–28.08.2017. Bremerhaven, Germany: Alfred Wegener Institute. **https://www.ldf.uni-hamburg.de/merian/wochenberichte/wochenberichte-merian/msm65-msm68/msm66-scr.pdf**

Dowdeswell, J.A., Hogan, K.A., Ó Cofaigh, C., Fugelli, E.M.G., Evans, J., and Noormets, R., 2014. Late Quaternary ice flow in a West Greenland fjord and cross-shelf trough system: submarine landforms from Rink Isbrae to Uummannaq shelf and slope. Quaternary Science Reviews, 92:292–309. **https://doi.org/10.1016/j.quascirev.2013.09.007**

Dowsett, H.J., Foley, K.M., Stoll, D.K., Chandler, M.A., Sohl, L.E., Bentsen, M., Otto-Bliesner, B.L., Bragg, F.J., Chan, W.-L., Contoux, C., Dolan, A.M., Haywood, A.M., Jonas, J.A., Jost, A., Kamae, Y., Lohmann, G., Lunt, D.J., Nisancioglu, K.H., Abe-Ouchi, A., Ramstein, G., Riesselman, C.R., Robinson, M.M., Rosenbloom, N.A., Salzmann, U., Stepanek, C., Strother, S.L., Ueda, H., Yan, Q., and Zhang, Z., 2013. Sea surface temperature of the mid-Piacenzian ocean: a data-model comparison. Scientific Reports, 3(1):2013. **https://doi.org/10.1038/srep02013**

Dutton, A., Carlson, A.E., Long, A.J., Milne, G.A., Clark, P.U., DeConto, R., Horton, B.P., Rahmstorf, S., and Raymo, M.E., 2015. Sea-level rise due to polar ice-sheet mass loss during past warm periods. Science, 349(6244):aaa4019. **https://doi.org/10.1126/science.aaa4019**

Dutton, A., and Lambeck, K., 2012. Ice volume and sea level during the last interglacial. Science, 337(6091):216–219. **https://doi.org/10.1126/science.1205749**

Eldrett, J.S., Harding, I.C., Wilson, P.A., Butler, E., and Roberts, A.P., 2007. Continental ice in Greenland during the Eocene and Oligocene. Nature, 446(7132):176–179. **https://doi.org/10.1038/nature05591**

Eyles, N., 1996. Passive margin uplift around the North Atlantic region and its role in Northern Hemisphere late Cenozoic glaciation. Geology, 24(2):103–106. **https://doi.org/10.1130/0091-7613(1996)024<0103:PMUATN>2.3.CO;2**

Fahnestock, M., Abdalati, W., Joughin, I., Brozena, J., and Gogineni, P., 2001. High geothermal heat flow, basal melt, and the origin of rapid ice flow in central Greenland. Science, 294(5550):2338–2342. **https://doi.org/10.1126/science.1065370**

Felikson, D., A. Catania, G., Bartholomaus, T.C., Morlighem, M., and Noël, B.P.Y., 2021. Steep glacier bed knickpoints mitigate inland thinning in Greenland. Geophysical Research Letters, 48(2):e2020GL090112. **https://doi.org/10.1029/2020GL090112**

Feng, R., Bhattacharya, T., Otto-Bliesner, B.L., Brady, E.C., Haywood, A.M., Tindall, J.C., Hunter, S.J., Abe-Ouchi, A., Chan, W.-L., Kageyama, M., Contoux, C., Guo, C., Li, X., Lohmann, G., Stepanek, C., Tan, N., Zhang, Q., Zhang, Z., Han, Z., Williams, C.J.R., Lunt, D.J., Dowsett, H.J., Chandan, D., and Peltier, W.R., 2022. Past terrestrial hydroclimate sensitivity controlled by Earth system feedbacks. Nature Communications, 13(1):1306. **https://doi.org/10.1038/s41467-022-28814-7**

Foster, G.L., Lear, C.H., and Rae, J.W.B., 2012. The evolution of pCO_2, ice volume and climate during the middle Miocene. Earth and Planetary Science Letters, 341–344:243–254. **https://doi.org/10.1016/j.epsl.2012.06.007**

Foster, G.L., Lunt, D.J., and Parrish, R.R., 2010. Mountain uplift and the glaciation of North America – a sensitivity study. Climate of the Past, 6(5):707–717. **https://doi.org/10.5194/cp-6-707-2010**

Funder, S., Bennike, O., Böcher, J., Israelson, C., Petersen, K.S., and Símonarson, L.A., 2001. Late Pliocene Greenland – the Kap København Formation in North Greenland. Bulletin of the Geological Society of Denmark, 48:117–134. **https://doi.org/10.37570/bgsd-2001-48-06**

Fyles, J.G., Hills, L.V., Matthews, J.V., Barendregt, R., Baker, J., Irving, E., and Jetté, H., 1994. Ballast Brook and Beaufort Formations (late Tertiary) on Northern Banks Island, Arctic Canada. Quaternary International, 22–23:141–171. **https://doi.org/10.1016/1040-6182(94)90010-8**

Golledge, N.R., Thomas, Z.A., Levy, R.H., Gasson, E.G.W., Naish, T.R., McKay, R.M., Kowalewski, D.E., and Fogwill, C.J., 2017. Antarctic climate and ice-sheet configuration during the early Pliocene interglacial at 4.23 Ma. Climate of the Past, 13(7):959–975. **https://doi.org/10.5194/cp-13-959-2017**

Graly, J.A., Corbett, L.B., Bierman, P.R., Lini, A., and Neumann, T.A., 2018. Meteoric ^{10}Be as a tracer of subglacial processes and interglacial surface exposure in Greenland. Quaternary Science Reviews, 191:118–131. **https://doi.org/10.1016/j.quascirev.2018.05.009**

Gregersen, U., Knutz, P.C., and Hopper, J.R., 2016. New geophysical and geological mapping of the eastern Baffin Bay region, offshore West Greenland. GEUS Bulletin, 35:83–86. **https://doi.org/10.34194/geusb.v35.4945**

Gregersen, U., Knutz, P.C., Pedersen, G.K., Nøhr-Hansen, H., Ineson, J.R., Larsen, L.M., Hopper, J.R., Bojesen-Koefoed, J.A., Dam, G., Funck, T., and Hovikoski, J., 2022. Stratigraphy of the West Greenland margin. In Dafoe, L.T., and Bingham-Koslowski, N. (Eds.), Geological Synthesis of Baffin Island (Nunavut) and the Labrador-Baffin Seaway. Geological Survey of Canada Bulletin, 608:247–309. **https://doi.org/10.4095/321849**

Gregersen, U., Hopper, J.R., and Knutz, P.C., 2013. Basin seismic stratigraphy and aspects of prospectivity in the NE Baffin Bay, Northwest Greenland. Marine and Petroleum Geology, 46:1–18. **https://doi.org/10.1016/j.marpetgeo.2013.05.013**

Guillermic, M., Misra, S., Eagle, R., and Tripati, A., 2022. Atmospheric CO_2 estimates for the Miocene to Pleistocene based on foraminiferal $\delta^{11}B$ at Ocean Drilling Program Sites 806 and 807 in the western equatorial Pacific. Climate of the Past, 18(2):183–207. **https://doi.org/10.5194/cp-18-183-2022**

Hamilton, J., and Wu, Y., 2013. Synopsis and trends in the physical environment of Baffin Bay and Davis Strait. Canadian Technical Report of Hydrography and Ocean Sciences, 282.

Hansen, J., Sato, M., Hearty, P., Ruedy, R., Kelley, M., Masson-Delmotte, V., Russell, G., Tselioudis, T., Cao, J., Rignot, E., Velicogna, I., Kandiana, E., von Schuckman, K., Kharecha, P., Legrande, A.N., Bauer, M., and Lo, K.-W., 2016. Ice melt, sea level rise and superstorms: evidence from paleoclimate data, climate modeling, and modern observations that 2°C global warming is highly dangerous. Atmospheric Chemistry and Physics, 15:20059–20179. **https://doi.org/10.5194/acpd-15-20059-2015**

Haywood, A.M., Dowsett, H.J., and Dolan, A.M., 2016. Integrating geological archives and climate models for the mid-Pliocene warm period. Nature Communications, 7(1):10646. **https://doi.org/10.1038/ncomms10646**

Haywood, A.M., Dowsett, H.J., Otto-Bliesner, B., Chandler, M.A., Dolan, A.M., Hill, D.J., Lunt, D.J., Robinson, M.M., Rosenbloom, N., Salzmann, U., and Sohl, L.E., 2010. Pliocene Model Intercomparison Project (PlioMIP): experi-

mental design and boundary conditions (Experiment 1). Geoscientific Model Development, 3(1):227–242. **https://doi.org/10.5194/gmd-3-227-2010**

Haywood, A.M., Tindall, J.C., Dowsett, H.J., Dolan, A.M., Foley, K.M., Hunter, S.J., Hill, D.J., Chan, W.L., Abe-Ouchi, A., Stepanek, C., Lohmann, G., Chandan, D., Peltier, W.R., Tan, N., Contoux, C., Ramstein, G., Li, X., Zhang, Z., Guo, C., Nisancioglu, K.H., Zhang, Q., Li, Q., Kamae, Y., Chandler, M.A., Sohl, L.E., Otto-Bliesner, B.L., Feng, R., Brady, E.C., von der Heydt, A.S., Baatsen, M.L.J., and Lunt, D.J., 2020. The Pliocene Model Intercomparison Project Phase 2: large-scale climate features and climate sensitivity. Climate of the Past, 16(6):2095–2123. **https://doi.org/10.5194/cp-16-2095-2020**

Henriksen, N., and Higgins, A.K., 2009. Descriptive text to Geological map of Greenland, 1:500,000, Dove Bugt, Sheet 10. Geological Survey of Denmark and Greenland Map Series, 4:1–32. **https://doi.org/10.34194/geusm.v4.4581**

Hodell, D.A., and Channell, J.E.T., 2016. Mode transitions in Northern Hemisphere glaciation: co-evolution of millennial and orbital variability in Quaternary climate. Climate of the Past, 12(9):1805–1828. **https://doi.org/10.5194/cp-12-1805-2016**

Hodson, A., Bøggild, C., Hanna, E., Huybrechts, P., Langford, H., Cameron, K., and Houldsworth, A., 2010. The cryoconite ecosystem on the Greenland ice sheet. Annals of Glaciology, 51(56):123–129. **https://doi.org/10.3189/172756411795931985**

Hofmann, J.C., Knutz, P.C., Nielsen, T., and Kuijpers, A., 2016. Seismic architecture and evolution of the Disko Bay trough-mouth fan, central West Greenland margin. Quaternary Science Reviews, 147:69–90. **https://doi.org/10.1016/j.quascirev.2016.05.019**

Hogan, K.A., Larter, R.D., Graham, A.G.C., Arthern, R., Kirkham, J.D., Totten Minzoni, R., Jordan, T.A., Clark, R., Fitzgerald, V., Wåhlin, A.K., Anderson, J.B., Hillenbrand, C.D., Nitsche, F.O., Simkins, L., Smith, J.A., Gohl, K., Arndt, J.E., Hong, J., and Wellner, J., 2020. Revealing the former bed of Thwaites Glacier using sea-floor bathymetry: implications for warm-water routing and bed controls on ice flow and buttressing. The Cryosphere, 14(9):2883–2908. **https://doi.org/10.5194/tc-14-2883-2020**

Holland, D.M., Thomas, R.H., de Young, B., Ribergaard, M.H., and Lyberth, B., 2008. Acceleration of Jakobshavn Isbræ triggered by warm subsurface ocean waters. Nature Geoscience, 1(10):659–664. **https://doi.org/10.1038/ngeo316**

Hu, A., Meehl, G.A., Han, W., Otto-Bliestner, B., Abe-Ouchi, A., and Rosenbloom, N., 2015. Effects of the Bering Strait closure on AMOC and global climate under different background climates. Progress in Oceanography, 132:174–196. **https://doi.org/10.1016/j.pocean.2014.02.004**

Hulbe, C.L., MacAyeal, D.R., Denton, G.H., Kleman, J., and Lowell, T.V., 2004. Catastrophic ice shelf breakup as the source of Heinrich event icebergs. Paleoceanography, 19(1):PA1004. **https://doi.org/10.1029/2003PA000890**

Jackson, R., Kvorning, A.B., Limoges, A., Georgiadis, E., Olsen, S.M., Tallberg, P., Andersen, T.J., Mikkelsen, N., Giraudeau, J., Massé, G., Wacker, L., and Ribeiro, S., 2021. Holocene polynya dynamics and their interaction with oceanic heat transport in northernmost Baffin Bay. Scientific Reports, 11(1):10095. **https://doi.org/10.1038/s41598-021-88517-9**

Jakobsson, M., Mayer, L., Coakley, B., Dowdeswell, J.A., Forbes, S., Fridman, B., Hodnesdal, H., and et al., 2012. The International Bathymetric Chart of the Arctic Ocean (IBCAO) Version 3.0. Geophysical Research Letters, 39(12):L12609. **https://doi.org/10.1029/2012GL052219**

Jansen, E., Fronval, T., Rack, F., and Channell, J.E.T., 2000. Pliocene-Pleistocene ice rafting history and cyclicity in the Nordic Seas during the last 3.5 Myr. Paleoceanography, 15(6):709–721. **https://doi.org/10.1029/1999PA000435**

Japsen, P., Bonow, J.M., Green, P.F., Chalmers, J.A., and Lidmar-Bergström, K., 2006. Elevated, passive continental margins: long-term highs or Neogene uplifts? New evidence from West Greenland. Earth and Planetary Science Letters, 248(1–2):330–339. **https://doi.org/10.1016/j.epsl.2006.05.036**

Jennings, A., Reilly, B., Andrews, J., Hogan, K., Walczak, M., Jakobsson, M., Stoner, J., Mix, A., Nicholls, K.W., O'Regan, M., Prins, M.A., and Troelstra, S.R., 2022. Modern and Early Holocene ice shelf sediment facies from Petermann Fjord and northern Nares Strait, northwest Greenland. Quaternary Science Reviews, 283:107460. **https://doi.org/10.1016/j.quascirev.2022.107460**

Jennings, A.E., Andrews, J.T., Ó Cofaigh, C., Onge, G.S., Sheldon, C., Belt, S.T., Cabedo-Sanz, P., and Hillaire-Marcel, C., 2017. Ocean forcing of ice sheet retreat in central west Greenland from LGM to the early Holocene. Earth and Planetary Science Letters, 472:1–13. **https://doi.org/10.1016/j.epsl.2017.05.007**

Jennings, A.E., Andrews, J.T., Ó Cofaigh, C., St-Onge, G., Belt, S., Cabedo-Sanz, P., Pearce, C., Hillaire-Marcel, C., and Calvin Campbell, D., 2018. Baffin Bay paleoenvironments in the LGM and HS1: resolving the ice-shelf question. Marine Geology, 402:5–16. **https://doi.org/10.1016/j.margeo.2017.09.002**

Jennings, A.E., Andrews, J.T., Oliver, B., Walczak, M., and Mix, A., 2019. Retreat of the Smith Sound ice stream in the Early Holocene. Boreas, 48(4):825–840. **https://doi.org/10.1111/bor.12391**

Keisling, B.A., Castañeda, I.S., and Brigham-Grette, J., 2017. Hydrological and temperature change in Arctic Siberia during the intensification of Northern Hemisphere Glaciation. Earth and Planetary Science Letters, 457:136–148. **https://doi.org/10.1016/j.epsl.2016.09.058**

Keisling, B.A., Nielsen, L.T., Hvidberg, C.S., Nuterman, R., and DeConto, R.M., 2020. Pliocene–Pleistocene megafloods as a mechanism for Greenlandic megacanyon formation. Geology, 48(7):737–741. **https://doi.org/10.1130/G47253.1**

Khan, S.A., Wahr, J., Bevis, M., Velicogna, I., and Kendrick, E., 2010. Spread of ice mass loss into northwest Greenland observed by GRACE and GPS. Geophysical Research Letters, 37(6):L06501. **https://doi.org/10.1029/2010GL042460**

Knies, J., Mattingsdal, R., Fabian, K., Grøsfjeld, K., Baranwal, S., Husum, K., De Schepper, S., Vogt, C., Andersen, N., Matthiessen, J., Andreassen, K., Jokat, W., Nam, S.-I., and Gaina, C., 2014. Effect of early Pliocene uplift on late Pliocene cooling in the Arctic–Atlantic gateway. Earth and Planetary Science Letters, 387:132–144. **https://doi.org/10.1016/j.epsl.2013.11.007**

Knutz, P.C., Gregersen, U., Harrison, C., Brent, T.A., Hopper, J.R., and Nøhr-Hansen, H., 2022. Baffin Bay composite tectono-sedimentary element. Memoirs - Geological Society of London, 57. **https://doi.org/10.1144/M57-2016-7**

Knutz, P.C., Hopper, J.R., Gregersen, U., Nielsen, T., and Japsen, P., 2015. A contourite drift system on the Baffin Bay–West Greenland margin linking Pliocene Arctic warming to poleward ocean circulation. Geology, 43(10):907–910. **https://doi.org/10.1130/G36927.1**

Knutz, P.C., Newton, A.M.W., Hopper, J.R., Huuse, M., Gregersen, U., Sheldon, E., and Dybkjær, K., 2019. Eleven phases of Greenland Ice Sheet shelf-edge advance over the past 2.7 million years. Nature Geoscience, 12(5):361–368. **https://doi.org/10.1038/s41561-019-0340-8**

Koenig, S.J., Dolan, A.M., de Boer, B., Stone, E.J., Hill, D.J., DeConto, R.M., Abe-Ouchi, A., Lunt, D.J., Pollard, D., Quiquet, A., Saito, F., Savage, J., and van de Wal, R., 2015. Ice sheet model dependency of the simulated Greenland ice sheet in the mid-Pliocene. Climate of the Past, 11(3):369–381. **https://doi.org/10.5194/cp-11-369-2015**

Larsen, H.C., Saunders, A.D., Clift, P.D., Beget, J., Wei, W., and Spezzaferri, S., 1994. Seven million years of glaciation in Greenland. Science, 264(5161):952–955. **https://doi.org/10.1126/science.264.5161.952**

Lear, C.H., Billups, K., Rickaby, R.E.M., Diester-Haass, L., Mawbey, E.M., and Sosdian, S.M., 2016. Breathing more deeply: deep ocean carbon storage during the mid-Pleistocene climate transition. Geology, 44(12):1035–1038. **https://doi.org/10.1130/G38636.1**

Lisiecki, L.E., and Raymo, M.E., 2005. A Pliocene–Pleistocene stack of 57 globally distributed benthic $\delta^{18}O$ records. Paleoceanography, 20(1):PA1003. **https://doi.org/10.1029/2004PA001071**

Loutre, M.F., 2003. Clues from MIS 11 to predict the future climate – a modelling point of view. Earth and Planetary Science Letters, 212(1–2):213–224. **https://doi.org/10.1016/S0012-821X(03)00235-8**

Lunt, D.J., Foster, G.L., Haywood, A.M., and Stone, E.J., 2008. Late Pliocene Greenland glaciation controlled by a decline in atmospheric CO_2 levels. Nature, 454(7208):1102–1105. **https://doi.org/10.1038/nature07223**

Matthews, J.V., and Ovenden, L.E., 1990. Late Tertiary plant macrofossils from localities in Arctic/subarctic North America: a review of the data. Arctic, 43:364–392. **https://doi.org/10.14430/ARCTIC1631**

Medvedev, S., Souche, A., and Hartz, E.H., 2013. Influence of ice sheet and glacial erosion on passive margins of Greenland. Geomorphology, 193:36–46. **https://doi.org/10.1016/j.geomorph.2013.03.029**

Melles, M., Brigham-Grette, J., Minyuk, P.S., Nowaczyk, N.R., Wennrich, V., DeConto, R.M., Anderson, P.M., Andreev, A.A., Coletti, A., Cook, T.L., Haltia-Hovi, E., Kukkonen, M., Lozhkin, A.V., Rosén, P., Tarasov, P., Vogel, H., and Wagner, B., 2012. 2.8 million years of Arctic climate change from Lake El'gygytgyn, NE Russia. Science, 337(6092):315–320. **https://doi.org/10.1126/science.1222135**

Miller, K.G., Mountain, G.S., Wright, J.D., and Browning, J.V., 2015. A 180-million-year record of sea level and ice volume variations from continental margin and deep-sea isotopic records. Oceanography, 24(2):40–53. **https://doi.org/10.5670/oceanog.2011.26**

Molnar, P., and England, P., 1990. Late Cenozoic uplift of mountain ranges and global climate change: chicken or egg? Nature, 346(6279):29–34. **https://doi.org/10.1038/346029a0**

Morlighem, M., Rignot, E., Mouginot, J., Seroussi, H., and Larour, E., 2014. Deeply incised submarine glacial valleys beneath the Greenland ice sheet. Nature Geoscience, 7(6):418–422. **https://doi.org/10.1038/ngeo2167**

Morlighem, M., Williams, C.N., Rignot, E., An, L., Arndt, J.E., Bamber, J.L., Catania, G., Chauché, N., Dowdeswell, J.A., Dorschel, B., Fenty, I., Hogan, K., Howat, I., Hubbard, A., Jakobsson, M., Jordan, T.M., Kjeldsen, K.K., Millan, R., Mayer, L., Mouginot, J., Noël, B.P.Y., O'Cofaigh, C., Palmer, S., Rysgaard, S., Seroussi, H., Siegert, M.J., Slabon, P., Straneo, F., van den Broeke, M.R., Weinrebe, W., Wood, M., and Zinglersen, K.B., 2017. BedMachine v3: complete bed topography and ocean bathymetry mapping of Greenland from multibeam echo sounding combined with mass conservation. Geophysical Research Letters, 44(21):11051–11061. **https://doi.org/10.1002/2017GL074954**

Neem Community Members, 2013. Eemian interglacial reconstructed from a Greenland folded ice core. Nature, 493(7433):489–494. **https://doi.org/10.1038/nature11789**

Newton, A.M.W., Huuse, M., Cox, D.R., and Knutz, P.C., 2021. Seismic geomorphology and evolution of the Melville Bugt trough mouth fan, northwest Greenland. Quaternary Science Reviews, 255:106798. **https://doi.org/10.1016/j.quascirev.2021.106798**

Newton, A.M.W., Knutz, P.C., Huuse, M., Gannon, P., Brocklehurst, S.H., Clausen, O.R., and Gong, Y., 2017. Ice stream reorganization and glacial retreat on the northwest Greenland shelf. Geophysical Research Letters, 44(15):7826–7835. **https://doi.org/10.1002/2017GL073690**

Nielsen, T., Andersen, C., Knutz, P.C., and Kuijpers, A., 2011. The Middle Miocene to Recent Davis Strait drift complex: implications for Arctic–Atlantic water exchange. Geo-Marine Letters, 31(5):419–426. **https://doi.org/10.1007/s00367-011-0245-z**

Nielsen, T., and Kuijpers, A., 2013. Only 5 southern Greenland shelf edge glaciations since the Early Pliocene. Scientific Reports, 3(1):1875. **https://doi.org/10.1038/srep01875**

Nøhr-Hansen, H., Pedersen, G.K., Knutz, P.C., Bojesen-Koefoed, J.A., Śliwińska, K.K., Hovikoski, J., Ineson, J.R., Kristensen, L., and Therkelsen, J., 2021. The Cretaceous succession of northeast Baffin Bay: stratigraphy, sedimentology and petroleum potential. Marine and Petroleum Geology, 133:105108. **https://doi.org/10.1016/j.marpetgeo.2021.105108**

Ó Cofaigh, C., Andrews, J.T., Jennings, A.E., Dowdeswell, J.A., Hogan, K.A., Kilfeather, A.A., and Sheldon, C., 2013. Glacimarine lithofacies, provenance and depositional processes on a West Greenland trough-mouth fan. Journal of Quaternary Science, 28(1):13–26. **https://doi.org/10.1002/jqs.2569**

O'Brien, C.L., Huber, M., Thomas, E., Pagani, M., Super, J.R., Elder, L.E., and Hull, P.M., 2020. The enigma of Oligocene climate and global surface temperature evolution. Proceedings of the National Academy of Sciences of the United States of America, 117(41):25302–25309. **https://doi.org/10.1073/pnas.2003914117**

Oakey, G.N., and Chalmers, J.A., 2012. A new model for the Paleogene motion of Greenland relative to North America: plate reconstructions of the Davis Strait and Nares Strait regions between Canada and Greenland. Journal of Geophysical Research: Solid Earth, 117(B10):B10401. **https://doi.org/10.1029/2011JB008942**

Ogg, J.G., 2020. Geomagnetic Polarity Time Scale. In Gradstein, F.M., Ogg, J.G., Schmitz, M., and Ogg, G. (Eds.), Geologic Time Scale 2020: Amsterdam (Elsevier), 159–192. **https://doi.org/10.1016/B978-0-12-824360-2.00005-X**

Otto-Bliesner, B.L., Jahn, A., Feng, R., Brady, E.C., Hu, A., and Löfverström, M., 2017. Amplified North Atlantic warming in the late Pliocene by changes in Arctic gateways. Geophysical Research Letters, 44(2):957–964. **https://doi.org/10.1002/2016GL071805**

Pagani, M., 2014. Biomarker-based inferences of past climate: the alkenone pCO_2 proxy. In Holland, H.D. and Turekian, K.K., Treatise on Geochemistry (Second Edition). Oxford (Elsevier), 361–378. **https://doi.org/10.1016/B978-0-08-095975-7.01027-5**

Pagani, M., Zachos, J.C., Freeman, K.H., Tipple, B., and Bohaty, S., 2005. Marked decline in atmospheric carbon dioxide concentrations during the Paleogene. Science, 309(5734):600–603. **https://doi.org/10.1126/science.1110063**

Paillard, D., 1998. The timing of Pleistocene glaciations from a simple multiple-state climate model. Nature, 391(6665):378–381. **https://doi.org/10.1038/34891**

Patton, H., Swift, D.A., Clark, C.D., Livingstone, S.J., and Cook, S.J., 2016. Distribution and characteristics of overdeepenings beneath the Greenland and Antarctic ice sheets: implications for overdeepening origin and evolution. Quaternary Science Reviews, 148:128-145. **https://doi.org/10.1016/j.quascirev.2016.07.012**

Paxman, G.J.G., Austermann, J., and Tinto, K.J., 2021. A fault-bounded palaeo-lake basin preserved beneath the Greenland ice sheet. Earth and Planetary Science Letters, 553:116647. **https://doi.org/10.1016/j.epsl.2020.116647**

Pearce, C., and Knutz, P., 2019. Baffin Bay Ice-Ocean-Sediment Interactions: Research Cruise on HDMS Lauge Koch Aasiat - Qaanaaq - Carey Islands - Aasiatt, 19 Aug–8 Sep 2019. **https://geo.au.dk/fileadmin/ingen_mappe_valgt/Paleoceanography_group/LAKO_BIOS19_cruise_report.pdf**

Pearson, P.N., and Palmer, M.R., 2000. Atmospheric carbon dioxide concentrations over the past 60 million years. Nature, 406(6797):695–699. **https://doi.org/10.1038/35021000**

Pedersen, V.K., Larsen, N.K., and Egholm, D.L., 2019. The timing of fjord formation and early glaciations in North and Northeast Greenland. Geology, 47(7):682–686. **https://doi.org/10.1130/G46064.1**

Pérez, L.F., Nielsen, T., Knutz, P.C., Kuijpers, A., and Damm, V., 2018. Large-scale evolution of the central-east Greenland margin: new insights to the North Atlantic glaciation history. Global and Planetary Change, 163:141–157. **https://doi.org/10.1016/j.gloplacha.2017.12.010**

Pollard, D., DeConto, R.M., and Alley, R.B., 2015. Potential Antarctic Ice Sheet retreat driven by hydrofracturing and ice cliff failure. Earth and Planetary Science Letters, 412:112–121. **https://doi.org/10.1016/j.epsl.2014.12.035**

Raymo, M.E., Grant, B., Horowitz, M., and Rau, G.H., 1996. Mid-Pliocene warmth: stronger greenhouse and stronger conveyor. Marine Micropaleontology, 27(1–4):313–326. **https://doi.org/10.1016/0377-8398(95)00048-8**

Raymo, M.E., and Huybers, P., 2008. Unlocking the mysteries of the ice ages. Nature, 451(7176):284–285. **https://doi.org/10.1038/nature06589**

Reyes, A.V., Carlson, A.E., Beard, B.L., Hatfield, R.G., Stoner, J.S., Winsor, K., Welke, B., and Ullman, D.J., 2014. South Greenland ice-sheet collapse during Marine Isotope Stage11. Nature, 510(7506):525–528. **https://doi.org/10.1038/nature13456**

Rial, J.A., Oh, J., and Reischmann, E., 2013. Synchronization of the climate system to eccentricity forcing and the 100,000-year problem. Nature Geoscience, 6(4):289–293. **https://doi.org/10.1038/ngeo1756**

Rogozhina, I., Petrunin, A.G., Vaughan, A.P.M., Steinberger, B., Johnson, J.V., Kaban, M.K., Calov, R., Rickers, F., Thomas, M., and Koulakov, I., 2016. Melting at the base of the Greenland ice sheet explained by Iceland hotspot history. Nature Geoscience, 9(5):366–369. **https://doi.org/10.1038/ngeo2689**

Ruddiman, W.F., 2006. Orbital changes and climate. Quaternary Science Reviews, 25(23):3092–3112. **https://doi.org/10.1016/j.quascirev.2006.09.001**

Ruddiman, W.F., and Kutzbach, J.E., 1989. Forcing of late Cenozoic northern hemisphere climate by plateau uplift in southern Asia and the American west. Journal of Geophysical Research: Atmospheres, 94(D15):18409–18427. **https://doi.org/10.1029/JD094iD15p18409**

Rybczynski, N., Gosse, J.C., Richard Harington, C., Wogelius, R.A., Hidy, A.J., and Buckley, M., 2013. Mid-Pliocene warm-period deposits in the High Arctic yield insight into camel evolution. Nature Communications, 4(1):1550. **https://doi.org/10.1038/ncomms2516**

Rysgaard, S., Boone, W., Carlson, D., Sejr, M.K., Bendtsen, J., Juul-Pedersen, T., Lund, H., Meire, L., and Mortensen, J., 2020. An updated view on water masses on the pan-West Greenland Continental Shelf and their link to proglacial fjords. Journal of Geophysical Research: Oceans, 125(2):e2019JC015564. **https://doi.org/10.1029/2019JC015564**

Scambos, T.A., Bell, R.E., Alley, R.B., Anandakrishnan, S., Bromwich, D.H., Brunt, K., Christianson, K., Creyts, T., Das, S.B., DeConto, R., Dutrieux, P., Fricker, H.A., Holland, D., MacGregor, J., Medley, B., Nicolas, J.P., Pollard, D., Siegfried, M.R., Smith, A.M., Steig, E.J., Trusel, L.D., Vaughan, D.G., and Yager, P.L., 2017. How much, how fast?: a science review and outlook for research on the instability of Antarctica's Thwaites Glacier in the 21st century. Global and Planetary Change, 153:16–34. **https://doi.org/10.1016/j.gloplacha.2017.04.008**

Schaefer, J.M., Finkel, R.C., Balco, G., Alley, R.B., Caffee, M.W., Briner, J.P., Young, N.E., Gow, A.J., and Schwartz, R., 2016. Greenland was nearly ice-free for extended periods during the Pleistocene. Nature, 540(7632):252–255. **https://doi.org/10.1038/nature20146**

Shackleton, N.J., Backman, J., Zimmerman, H., Kent, D.V., Hall, M.A., Roberts, D.G., Schnitker, D., Baldauf, J.G., Desprairies, A., Homrighausen, R., Huddlestun, P., Keene, J.B., Kaltenback, A.J., Krumsiek, K.A.O., Morton, A.C., Murray, J.W., and Westberg-Smith, J., 1984. Oxygen isotope calibration of the onset of ice-rafting and history of glaciation in the North Atlantic region. Nature, 307(5952):620–623. **https://doi.org/10.1038/307620a0**

Slabon, P., Dorschel, B., Jokat, W., Myklebust, R., Hebbeln, D., and Gebhardt, C., 2016. Greenland ice sheet retreat history in the northeast Baffin Bay based on high-resolution bathymetry. Quaternary Science Reviews, 154:182–198. **https://doi.org/10.1016/j.quascirev.2016.10.022**

Solgaard, A.M., Bonow, J.M., Langen, P.L., Japsen, P., and Hvidberg, C.S., 2013. Mountain building and the initiation of the Greenland Ice Sheet. Palaeogeography, Palaeoclimatology, Palaeoecology, 392:161–176. **https://doi.org/10.1016/j.palaeo.2013.09.019**

St. John, K., 2008. Cenozoic ice-rafting history of the central Arctic Ocean: terrigenous sands on the Lomonosov Ridge. Paleoceanography and Paleoclimatology, 23(1):PA1S05. **https://doi.org/10.1029/2007PA001483**

St. John, K.E.K., and Krissek, L.A., 2002. The late Miocene to Pleistocene ice-rafting history of southeast Greenland. Boreas, 31(1):28–35. **https://doi.org/10.1111/j.1502-3885.2002.tb01053.x**

Straneo, F., Sutherland, D.A., Holland, D., Gladish, C., Hamilton, G.S., Johnson, H.L., Rignot, E., Xu, Y., and Koppes, M., 2012. Characteristics of ocean waters reaching Greenland's glaciers. Annals of Glaciology, 53(60):202–210. **https://doi.org/10.3189/2012AoG60A059**

Tan, N., Ladant, J.-B., Ramstein, G., Dumas, C., Bachem, P., and Jansen, E., 2018. Dynamic Greenland ice sheet driven by pCO_2 variations across the Pliocene Pleistocene transition. Nature Communications, 9(1):4755. **https://doi.org/10.1038/s41467-018-07206-w**

Tang, C.C.L., Ross, C.K., Yao, T., Petrie, B., DeTracey, B.M., and Dunlap, E., 2004. The circulation, water masses and sea-ice of Baffin Bay. Progress in Oceanography, 63(4):183–228. **https://doi.org/10.1016/j.pocean.2004.09.005**

Thiede, J., Jessen, C., Knutz, P., Kuijpers, A., Mikkelsen, N., Norgaard-Pedersen, N., and Spielhagen, R.F., 2011. Millions of years of Greenland ice sheet history recorded in ocean sediments. Polarforschung, 80(3):141–159. **https://epic.awi.de/id/eprint/30005/1/15-33.pdf**

Thiede, J., and Myhre, A.M., 1996. The paleoceanographic history of the North Atlantic-Arctic gateways: synthesis of the Leg 151 drilling results. In Thiede, J., Myhre, A.M., Firth, J.V., Johnson, G.L., and Ruddiman, W.F. (Eds.), Proceedings of the Ocean Drilling Program, Scientific Results. 151: College Station, TX (Ocean Drilling Program), 645–658. **https://doi.org/10.2973/odp.proc.sr.151.147.1996**

Tripati, A.K., Eagle, R.A., Morton, A., Dowdeswell, J.A., Atkinson, K.L., Bahé, Y., Dawber, C.F., and et al., 2008. Evidence for glaciation in the Northern Hemisphere back to 44 Ma from ice-rafted debris in the Greenland Sea. Earth and Planetary Science Letters, 265(1):112–122. **https://doi.org/10.1016/j.epsl.2007.09.045**

Tripati, A.K., Roberts, C.D., and Eagle, R.A., 2009. Coupling of CO_2 and ice sheet stability over major climate transitions of the last 20 million years. Science, 326(5958):1394–1397. **https://doi.org/10.1126/science.1178296**

Whittaker, R.C., Hamann, N.E., and Pulvertaft, T.C.R., 1997. A new frontier province offshore northwest Greenland: structure, basin development, and petroleum potential of the Melville Bay area. AAPG Bulletin, 81:978–998. **https://www.osti.gov/biblio/494206**

Willeit, M., Ganopolski, A., Calov, R., and Brovkin, V., 2019. Mid-Pleistocene transition in glacial cycles explained by declining CO_2 and regolith removal. Science Advances, 5(4):eaav7337. **https://doi.org/10.1126/sciadv.aav7337**

Willerslev, E., Cappellini, E., Boomsma, W., Nielsen, R., Hebsgaard, M.B., Brand, T.B., Hofreiter, M., Bunce, M., Poinar, H.N., Dahl-Jensen, D., Johnsen, S., Steffensen, J.P., Bennike, O., Schwenninger, J.L., Nathan, R., Armitage, S., de Hoog, C.J., Alfimov, V., Christl, M., Beer, J., Muscheler, R., Barker, J., Sharp, M., Penkman, K.E., Haile, J., Taberlet, P., Gilbert, M.T., Casoli, A., Campani, E., and Collins, M.J., 2007. Ancient biomolecules from deep ice cores reveal a forested southern Greenland. Science, 317(5834):111–114. **https://doi.org/10.1126%2Fscience.1141758**

Wolf, T.C.W., and Thiede, J., 1991. History of terrigenous sedimentation during the past 10 m.y. in the North Atlantic (ODP Legs 104 and 105 and DSDP Leg 81). Marine Geology, 101(1–4):83–102. **https://doi.org/10.1016/0025-3227(91)90064-B**

Yang, H., Krebs-Kanzow, U., Kleiner, T., Sidorenko, D., Rodehacke, C.B., Shi, X., Gierz, P., Niu, L., Gowan, E.J., Hinck, S., Liu, X., Stap, L.B., and Lohmann, G., 2022. Impact of paleoclimate on present and future evolution of the Greenland Ice Sheet. PloS One, 17(1):e0259816. **https://doi.org/10.1371/journal.pone.0259816**

Yao, T., and Tang, C.L., 2003. The formation and maintenance of the North Water polynya. Atmosphere-Ocean, 41(3):187–201. **https://doi.org/10.3137/ao.410301**

Yin, J., Overpeck, J.T., Griffies, S.M., Hu, A., Russell, J.L., and Stouffer, R.J., 2011. Different magnitudes of projected subsurface ocean warming around Greenland and Antarctica. Nature Geoscience, 4(8):524–528. **https://doi.org/10.1038/ngeo1189**

Yin, Q.Z., and Berger, A., 2010. Insolation and CO_2 contribution to the interglacial climate before and after the Mid-Brunhes Event. Nature Geoscience, 3(4):243–246. **https://doi.org/10.1038/ngeo771**

Zachos, J.C., Dickens, G.R., and Zeebe, R.E., 2008. An early Cenozoic perspective on greenhouse warming and carbon-cycle dynamics. Nature, 451(7176):279–283. **https://doi.org/10.1038/nature06588**

Zhang, Y.G., Pagani, M., Liu, Z.H., Bohaty, S.M., and DeConto, R., 2013. A 40-million-year history of atmospheric CO_2. Philosophical Transactions of the Royal Society A: Mathematical Physical and Engineering Sciences, 371:20130096. **https://doi.org/10.1098/rsta.2013.0096**

Site summaries

Site MB-23A

Priority:	Primary
Position:	72.9840, −62.9805
Water depth (m):	1821
Target drilling depth (mbsf):	422
Approved maximum penetration (mbsf):	422
Survey coverage (track map; seismic profile):	High-resolution seismic reflection primary: LAKO_1012; SP 14841 High-resolution seismic reflection crossing: LAKO_1015; SP 18017 Deep-penetration seismic reflection primary: BB10-5068125; SP 13370
Objective(s):	Recover high-resolution paleoceanographic record of an early/middle–late Pleistocene sediment drift system corresponding to the most recent part of the trough-mouth-fan history; expanded Units 9, 10, and 11
Coring program:	Hole A: APC to refusal (~250 mbsf) Hole B: APC to refusal (~250 mbsf) Hole C: APC/XCB to 422 mbsf
Downhole measurements program:	Hole C (0–422 mbsf): • Triple combo • FMS-sonic • VSI
Nature of rock anticipated:	Mud with dropstones

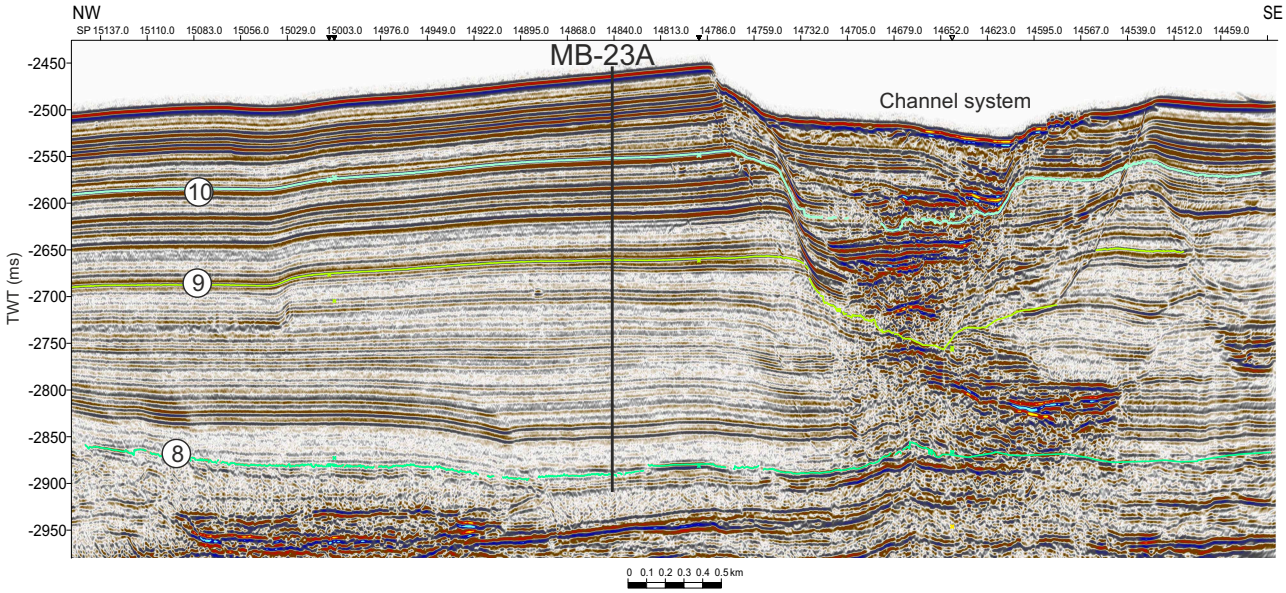

Figure AF1. Top: bathymetric map and locations of high-resolution Seismic Reflection Line LAKO_1012, Crossing Line LAKO_1022, and primary Site MB-23A on the lower slope of the Melville Bugt TMF. Bottom: location of primary Site MB-23A in Seismic Reflection Profile LAKO_1012 at Shotpoint (SP) 14841 shown with interpreted horizons. Primary seismic section is shown with interpreted horizons. The sedimentary package is interpreted as a contourite drift incised by downslope channels. The section below the stratified units displays discontinuous to chaotic reflections interpreted as mass transport deposits and buried channels. Site MB-23A is expected to recover silty mud with scattered dropstones likely of middle to late Quaternary age. The site is located 0.45 km from the nearest crossing point to avoid disturbances seen at the edge of the channel.

Site MB-02C

Priority:	Primary
Position:	73.1150, −63.7904
Water depth (m):	1957
Target drilling depth (mbsf):	522
Approved maximum penetration (mbsf):	522
Survey coverage (track map; seismic profile):	Primary: LAKO_1010; SP 10145 Crossing: LAKO_1005; SP 5190 Primary: BB10-5063125; SP 12768 Crossing: BB09-1055; SP 13471
Objective(s):	Recover high-resolution paleoceanographic record of an early/middle–late Pleistocene sediment drift system corresponding to the most recent part of the trough-mouth-fan history; expanded Unit 8; overlaps strata of 23C
Coring program:	Hole A: APC/XCB to 522 mbsf Hole B: APC/XCB to 522 mbsf
Downhole measurements program:	Hole B (0–522 mbsf): • Triple combo • FMS-sonic • VSI
Nature of rock anticipated:	Mud with dropstones

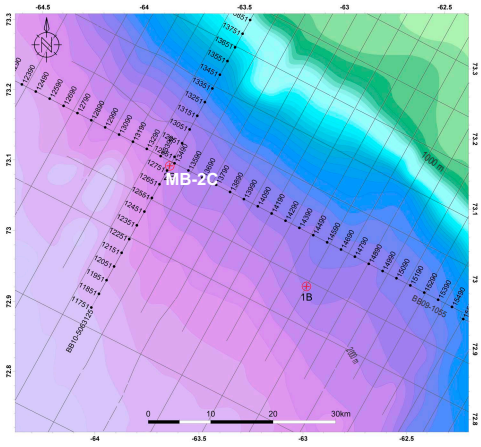

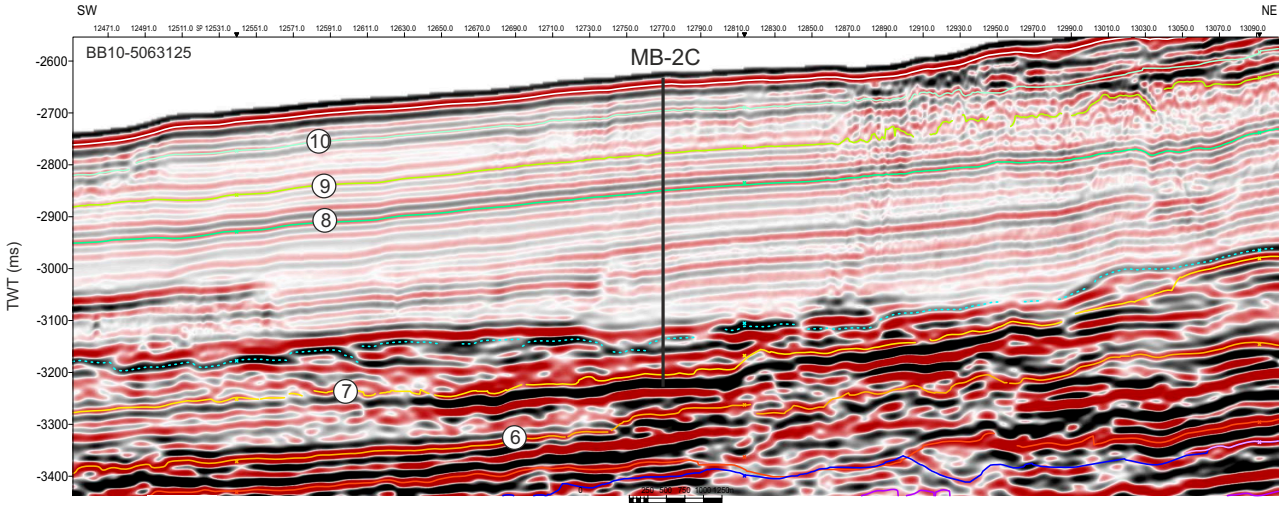

Figure AF2. Top: bathymetric map (IBCAO V3) and locations of Seismic Reflection Line BB10-5063125, Crossing Line BB09-1055, and primary Site MB-02C on the lower slope of the Melville Bugt TMF. Bottom: location of primary Site MB-02C in Seismic Reflection Profile Line BB10-5063125 at Shotpoint (SP) 12768 shown with interpreted horizons. The strata package above target Horizon 7, displaying a continuous reflection character, is interpreted as a contourite drift abounding a channel system. Site MB-02C is expected to recover silty-sandy muds, presumably of Early/Middle to Late Pleistocene age. The site is located 1 km off the nearest crossline (BB09-1055) to obtain optimal stratigraphic coverage of Unit 8 (between Horizons 7 and 8) and avoid amplitude anomaly at the base of this unit.

Site MB-31A

Priority:	Primary
Position:	73.5607, −62.1512
Water depth (m):	531
Target drilling depth (mbsf):	282
Approved maximum penetration (mbsf):	282
Survey coverage (track map; seismic profile):	High-resolution primary: LAKO_1033; SP 46083 Deep-penetration primary: ANU-3D_IL-13392; XL-6920 Deep-penetration crossing: ANU-3D_XL-6920; IL-13392
Objective(s):	Recover deglacial and interglacial intervals of potentially early to middle Pleistocene age within top-set strata of the trough-mouth fan; onlap glacial unconformities of Units 6, 7, and 8
Coring program:	Hole A: RCB to 282 mbsf Hole B: drill down to 70 mbsf; APC/XCB to 282 mbsf
Downhole measurements program:	Hole A (0–282 mbsf): • Triple combo • FMS-sonic • VSI
Nature of rock anticipated:	Diamicton with intercalated pebbly mud and marine mud units

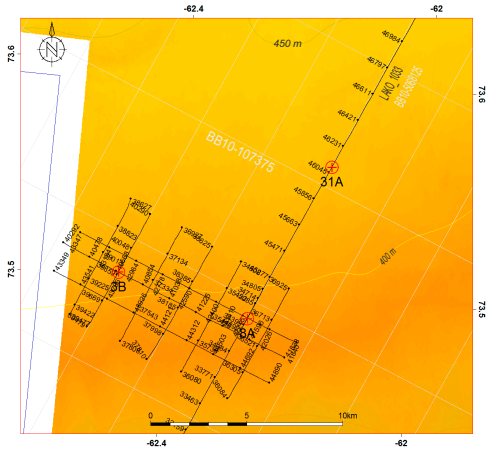

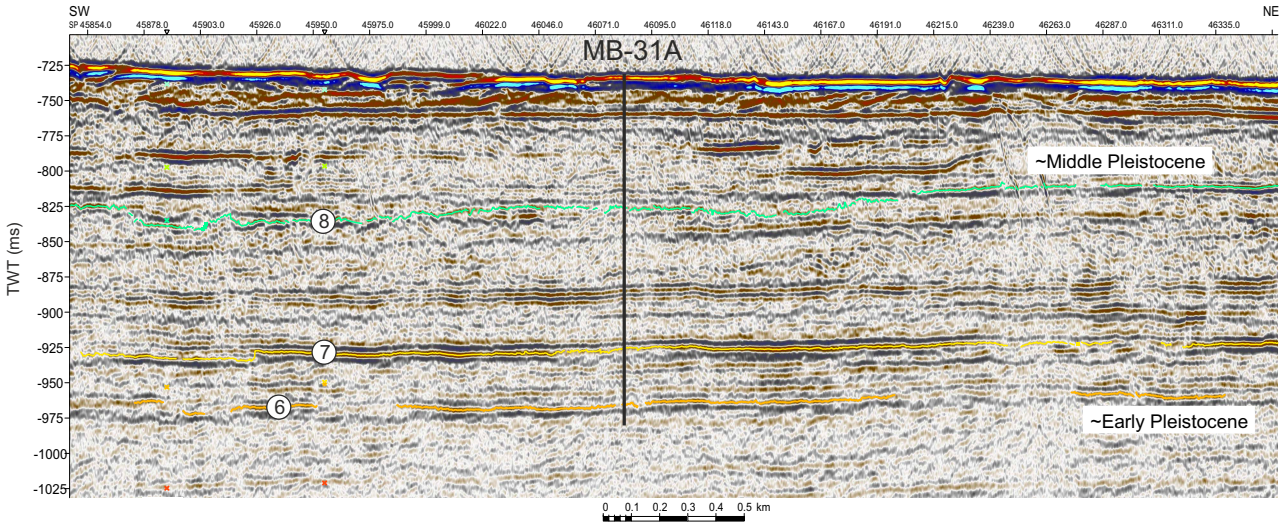

Figure AF3. Top: bathymetric map with locations of Seismic Reflection Line LAKO_1033 and primary Site MB-31A on the outer shelf margin of the Melville Bugt TMF. Bottom: location of primary Site MB-31A in Seismic Reflection Profile Line LAKO_1033 at Shotpoint (SP) 46083 showing interpreted horizons. Site MB-31A is aimed at recovering the stratified intervals between Horizons 6, 7, and 8. The expected lithologies are proximal glacigenic deposits (e.g., tills interlayered with muddy marine/glacial-marine strata), probably of Early–Middle Pleistocene age. The site is placed ~1 km off the nearest crossline (BB10-107375) to optimize penetration of flat lying/onlapping reflections and avoid strong reflections in the upper 100 ms interval.

Site MB-30A

Priority:	Primary
Position:	73.9013, −61.8540
Water depth (m):	618
Target drilling depth (mbsf):	303
Approved maximum penetration (mbsf):	303
Survey coverage (track map; seismic profile):	High-resolution primary: LAKO_1035; SP 71423 High-resolution crossing: LAKO_1036; SP 72941 Deep-penetration primary: ANU-3D_IL-14776; Xline 13020 Deep-penetration crossing: ANU-3D_XL-13020; In-line 14776
Objective(s):	Recover deglacial and interglacial intervals of potentially early Pleistocene age within top-set strata of the trough-mouth fan; onlap glacial unconformity (Horizon 3)
Coring program:	Hole A: RCB to 303 mbsf Hole B: drill down to 100 mbsf; APC/XCB to 303 mbsf
Downhole measurements program:	Hole A (0–303 mbsf): • Triple combo • FMS-sonic
Nature of rock anticipated:	Diamicton with intercalated pebbly mud and mud units

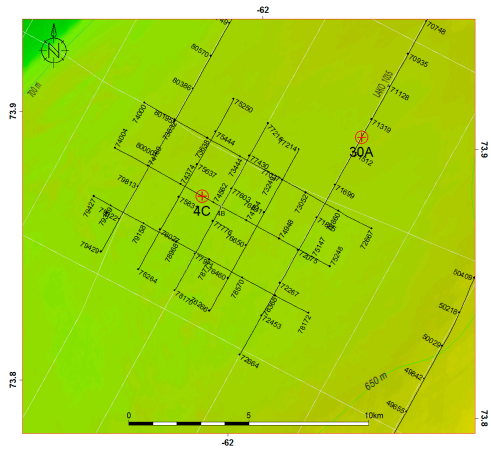

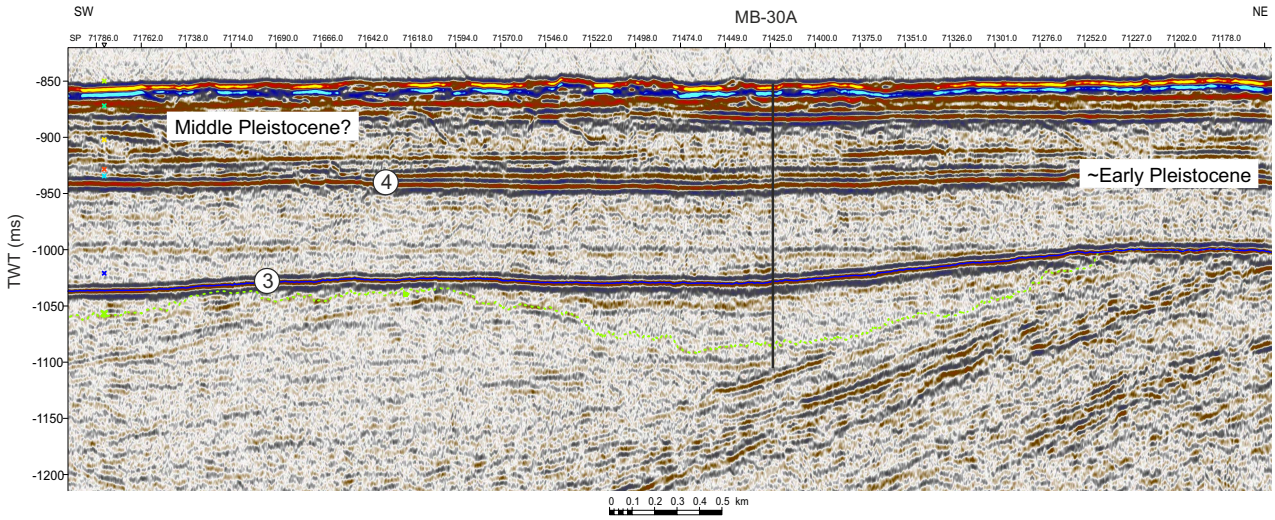

Figure AF4. Top: bathymetric map and location of primary Site MB-30A on high-resolution Seismic Reflection Line LAKO_1035. High-resolution seismic data (LAKO) with shot numbers (black), TGS regional 2D data (gray) and core sites (red) are shown. Bottom: location of primary Site MB-30A in seismic reflection profile with interpreted horizons and ages on Line LAKO_1035 at Shotpoint (SP) 71423. Site MB-30A captures the pinch-out of a basal unit within TMF Unit 4 over Horizon 3. The depth target is the bottom of a minibasin developed at this position below Horizon 3 (light green). Proximal glacigenic deposits interlayered with muddy marine/glaciomarine strata of likely Early Pleistocene age are expected. Site MB-30A is offset 3.2 km from the nearest high-resolution crossline to achieve optimal stratigraphic coverage of Units 3 and 4 and was selected as a primary site due to overall high reflection continuity.

Site MB-06D

Priority:	Primary
Position:	74.1283, –60.9744
Water depth (m):	614
Target drilling depth (mbsf):	561
Approved maximum penetration (mbsf):	561
Survey coverage (track map; seismic profile):	High-resolution primary: LAKO_1044; SP 88383 Deep-penetration primary: ANU-3D_IL-18992; XL 19032 Deep-penetration crossing: ANU-3D_XL-19032; IL 18992
Objective(s):	Recover Neogene contourite drift sediments that can elucidate paleoceanographic conditions prior to the major basinward expansion of the Greenland Ice Sheet
Coring program:	Hole A: RCB to 561 mbsf Hole B: RCB to 400 mbsf
Downhole measurements program:	Hole A (0–561 mbsf): • Triple combo • FMS-sonic • VSI
Nature of rock anticipated:	Diamicton; mudstone with silty-sandy intervals

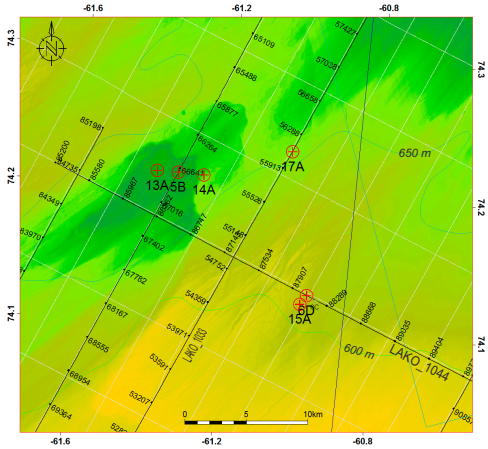

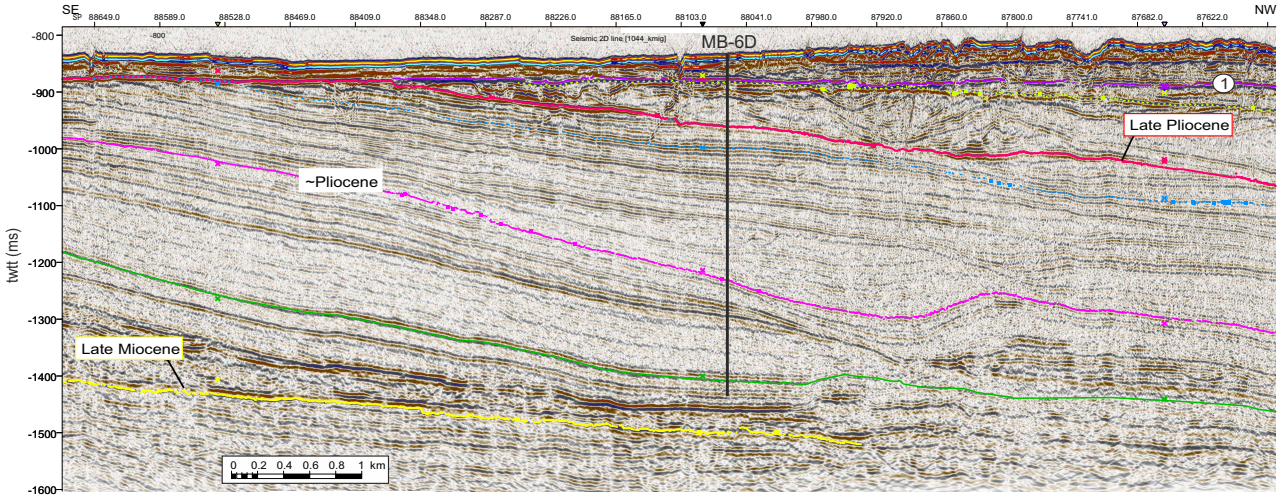

Figure AF5. Top: bathymetric map with location of primary Site MB-06D on high-resolution Seismic Reflection Line LAKO_1044 on the middle shelf region fringing the Melville Bugt trough. Bottom: location of primary Site MB-06D on LAKO_1044 at Shotpoint (SP) 88383. High-resolution seismic section with interpreted horizons and ages penetrates an expanded interval of contourite drift sediments of likely Pliocene age. Site MB-06D overlaps with primary Site MB-17A and alternate Sites MB-05B, MB-13A, and MB-14A to produce a composite succession. Total depth is placed above a strong reflector covering a major slide scar.

Site MB-17A

Priority:	Primary
Position:	74.2323, −61.0374
Water depth (m):	655
Target drilling depth (mbsf):	411
Approved maximum penetration (mbsf):	411
Survey coverage (track map; seismic profile):	High-resolution primary: LAKO_1033; SP 56182 Deep-resolution primary: ANU_Inline_18624.sgy; Xline 19032 Deep-resolution crossing: ANU_XLine_19032.sgy; In-line 18624
Objective(s):	(1) Capture deposits corresponding to the earliest shelf-based glaciations in northwest Greenland; (2) recover Neogene sediments of likely early Pliocene age that can elucidate paleoceanographic conditions prior to the major expansion of the Greenland Ice Sheet
Coring program:	Hole A: RCB to 411 mbsf
Downhole measurements program:	Hole A (0–411 mbsf): • Triple combo • FMS-sonic
Nature of rock anticipated:	Diamicton; mudstone with silty-sandy intervals

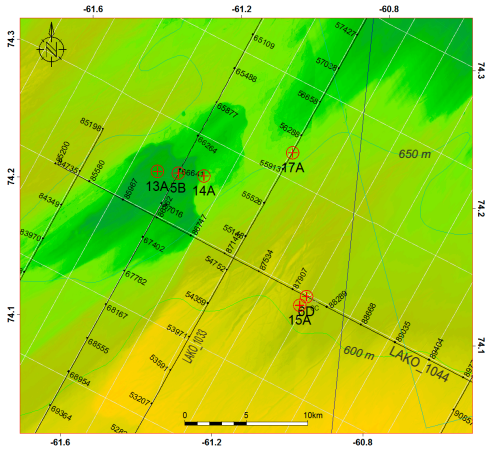

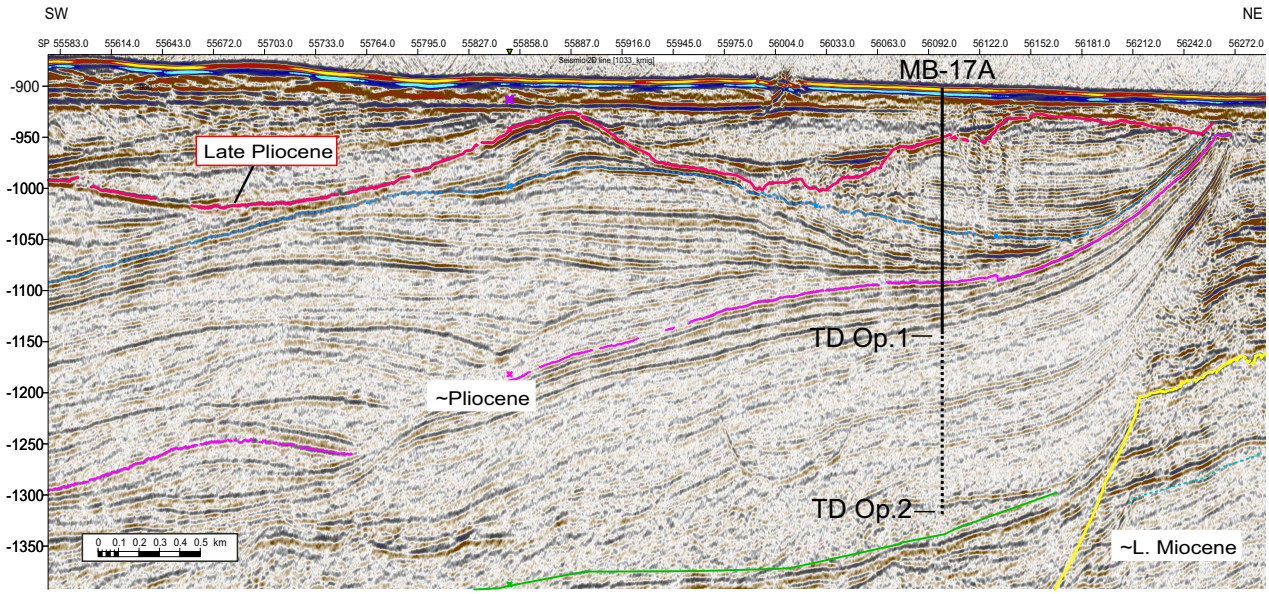

Figure AF6. Top: bathymetric map with location of primary Site MB-17A on high-resolution Seismic Reflection Line LAKO_1033 in the middle shelf region of Melville Bugt trough. High-resolution seismic data (LAKO; black lines) with shot points (SP), regional TGS 2D data (gray lines), and drilling sites (red) are indicated. Bottom: location of primary Site MB-17A on LAKO_1033 at Shotpoint 56182 with interpreted horizons and ages. This site is aimed at recovering a composite sequence of high–accumulation rate contourite drifts of Mega-unit B (likely Pliocene age) and the earliest glacial clinoforms of Mega-unit A (Late Pliocene and Early Pleistocene).

Site MB-07B

Priority:	Primary
Position:	74.4925, –60.5832
Water depth (m):	736
Target drilling depth (mbsf):	978
Approved maximum penetration (mbsf):	978
Survey coverage (track map; seismic profile):	High-resolution primary: LAKO_1033; SP 60045 Deep-penetration primary: PITU 3D: In-line 2499: Xline 7230 Deep-penetration crossing: Line: Site-7B_PITU-3D_XL-7230.segy: In-line 2499
Objective(s):	Recover an upper Miocene interval and continue coring through the Middle Miocene horizon to the top of a sedimentary wedge of possible Oligocene age to elucidate past ocean and terrestrial climates in northeast Baffin Bay/Greenland and the onset of ephemeral glaciation in northwest Greenland
Coring program:	Hole A: RCB to 620 mbsf Hole B: Install HRT with 600 m of casing; RCB 600–978 mbsf
Downhole measurements program:	Hole A (0–620 mbsf): • Triple combo • FMS-sonic • VSI Hole B (600–978 mbsf): • Triple combo • FMS-sonic • VSI
Nature of rock anticipated:	Claystone with silty to sandy intervals and siliceous ooze

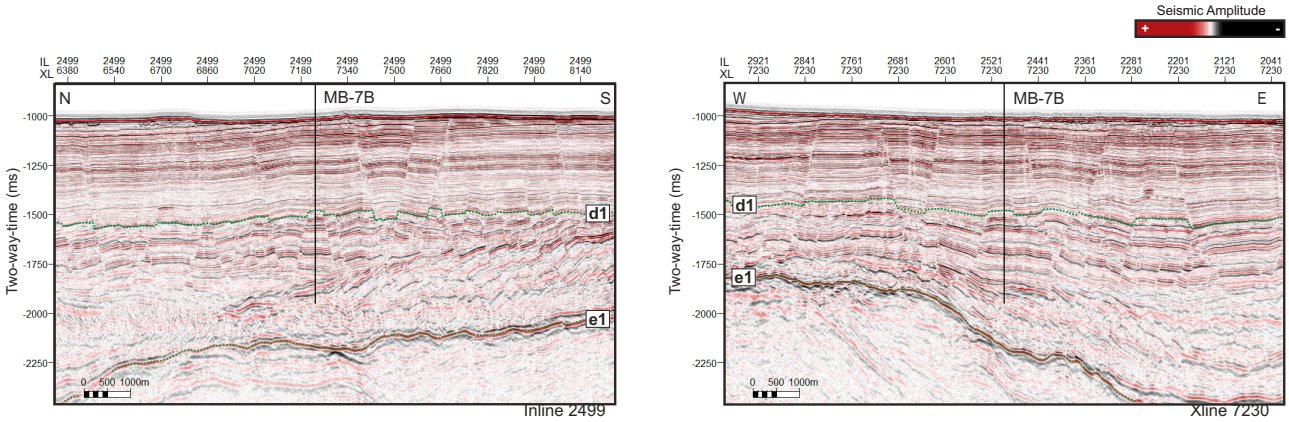

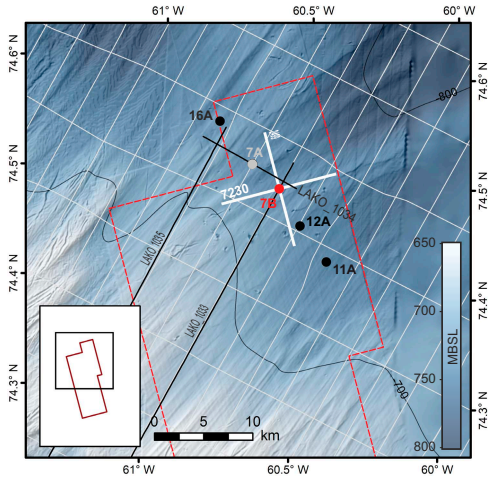

Figure AF7. Top: shaded relief bathymetric map of the middle shelf region within the Melville Bugt trough showing location of primary Site MB-07B on Seismic Reflection Lines PITU 3D inline 2499 and Xline 7230. Seismic crossing lines displayed in the bottom panel are shown in thick white lines. Thin white lines show the 2D seismic grid. Inset shows the aerial coverage of 3D seismic data used to help refine target location. Black circles show the proposed alternate drill site locations, and the red circle shows the location for Site MB-07B. Bottom: Line PITU 2499 and Crossing Line PITU 7230 with location of primary Site MB-07B. SP = shot point. Key Inline and Xline seismic sections from the 3D seismic cube (zero-phase). Mega-unit boundaries are shown. This drill site is aimed at recovering Oligocene and Miocene successions that are expected to be fine-grained hemipelagic sediments of Mega-units C and D.

Site MB-01C

Priority:	Alternate
Position:	73.0001, −63.0065
Water depth (m):	1809
Target drilling depth (mbsf):	473
Approved maximum penetration (mbsf):	473
Survey coverage (track map; seismic profile):	High-resolution seismic reflection primary: LAKO_1011; SP 14035 High-resolution seismic reflection crossing: LAKO_1022; SP 24911 Deep-penetration seismic reflection primary: BB10-5068125 Deep-penetration seismic reflection crossing: BB10-10525; SP 14612
Objective(s):	Recover high-resolution paleoceanographic record of an early/middle–late Pleistocene sediment drift system corresponding to the most recent part of the trough-mouth-fan history; expanded Units 9, 10, and 11
Coring program:	Hole A: APC to refusal (~250 mbsf) Hole B: APC to refusal (~250 mbsf) Hole C: APC to refusal; XCB to 473 mbsf
Downhole measurements program:	Hole C (0–473 mbsf): • Triple combo • FMS-sonic • VSI
Nature of rock anticipated:	Mud with dropstones

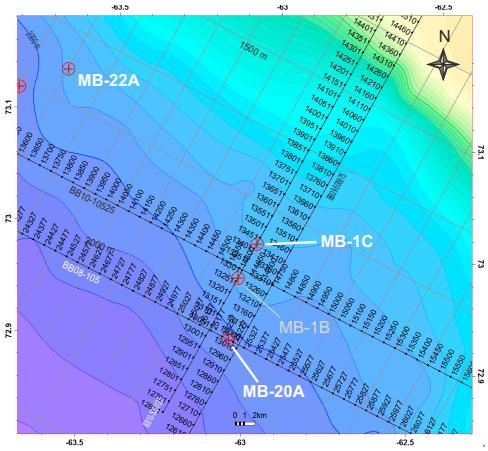

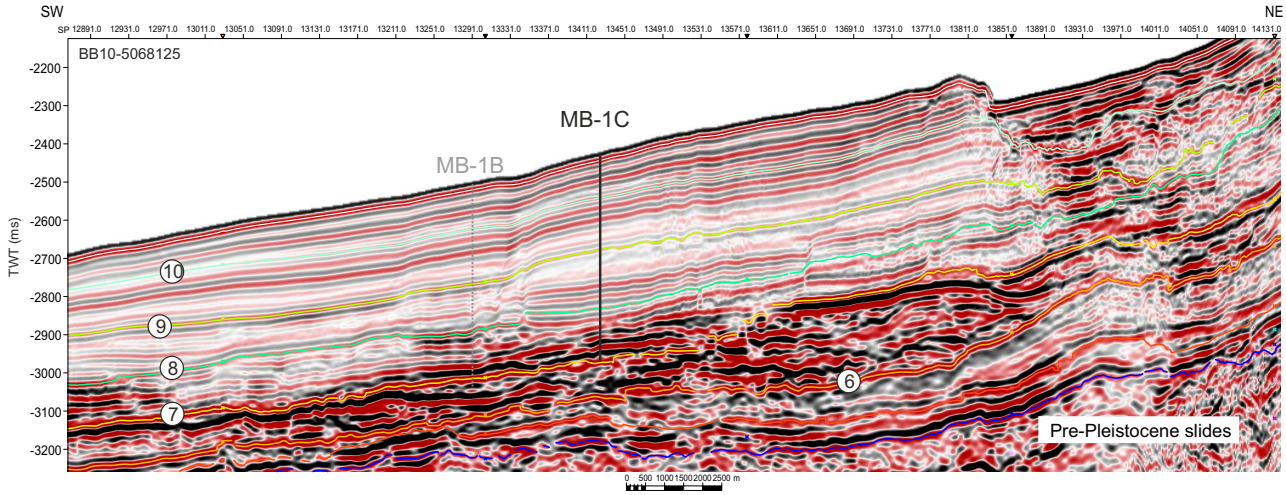

Figure AF8. Top: bathymetric map of the lower slope below the Melville Bugt TMF showing location of alternate Site MB-01C on Seismic Reflection Line BB10-5068125 and nearby Crossing Line BB10-10525. SP = shot point. Bottom: Line BB10-5068125 with location of alternate Site MB-01C at position 13424 shown with interpreted horizons. The strata package above Horizon 7 (depth target), displaying a wavy, semicontinuous reflection character, is interpreted as a contourite drift formed in juxtaposition to a channel system. The strong reflections below Horizon 7 are interpreted as channel deposits (e.g., slumps or turbidites). Site MB-01C is expected to recover silty-sandy muds presumably of Early/Middle to Late Pleistocene age.

Site MB-20A

Priority:	Alternate
Position:	72.9118, −63.0642
Water depth (m):	1928
Target drilling depth (mbsf):	450
Approved maximum penetration (mbsf):	450
Survey coverage (track map; seismic profile):	Deep-penetration primary: BB08-105; SP 25254 Deep-penetration crossing: BB09-506875; SP 13028
Objective(s):	Recover high-resolution paleoceanographic record of an early/middle–late Pleistocene sediment drift system corresponding to the most recent part of the trough-mouth-fan history; expanded Units 9, 10, and 11
Coring program:	Hole A: APC to refusal (~250 mbsf) Hole B: APC to refusal (~250 mbsf) Hole C: APC to refusal; XCB to 450 mbsf
Downhole measurements program:	Hole C (0–450 mbsf): • Triple combo • FMS-sonic • VSI
Nature of rock anticipated:	Mud with dropstones

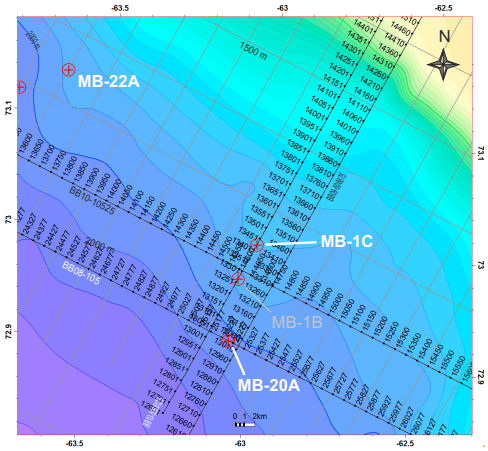

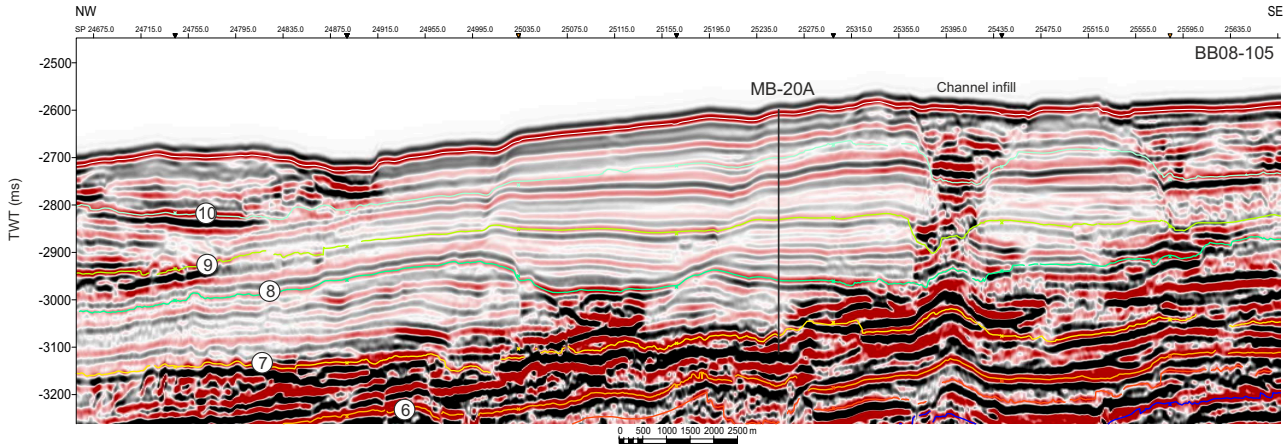

Figure AF9. Top: bathymetric map of the lower slope below the Melville Bugt TMF showing location of alternate Site MB-20A on Seismic Reflection Line BB08-105 and nearby Crossing Line BB09-506875. SP = shot point. Bottom: section of seismic Line BB08-105 with location of alternate Site MB-20A at position 25254 showing interpreted horizons. The strata package above Horizon 7 (depth target), displaying a wavy, semicontinuous reflection character, is interpreted as a contourite drift formed in juxtaposition to a channel system. The strong reflections below Horizon 7 are interpreted as channel deposits (e.g., slumps, turbidites, or plumites?). Site MB-20A is expected to recover silty-sandy muds presumably of Middle to Late Pleistocene age. Site is located ~1.2 km away from crossing line to avoid strong reflections at target depth that might be channel sands.

Site MB-22A

Priority:	Alternate
Position:	73.1388, –63.6402
Water depth (m):	1850
Target drilling depth (mbsf):	611
Approved maximum penetration (mbsf):	611
Survey coverage (track map; seismic profile):	BB09-506375; SP 12939 Crossing: BB09-1055; SP 13610
Objective(s):	Recover high-resolution paleoceanographic record of an early/middle–late Pleistocene sediment drift system corresponding to the most recent part of the trough-mouth-fan history; expanded Unit 8; overlaps strata of 23C.
Coring program:	Hole A: APC/XCB to 611 mbsf Hole B: APC/XCB to 611 mbsf
Downhole measurements program:	Hole B (0–611 mbsf): • Triple combo • FMS-sonic • VSI
Nature of rock anticipated:	Mud with dropstones

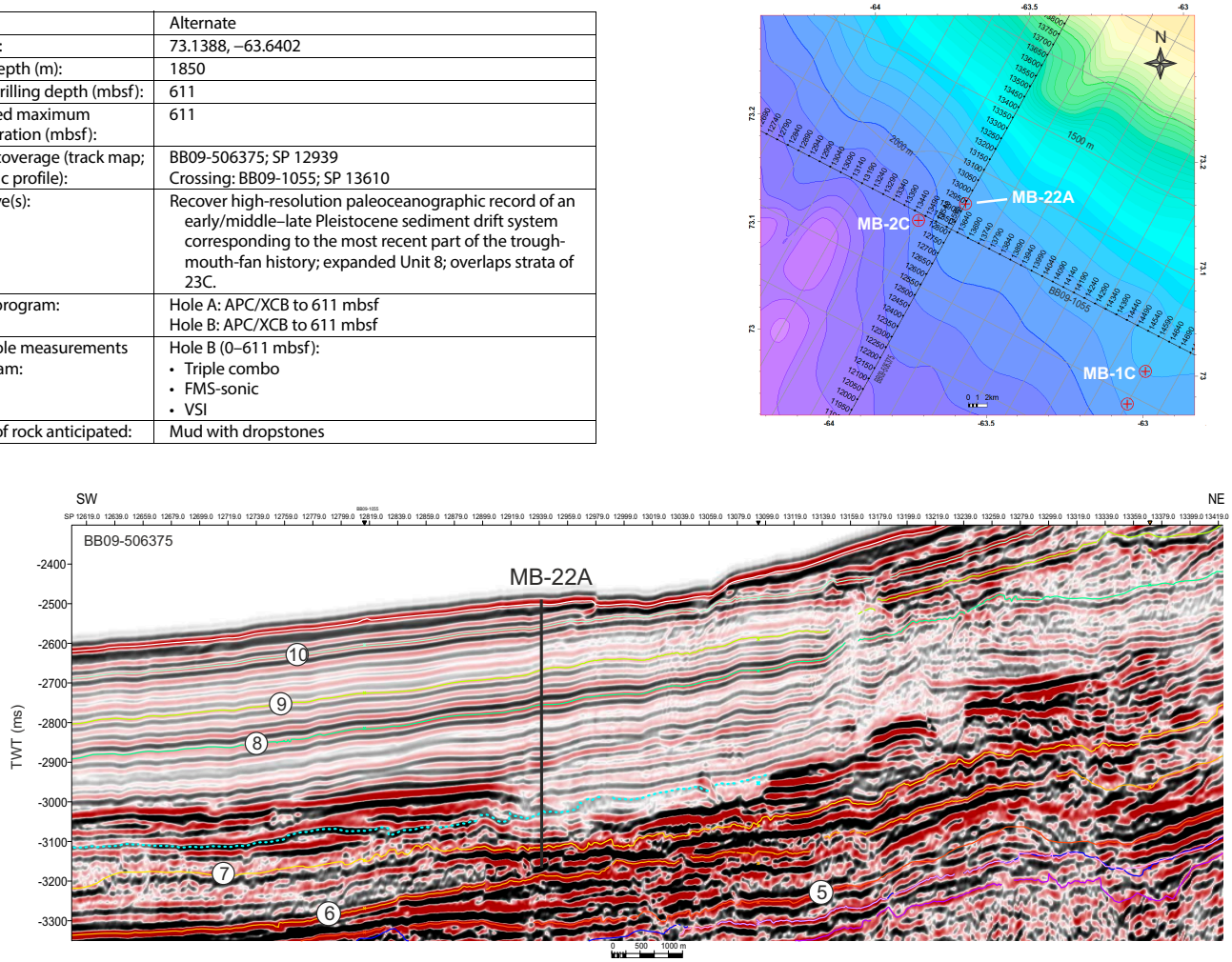

Figure AF10. Top: bathymetric map of the lower slope below the Melville Bugt TMF showing location of alternate Site MB-22A on Seismic Reflection Line BB09-506375 at Shotpoint (SP) 12939 and Crossing Line BB09-0155. Bottom: section of Seismic Line BB09-506375 with location of alternate Site MB-22A showing interpreted horizons. The strata package above target Horizon 7, displaying a semicontinuous reflection character, is interpreted as a contourite drift abounding a channel system. Site MB-22A is expected to recover silty-sandy muds presumably of Early/Middle to Late Pleistocene age. Early depositional stage of Unit 8 is marked by a blue dotted line. The site is placed between two crosslines to optimize stratigraphic coverage of Unit 8 (between Horizons 7 and 8) and avoid drilling into strong reflectors (e.g., channel sands).

Site MB-08A

Priority:	Alternate
Position:	73.4870, −62.2682
Water depth (m):	497
Target drilling depth (mbsf):	370
Approved maximum penetration (mbsf):	370
Survey coverage (track map; seismic profile):	BB10-5068125; SP 15796 BB09-10725; SP 21378
Objective(s):	Recover deglacial and interglacial intervals of potentially early to middle Pleistocene age within top-set strata of the trough-mouth fan; onlap glacial unconformities of Units 6, 7, 8, and 9
Coring program:	Hole A: RCB to 370 mbsf Hole B: Drill down to 70 mbsf; APC/XCB to 370 mbsf
Downhole measurements program:	Hole A (0–370 mbsf): • Triple combo • FMS-sonic • VSI
Nature of rock anticipated:	Diamicton with intercalated pebbly mud and sandy mud units

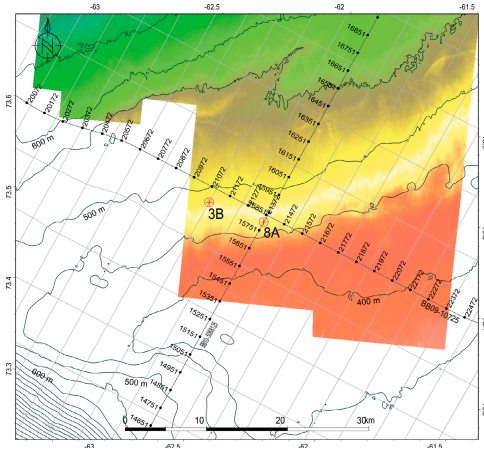

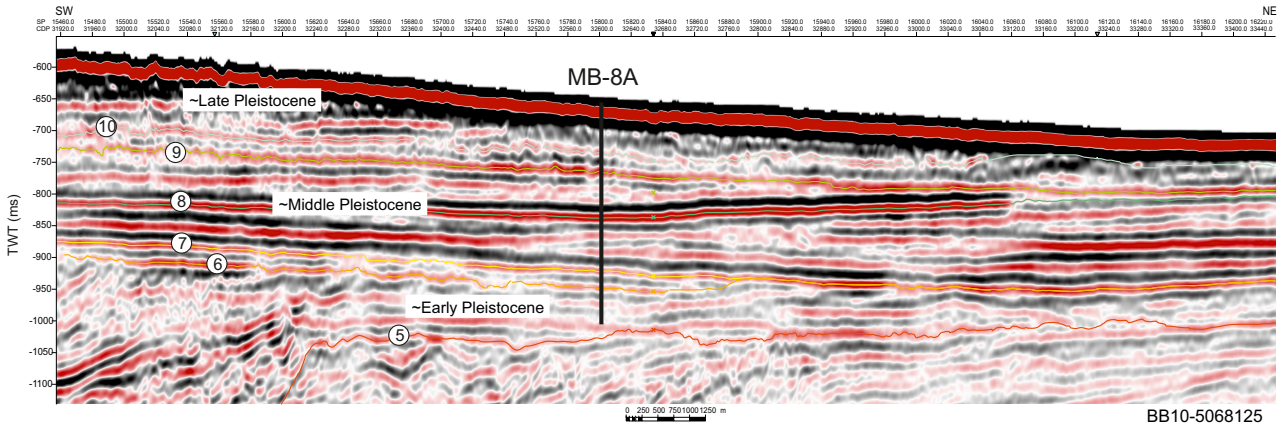

Figure AF11. Top: bathymetric map of the outer margin of the Melville Bugt TMF showing location of alternate Site MB-08A on Seismic Reflection Lines BB10-5068125 at Shotpoints (SP) 15796 and BB09-10725. Bottom: section of Seismic Line B10-5068125 with location of alternate Site MB-08A and interpreted horizons and ages. This site will recover the stratified section above seismic Horizon 5. The expected lithologies are proximal glacigenic deposits (e.g., tills interlayered with muddy marine/glacial-marine strata, probably of Early to Middle Pleistocene age). The site is placed ~1 km off the nearest crossline to optimize penetration of flat lying, onlapping reflections.

Site MB-03B

Priority:	Alternate
Position:	73.5032, −62.4861
Water depth (m):	498
Target drilling depth (mbsf):	375
Approved maximum penetration (mbsf):	375
Survey coverage (track map; seismic profile):	BB10-5066845; SP 15463 BB09-10725; SP 21096
Objective(s):	Recover deglacial and interglacial intervals of potentially early to middle Pleistocene age within top-set strata of the trough-mouth fan; onlap glacial unconformities of Units 6, 7, 8, and 9
Coring program:	Hole A: RCB to 375 mbsf Hole B: Drill down to 70 mbsf; APC/XCB to 375 mbsf
Downhole measurements program:	Hole A (0–375 mbsf): • Triple combo • FMS-sonic • VSI
Nature of rock anticipated:	Diamicton with intercalated pebbly mud and sandy mud units

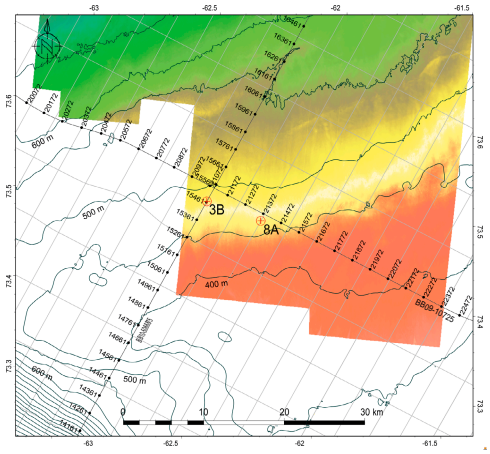

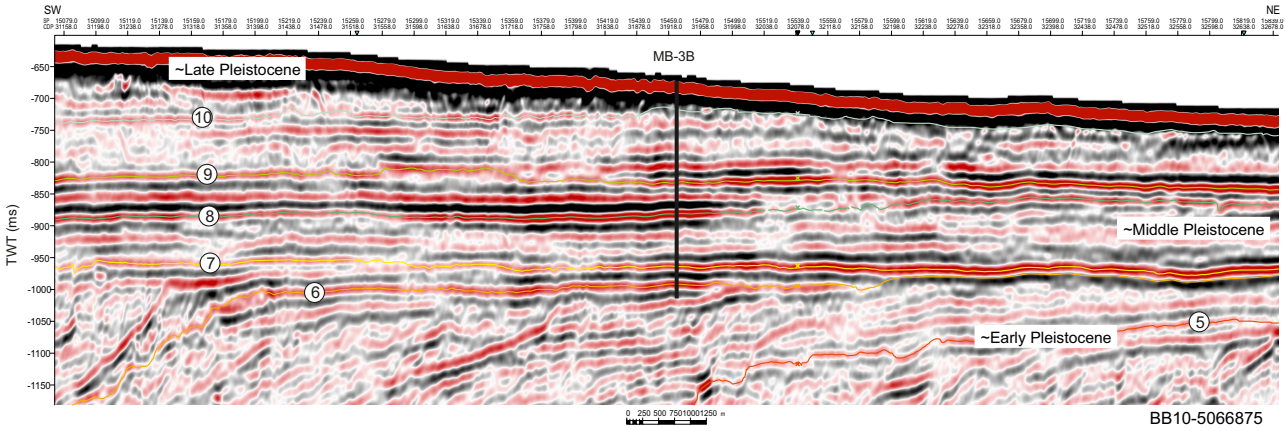

Figure AF12. Top: bathymetric map of the outer margin of the Melville Bugt TMF showing location of alternate Site MB-03B on Seismic Reflection Line BB10-5066875. Bottom: section of Seismic Line BB10-5066875 with interpreted horizons and location of alternate Site MB-03B at Shotpoint (SP) 15463. Site MB-03B will recover the stratified section above Seismic Unit 6 (depth target). The expected lithologies are proximal glacigenic deposits (e.g., tills interlayered with muddy marine/glacial-marine strata, probably of Early to Middle Pleistocene age). The site is placed ~2.7 km off the nearest crossline to optimize penetration of flat lying, onlapping reflections.

Site MB-04C

Priority:	Alternate
Position:	73.8734, −62.0528
Water depth (m):	628
Target drilling depth (mbsf):	305
Approved maximum penetration (mbsf):	305
Survey coverage (track map; seismic profile):	High-resolution primary: LAKO_1037; SP 74530 High-resolution crossing: LAKO_1041; SP 77698 Deep-penetration primary: ANU_Inline_13756.sgy; Xline 12520 Deep-penetration crossing: ANU_XLine_12520.sgy; In-line 13756
Objective(s):	Recover deglacial and interglacial intervals of potentially early Pleistocene age within top-set strata of the trough-mouth fan; onlap glacial unconformity (Horizon 3)
Coring program:	Hole A: RCB to 305 mbsf
Downhole measurements program:	Hole A (0–305 mbsf): • Triple combo • FMS-sonic
Nature of rock anticipated:	Diamicton with intercalated pebbly mud and mud units

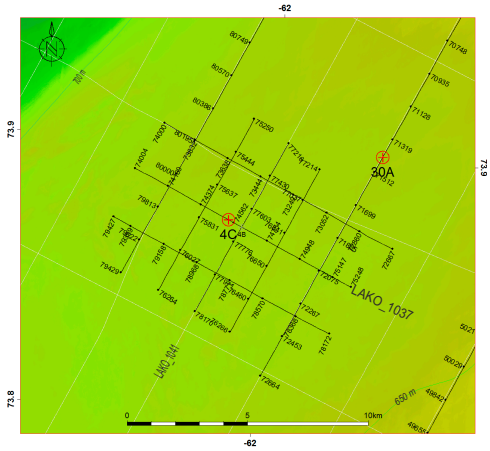

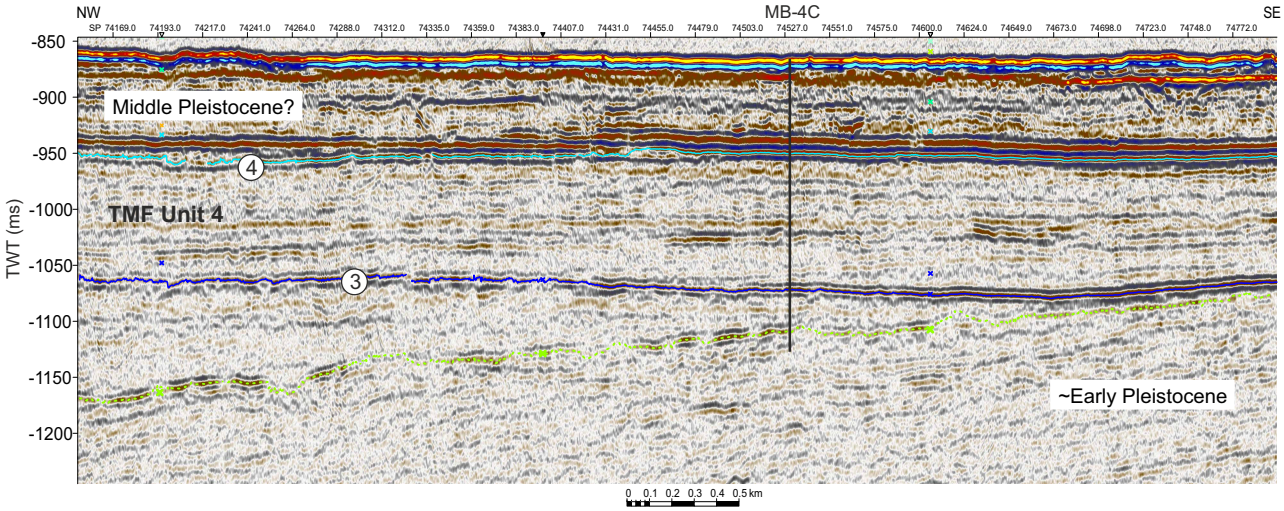

Figure AF13. Top: bathymetric map of the middle shelf region south of the Melville Bugt trough showing location of alternate Site MB-04C on Seismic Reflection Line LAKO_1037. Seismic lines include shot point (SP) numbers. Bottom: section of Seismic Line LAKO_1037 showing interpreted horizons and ages and location of alternate Site MB-04C at SP 74530. This site captures the pinch-out of a basal unit with TMF Unit 4 over Horizon 3. Depth target is a reflection onlap over an internal unconformity (light green) below Horizon 3. The site is expected to recover proximal glacigenic deposits interlayered with muddy marine/glacial-marine strata of probable Early Pleistocene age. Site MB-04C is offset 0.6 km from the nearest high-resolution crossline to achieve optimal stratigraphic coverage of the depth target.

Site MB-15A

Priority:	Alternate
Position:	74.1217, –60.9909
Water depth (m):	605
Target drilling depth (mbsf):	582
Approved maximum penetration (mbsf):	648
Survey coverage (track map; seismic profile):	Deep-penetration primary: ANU-3D: In-line 18916.segy; Xline 17068 Deep-penetration crossing: ANU-3D_XL-17068.segy; IL 18916
Objective(s):	Recover Neogene contourite drift sediments that can elucidate paleoceanographic conditions prior to the major basinward expansion of the Greenland Ice Sheet
Coring program:	Hole A: RCB to 582 mbsf Hole B: RCB to 400 mbsf
Downhole measurements program:	Hole A (0–582 mbsf): • Triple combo • FMS-sonic • VSI
Nature of rock anticipated:	Diamicton; mudstone with silty-sandy intervals

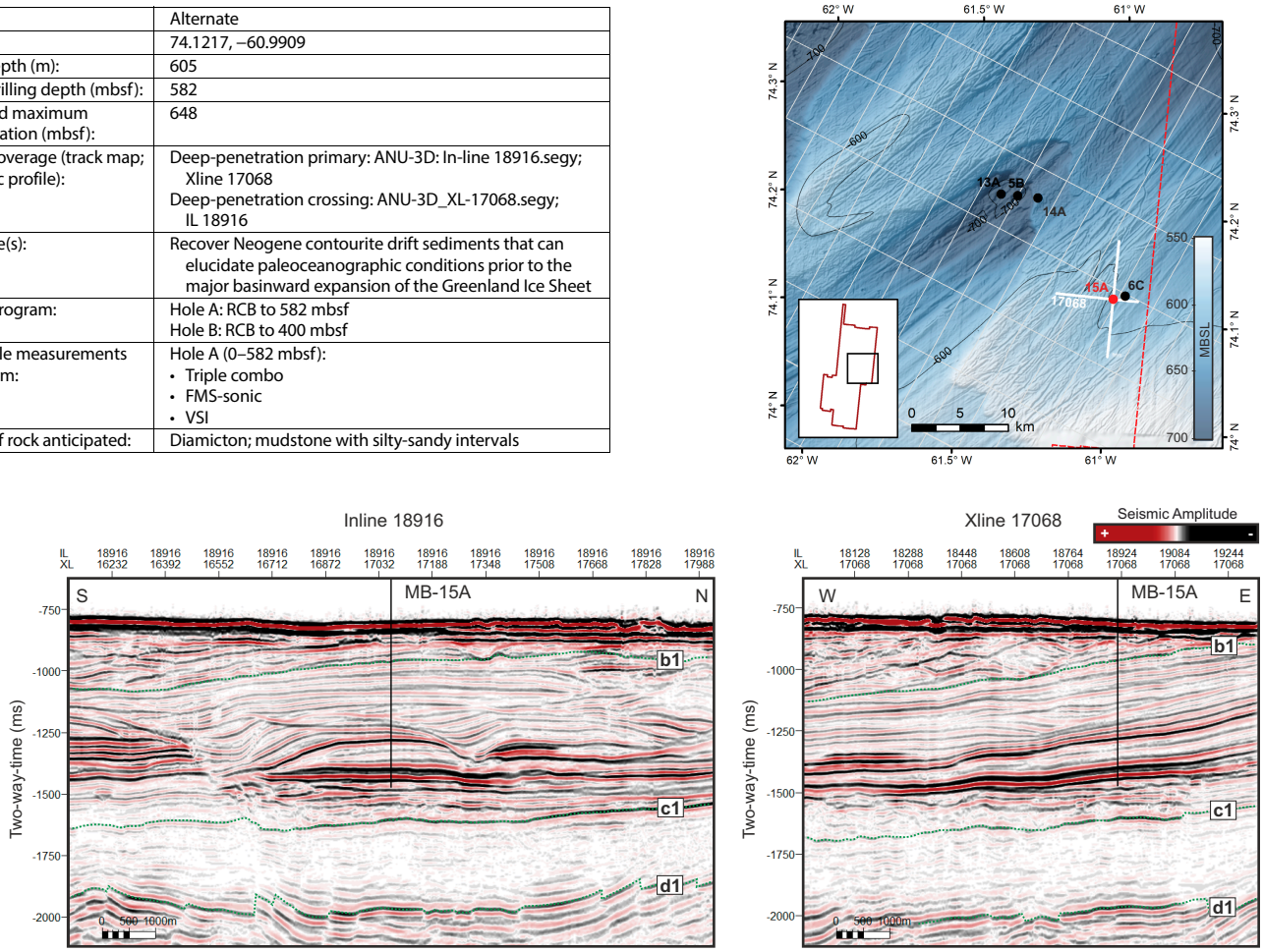

Figure AF14. Top: shaded relief bathymetric map of the middle shelf region within the Melville Bugt trough showing location of alternate Site MB-15A on seismic reflection crossing lines shown in bottom panel as thick white lines. Inline-Xline: 18916, 17068. Thin white lines show the 2D seismic grid. Inset shows the area coverage of 3D seismic data used to help refine target location. Black circles show the proposed alternate drill site location, and the red circle shows the drill site location for Site MB-15A. Bottom: key Inline and Xline seismic sections from the 3D seismic cube (zero-phase). Mega-unit boundaries are shown. Inline (left)-Xline (right): 18916, 17068 sections with location of alternate Site MB-15A.

Site MB-05B

Priority:	Alternate
Position:	74.2116, –61.3397
Water depth (m):	704
Target drilling depth (mbsf):	520
Approved maximum penetration (mbsf):	520
Survey coverage (track map; seismic profile):	High-resolution primary: LAKO_1022; SP 66675 Deep-penetration primary: ANU-3D_IL-17168.segy; XL 18616 Deep-penetration crossing: ANU-3D_XL-18616.segy; IL 17168
Objective(s):	(1) Capture deposits corresponding to the earliest shelf-based glaciations in northwest Greenland; (2) recover contourite drift sediments of likely early Pliocene age that can elucidate paleoceanographic conditions prior to the major expansion of the Greenland Ice Sheet
Coring program:	Hole A: RCB to 520 mbsf
Downhole measurements program:	Hole A (0–520 mbsf): • Triple combo • FMS-sonic
Nature of rock anticipated:	Diamicton; mudstone with silty-sandy intervals

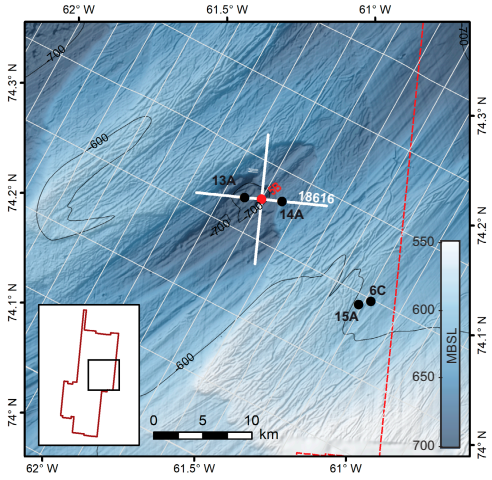

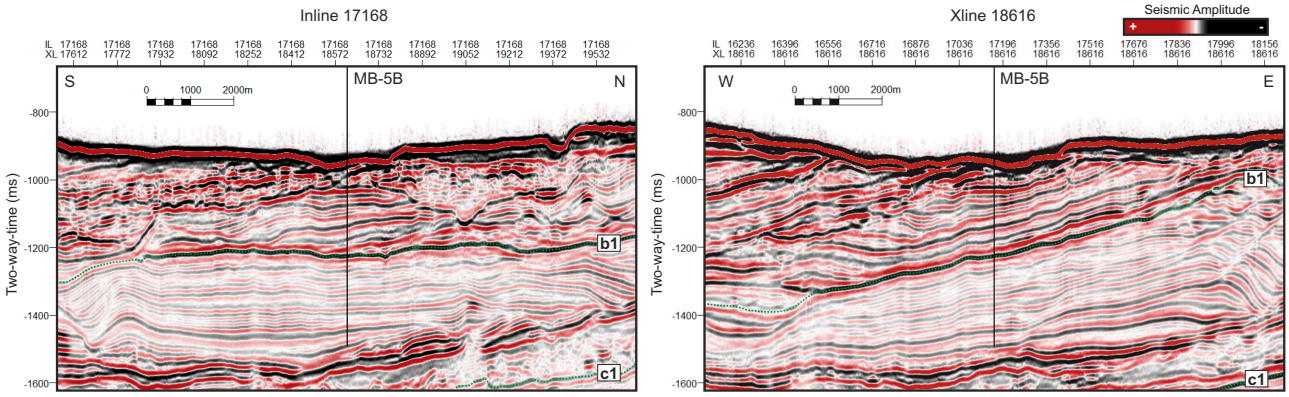

Figure AF15. Top: shaded relief bathymetry map of the middle shelf region within the Melville Bugt trough showing location of alternate Site MB-05B on seismic reflection crossing lines shown as thick white lines in bottom panel. Inline-Xline: 17168, 18616. Thin white lines show the 2D seismic grid. Inset shows the aerial coverage of 3D seismic data used to help refine target location. Red circle shows the drill site location for MB-05B. Bottom: key Inline and Xline seismic sections from the 3D seismic cube (zero-phase). Mega-unit boundaries are shown. Inline (left)-Xline (right): 17168, 18616 sections with location of alternate Site MB-05B.

Site MB-13A

Priority:	Alternate
Position:	74.2118, –61.3958
Water depth (m):	707
Target drilling depth (mbsf):	540
Approved maximum penetration (mbsf):	540
Survey coverage (track map; seismic profile):	Primary: ANU-3D: In-line 16896.segy; Xline 18616 Crossing: Site-13A_ANU-3D_XL-18616.segy; IL 16896
Objective(s):	(1) Capture deposits corresponding to the earliest shelf-based glaciations in northwest Greenland; (2) recover Contourite drift sediments of likely early Pliocene age that can elucidate paleoceanographic conditions prior to the major expansion of the Greenland Ice Sheet
Coring program:	Hole A: RCB to 540 mbsf
Downhole measurements program:	Hole A (0–540 mbsf): • Triple combo • FMS-sonic
Nature of rock anticipated:	Diamicton; mudstone with silty-sandy intervals

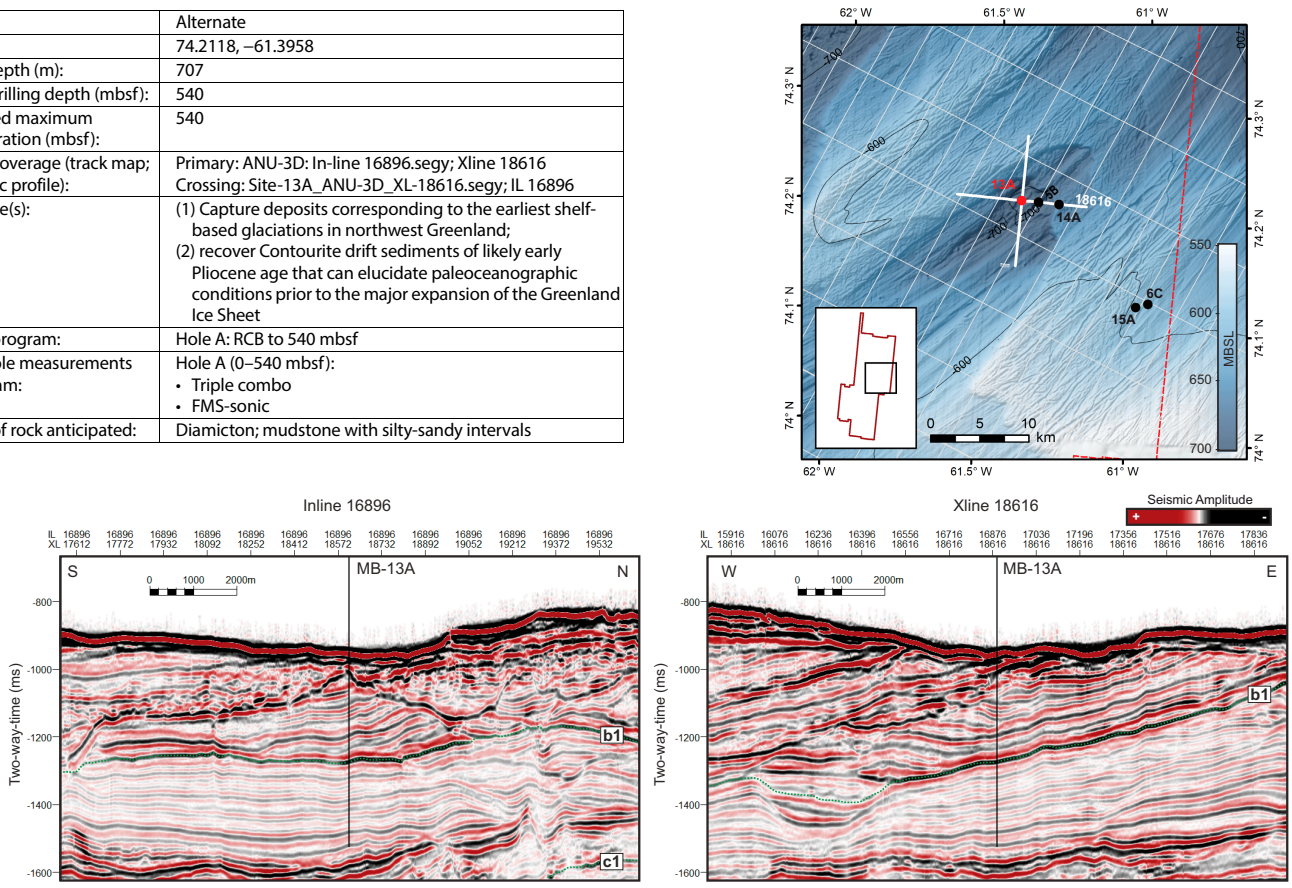

Figure AF16. Top: shaded relief bathymetry map of the middle shelf region within the Melville Bugt trough showing location of alternate Site MB-13A on seismic reflection crossing lines shown as thick white lines in bottom panel; Inline-Xline: 16896, 18616. Thin white lines show the 2D seismic grid. Inset shows the aerial coverage of 3D seismic data used to help refine target location. Red circle shows the drill site location for Site MB-13A. Bottom: key (left) Inline and (right) Xline seismic sections from the 3D seismic cube (zero-phase). Mega-unit boundaries are shown.

Site MB-14A

Priority:	Alternate
Position:	74.2109, –61.2704
Water depth (m):	663
Target drilling depth (mbsf):	510
Approved maximum penetration (mbsf):	510
Survey coverage (track map; seismic profile):	Deep-penetration primary: ANU-3D: In-line 17504.segy; Xline 18616 Deep-penetration crossing: Site-14A_ANU-3D_XL-18616.segy; IL 17504
Objective(s):	(1) Capture deposits corresponding to the earliest shelf-based glaciations in northwest Greenland; (2) recover contourite drift sediments of likely early Pliocene age that can elucidate paleoceanographic conditions prior to the major expansion of the Greenland Ice Sheet
Coring program:	Hole A: RCB to 510 mbsf
Downhole measurements program:	Hole A (0–510 mbsf): • Triple combo • FMS-sonic
Nature of rock anticipated:	Diamicton; mudstone with silty-sandy intervals

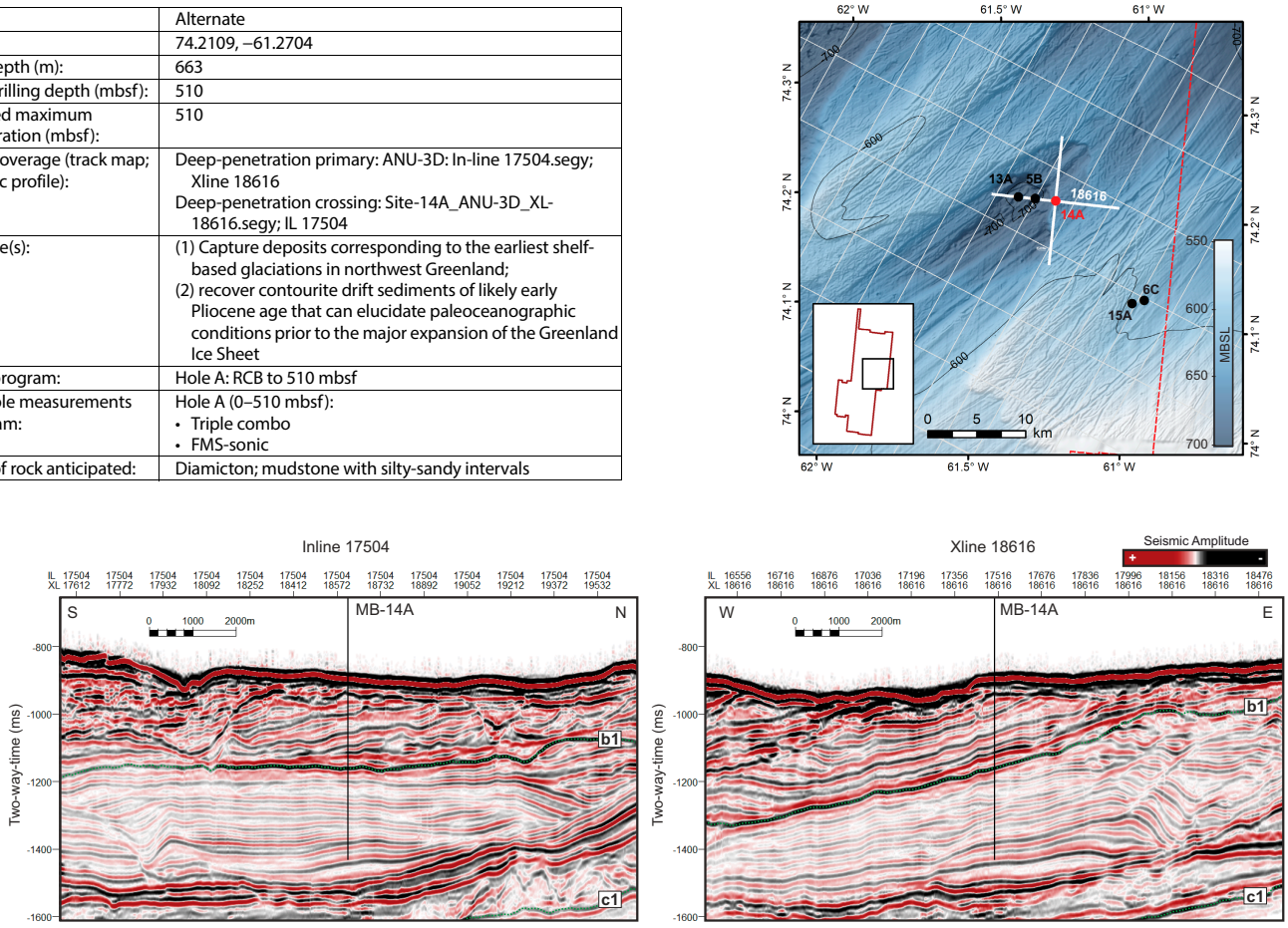

Figure AF17. Alternate Site MB-14A is aimed at recovering a composite sequence of high–accumulation rate contourite drifts of Mega-unit B (likely Pliocene age) and the earliest glacial clinoforms of Mega-unit A (Late Pliocene and Early Pleistocene). Top: shaded relief bathymetric map of the middle shelf region within the Melville Bugt trough showing location of alternate Site MB-14A on seismic reflection crossing lines shown as thick white lines in bottom panel. Inline-Xline: 17504, 18616. Thin white lines show the 2D seismic grid. Inset shows the aerial coverage of 3D seismic data used to help refine target location. Red circle shows the drill site location for Site MB-14A Bottom: seismic reflection profiles with location of alternate Site MB-14A: (left) Inline 17504 and (right) Xline 18616. SP = shotpoint.

Site MB-16A

Priority:	Alternate
Position:	74.5507, –60.7990
Water depth (m):	734
Target drilling depth (mbsf):	1080
Approved maximum penetration (mbsf):	1089
Survey coverage (track map; seismic profile):	High-resolution crossing: LAKO_1035; SP 61758 Deep-penetration primary: PITU 3D: In-line 2825; Xline 2960 Deep-penetration crossing: PITU-3D-Full-Volume_XL-2960.segy; In-line 2825
Objective(s):	Recover an upper Miocene interval and continue coring through the Middle Miocene horizon to the top of a sedimentary wedge of possible Oligocene age to elucidate past ocean and terrestrial climates in northeast Baffin Bay/Greenland and the onset of ephemeral glaciation in northwest Greenland
Coring program:	Hole A: RCB to 630 mbsf Hole B: Install HRT with 600 m of casing; RCB 600–1080 mbsf
Downhole measurements program:	Hole A (0–630 mbsf): • Triple combo • FMS-sonic • VSI Hole B (600–1080 mbsf): • Triple combo • FMS-sonic • VSI
Nature of rock anticipated:	Claystone with silty to sandy intervals and siliceous ooze

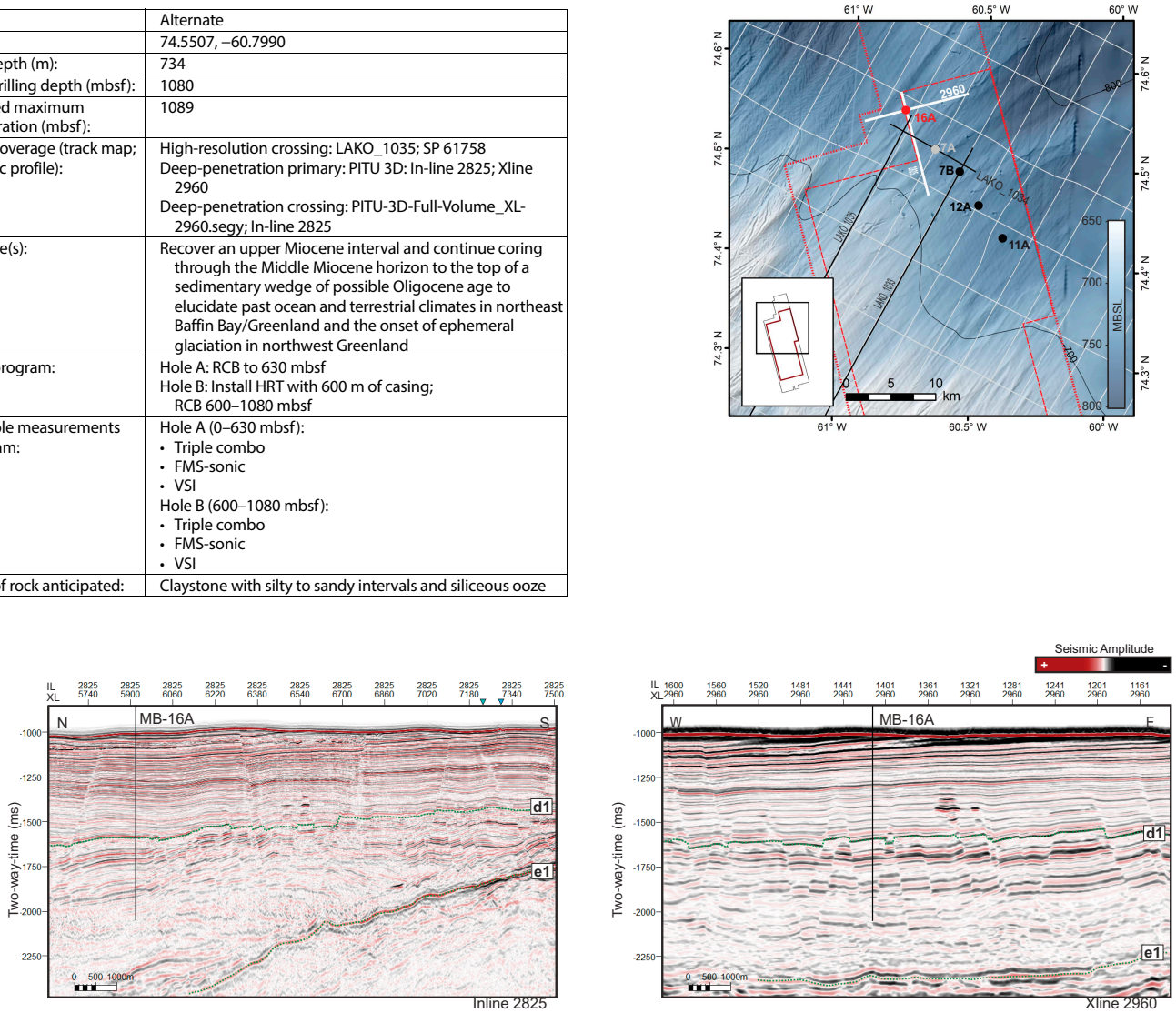

Figure AF18. Alternate Site MB-16A aimed at recovering Oligocene and Miocene successions that are expected to be fine-grained hemipelagic sediments of Mega-units C and D. Top: shaded relief bathymetry map of the middle shelf region within the Melville Bugt trough, shown with 100 m contours. Seismic crossing lines displayed in the bottom panel are shown as thick white lines: Inline-Xline: 2825, 2960. Thin white lines show the 2D seismic grid. Inset shows the aerial coverage of 3D seismic data used to help refine target location. Red circle shows the drill site location for alternate Site MB-16A. Dashed and dotted red lines show the high-resolution subcrop and standard 3D data outlines, respectively. Bottom: seismic reflection profiles with location of MB-16A. Left, Inline 2825; right, Xline 2960. SP = shotpoint.

Site MB-11A

Priority:	Alternate
Position:	74.4283, –60.4086
Water depth (m):	747
Target drilling depth (mbsf):	1015
Approved maximum penetration (mbsf):	1200
Survey coverage (track map; seismic profile):	Primary: PITU 3D: In-line 2280.segy; Xline 8578 Crossing: PITU-3D_XL-8578.segy; IL 2280
Objective(s):	Recover an upper Miocene interval and continue coring through the Middle Miocene horizon to the top of a sedimentary wedge of possible Oligocene age to elucidate past ocean and terrestrial climates in northeast Baffin Bay/Greenland and the onset of ephemeral glaciation in northwest Greenland
Coring program:	Hole A: RCB to 630 mbsf Hole B: Install HRT with 600 m of casing; RCB 600–1015 mbsf
Downhole measurements program:	Hole A (0–630 mbsf): • Triple combo • FMS-sonic • VSI Hole B (600–1015 mbsf): • Triple combo • FMS-sonic • VSI
Nature of rock anticipated:	Claystone with silty to sandy intervals and siliceous ooze

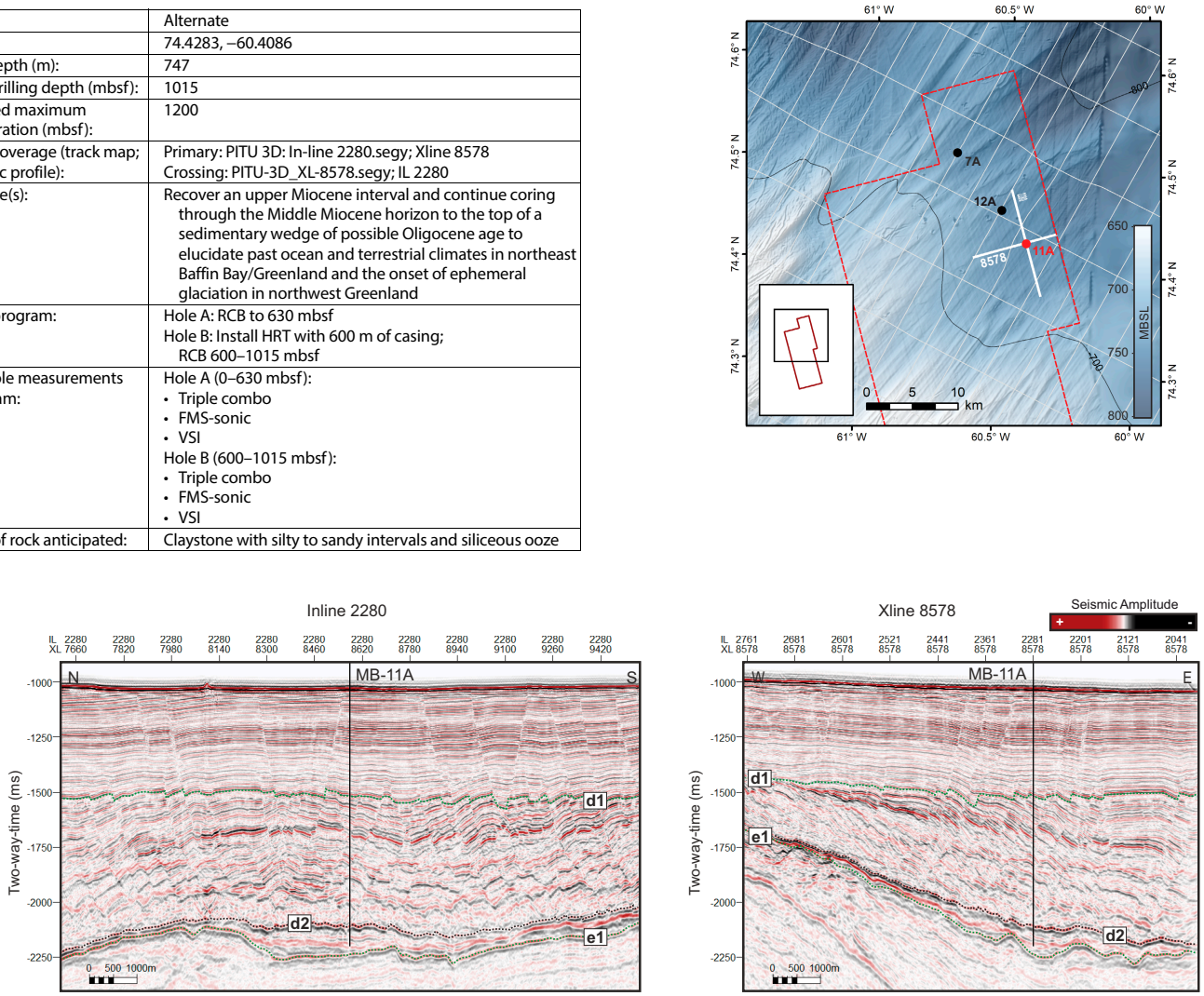

Figure AF19. Alternate drill Site MB-11A is aimed at recovering Oligocene and Miocene successions that are expected to be fine-grained hemipelagic sediments of Mega-units C and D. Top: shaded relief bathymetry map of the middle shelf region within the Melville Bugt trough, shown with 100 m contours. Seismic crossing lines displayed in the bottom panel are shown as thick white lines: Inline-Xline: 2280, 8578. Thin white lines show the 2D seismic grid. Inset shows the aerial coverage of 3D seismic data used to help refine the target location. Red circle shows location of Site MB-11A. Dashed and dotted red lines show the high-resolution subcrop and standard 3D data outlines, respectively. Bottom: seismic reflection profiles with location of Site MB-11A. Left, Inline 2825; right, Xline 2960. SP = shotpoint.

Site MB-12A

Priority:	Alternate
Position:	74.4597, –60.5049
Water depth (m):	739
Target drilling depth (mbsf):	971
Approved maximum penetration (mbsf):	1186
Survey coverage (track map; seismic profile):	Primary: PITU 3D: In-line 2413.segy; Xline 7902 Crossing: PITU-3D_XL-7902.segy; IL 2413
Objective(s):	Recover an upper Miocene interval and continue coring through the Middle Miocene horizon to the top of a sedimentary wedge of possible Oligocene age to elucidate past ocean and terrestrial climates in northeast Baffin Bay/Greenland and the onset of ephemeral glaciation in northwest Greenland
Coring program:	Hole A: RCB to 630 mbsf Hole B: Install HRT with 600 m of casing; RCB 630–971 mbsf
Downhole measurements program:	Hole A (0–630 mbsf): • Triple combo • FMS-sonic • VSI Hole B (600–971 mbsf): • Triple combo • FMS-sonic • VSI
Nature of rock anticipated:	Claystone with silty to sandy intervals and siliceous ooze

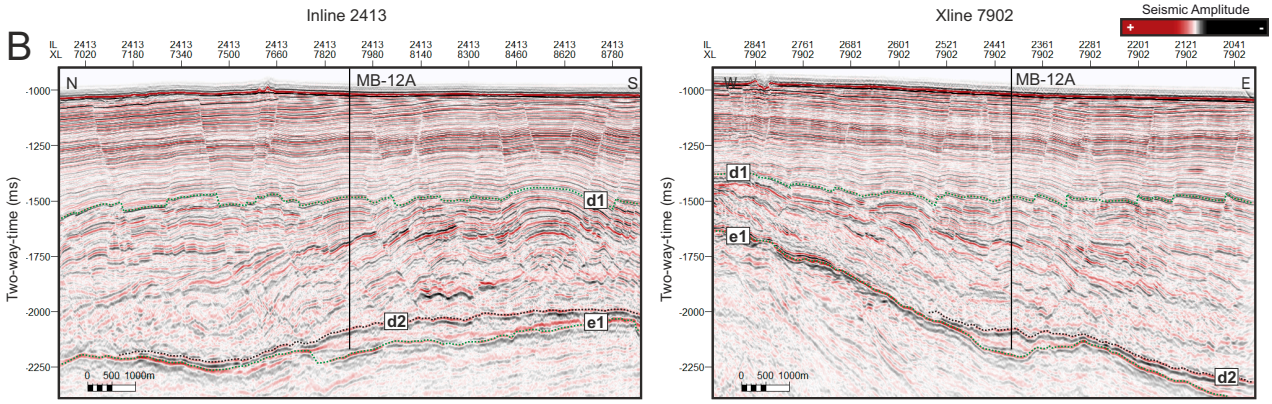

Figure AF20. Alternate drill Site MB-12A is aimed at recovering Oligocene and Miocene successions that are expected to be fine-grained hemipelagic sediments of Mega-units C and D. Top: shaded relief bathymetry map of the middle shelf region within the Melville Bugt trough, shown with 100 m contours. Seismic crossing lines displayed in the bottom panel are shown as thick white lines: Inline-Xline: 2413, 7902. Thin white lines show the 2D seismic grid. Inset shows the aerial coverage of 3D seismic data used to help refine the target location. Red circle shows the location of Site MB-12A. Dashed and dotted red lines show the high-resolution subcrop and standard 3D data outlines, respectively. Bottom: seismic reflection profiles with location of Site MB-12A. Left, Inline 2413; right, Xline 7902. SP = shotpoint.

Site MB-10A

Priority:	Alternate
Position:	74.4584, –61.1792
Water depth (m):	698
Target drilling depth (mbsf):	1200
Approved maximum penetration (mbsf):	1288
Survey coverage (track map; seismic profile):	Primary: BB10-5065625; SP 19946 Crossing: BB10-109125; SP 25337
Objective(s):	Recover an upper Miocene interval and continue coring through the Middle Miocene horizon to the top of a sedimentary wedge of possible Oligocene age to elucidate past ocean and terrestrial climates in northeast Baffin Bay/Greenland and the onset of ephemeral glaciation in northwest Greenland
Coring program:	Hole A: RCB to 630 mbsf Hole B: Install HRT with 600 m of casing; RCB 630–1200 mbsf
Downhole measurements program:	Hole A (0–630 mbsf): • Triple combo • FMS-sonic • VSI Hole B (600–1200 mbsf): • Triple combo • FMS-sonic • VSI
Nature of rock anticipated:	Claystone with silty to sandy intervals and siliceous ooze

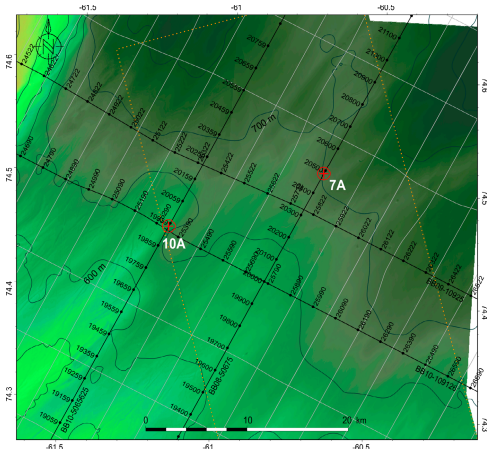

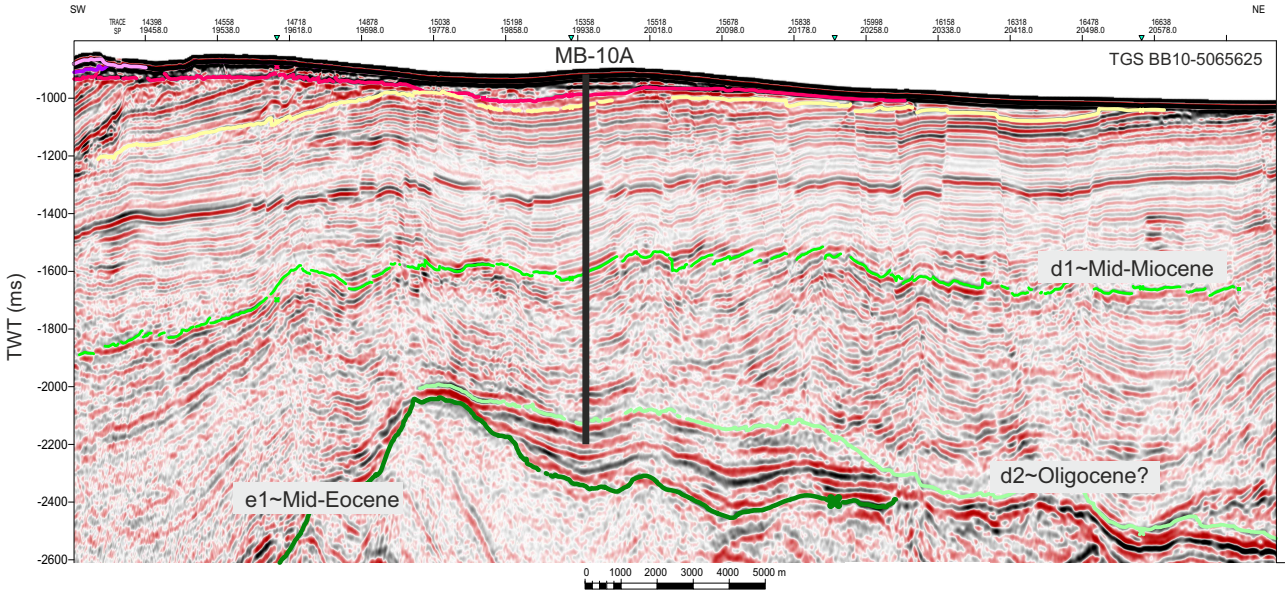

Figure AF21. Top: multibeam bathymetry map of the middle shelf region, situated within the Melville Bugt trough, shown with 50 m depth contours. 3D data cube outlined in orange. Alternate Site MB-10A is on seismic reflection Line BB10-5065625 at Shotpoint (SP) 19946 and on Crossing Line BB10-109125 at SP 25337. Bottom: key Seismic Profile BB10-5065625 with location of alternate Site MB-10A and interpreted horizons and assumed ages. TD is Horizon d2 of possible Oligocene age. Site MB-10A is expected to recover Late and Early Miocene successions composed mainly of fine-grained hemipelagic sediments, possibly with smectite and intervals rich in opal-CT.